SK CHANNELS AND SIGNALING MICRODOMAINS IN DENDRITIC SPINES

by

Kang Wang

A DISSERTATION

Presented to the Cell & Developmental Biology

and the Oregon Health & Science University

School of Medicine

in partial fulfillment of

the requirements for the degree of

Doctor of Philosophy

September 2014

School of Medicine
Oregon Health & Science University

CERTIFICATE OF APPROVAL

This is to certify that the PhD dissertation of

Kang Wang

has been approved

_____
Mentor/Advisor

_____
Mentor/Advisor

_____
Committee Member

_____
Committee Member

_____
Committee Member

_____
Committee Member

TABLE OF CONTENTS

Special thanks to my mentor John Adelman and James Maylie

And to my family

Abbreviations

1-EBIO 1-Ethyl-2-benzimidazolinone

4-AP 4-Aminopyridine

AHP afterhyperpolarization

AMPA α-amino-3-hydroxy-5-methyl-4-isoxazolepropionic acid

AP action potential

BAPTA 1,2-bis(o-aminophenoxy)ethane-N'N'N'-tetraacetic acid

BK big-conductance potassium channel

CaM calmodulin

CaMBD calmodulin-binding domain

CNS central nervous system

CyPPA *N*-cyclohexyl-*N*-[2-(3,4-dimethyl-pyrazol-1-yl)-6-methyl-4-pyrimidinamine]

D-AP5 D-2-amino-5-phosphonovalerate

EGTA ethylenediaminetetraacetate

EPSC excitatory postsynaptic current

EPSP excitatory postsynaptic potential

IbTx Iberiotoxin

iEM immunoelectron microscopy

IK intermediate-conductance potassium channel

IP3 inositol 1,4,5-trisphosphate

IPSC inhibitory postsynaptic current

IPSP inhibitory postsynaptic potential

KChIP potassium channel interacting protein

K_{2P} two-pore potassium channel

K_{Ca} calcium activated potassium channel

K_{ir} inward rectifier potassium channel

Kv voltage gated potassium channel

LTD long-term depression

LTP long-term potentiation

mAChR muscarinic acetylcholine receptor

nAChR nicotinic acetylcholine receptor

NMDA N-methyl-D-aspartate

NS309 6,7-dichloro-1*H*-indole-2,3-dione 3-oxime

NS4591 4,5-dichloro-1,3-diethyl-1,3-dihydro-benzoimidazol-2-one

PKA protein kinase A

PP2A protein phosphatase 2A

PSD postsynaptic density

SK small-conductance potassium channel

SK2-L SK2-long

SK2-S SK2-short

TEA tetraethylammonium

TRAM-34 1-[(2-Chlorophenyl) diphenylmethyl]-1*H*-pyrazole

VGCC voltage gated Ca^{2+} channel

I. ABSTRACT

Small-conductance Ca^{2+} activated potassium channels (SK) channels play a fundamental role in all excitable cells. They are potassium selective, voltage-insensitive, and activated by increases in the level of intracellular Ca^{2+} ions and selectively blocked by peptide toxin apamin. Increases in the intracellular Ca^{2+} concentration activated SK channels, leading to hyperpolarization of membrane potential, which in turn reduces the Ca^{2+} transient in the cell. For example, in the spine of hippocampal CA1 pyramidal neurons and in lateral amygdala pyramidal neurons, Ca^{2+} influx through N-methyl-D-aspartate receptors (NMDARs) activates the SK2-containing channels, the efflux of K^{+} ions through SK channels repolarizes the spine, promoting the Mg^{2+} blockage of NMDARs, therefore reducing the Ca^{2+} transient in the cell. Thus, blocking SK2-containing channels with apamin facilitates the induction of long-term potentiation (LTP) by enhancing NMDAR-dependent Ca^{2+} signals within dendritic spines.

The *SK2* gene encodes two isoforms that differ only in the length of their N-terminal domains. SK2-long (SK2-L) and SK2-short (SK2-S) are co-expressed in CA1 pyramidal neurons and likely form heteromeric channels. In mice lacking SK2-L, SK2-S-containing channels are expressed in the extrasynaptic membrane, but are excluded from the postsynaptic density (PSD). The SK channel contribution to excitatory postsynaptic potentials (EPSP) is absent in SK2-S only mice and could be restored by SK2-L re-expression. The first aim of this thesis was to assess the contribution of SK-L isoform to the induction of LTP in hippocampal neurons. We found that blocking SK channels increased the amount of LTP induced in area CA1 in

slices from wild-type mice but had no effect in slices from SK2-S only mice. Taken together with the SK2-S expression pattern and the effect of SK2-L on EPSP, these results indicate that SK2-L directs synaptic SK2-containing channels expression and is important for normal synaptic signaling and plasticity.

There are many Ca^{2+} sources for activating SK channels in excitable cells, for example, Ca^{2+} influx through NMDAR or via voltage gated Ca^{2+} channels, or Ca^{2+} induced Ca^{2+} release from intracellular store. In hippocampal CA1 pyramidal neurons, synaptically evoked Ca^{2+} influx through NMDARs activates spine SK channels, reducing EPSPs and the associated spine head Ca^{2+} transient. However, results using glutamate uncaging implicated Ca^{2+} influx through SNX-482 sensitive R-type (Cav2.3) Ca^{2+} channels as the Ca^{2+} source for SK channel activation. The second aim of this thesis was to study the two Ca^{2+} sources, one from Ca^{2+} influx through NMDARs and the other from R-type Ca^{2+} channels, and their downstream targets of potassium channels. By using synaptic stimulation, we found that both apamin and SNX-482 boosted synaptically evoked EPSPs and their effects were not mutually exclusive. Ca^{2+} influx through R-type Ca^{2+} channels activates voltage dependent Kv4.2 containing potassium channels in a Kv channel interacting protein (KChIP) dependent manner. These results suggest two distinct Ca^{2+} signaling pathways within dendritic spine that link Ca^{2+} influx through NMDARs to SK channels and Ca^{2+} influx through R-type Ca^{2+} channels to Kv4.2-containing channels.

II. INTRODUCTION

II.1. Potassium channels

II.1.1. Ion channels overview

Ion channels are pore-forming protein complexes that traverse the lipid bilayer of cell membranes and conduct the movement of specific inorganic ions - primarily Na^+, K^+, Ca^{2+}, or Cl^- - across the membrane. The channel's response to specific ions, molecules or voltage changes leads to the opening and closing of the pore, which contributes to one of the ion channels properties: gating. Therefore, ion channels are not continuously open but fluctuate between open and close states. When the pore is open, many ion channels have the important property of 'selective permeability', allowing some ions to flow passively down their electrochemical activity gradients at a high rate, while excluding the passage of other ions. According to different types of stimuli that cause channels to open, ion channels are classified into several subtypes: voltage-gated ion channels open and close in response to membrane potential; ligand-gated ion channels respond to the binding of either an extracellular mediator such as neurotransmitter or an intracellular mediator such as nucleotide or an ion such as Ca^{2+}; other ion channels such as mechanically-gated channels, temperature-gated channels and light-gated channels are gated by mechanical stress, change of temperature and the action of light respectively. Channels are also grouped into families according to their selectivity: chloride channels, potassium channels, sodium channels and calcium channels, with a small group of proton channels and non-selective cation channels[1,2].

II.1.2. Potassium channels: types, structure and function.

As the biggest ion channel family, potassium channels, originally identified as the molecular entities conducting K^+ ions across the cell membrane, are now known in virtually all types of cells in all living organisms, where they contribute to the complex and diverse functional repertoires of neurons in the nervous system and cells in other organ systems[2]. All potassium channels display a highly conserved segment with the consensus sequence of TVGYG with some variations, which is located in the narrowest region of the pore, and functions as the selectivity filter to allow K^+ but not Na^+ or other ions to cross the membrane[3,4]. The majority of potassium channels are formed as homotetramers or heterotetramers, whose subunits are arranged in four-fold symmetry surrounding the K^+-selective pore[4,5]. Each subunit contains either six (shaker-like[6,7]) or two (inward-rectifier[8,9,10]) transmembrane segments. There is an additional subfamily that comprise tandem pore domains, the potassium (K_{2P}) channels, which are presumably dimers with four transmembrane segments in each subunit[11,12].

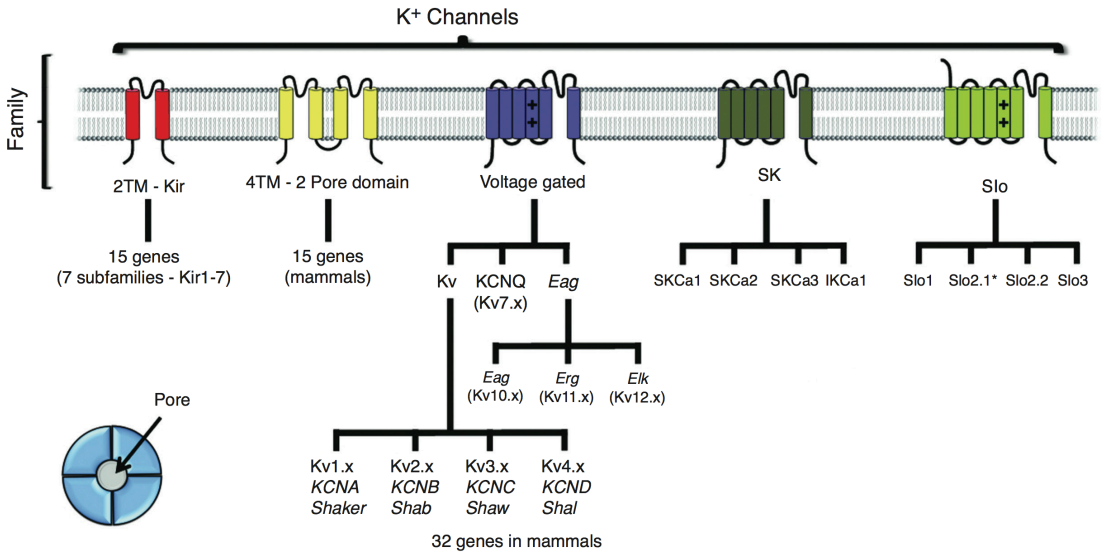

González et al. (2012) K^+ channels: function-structural overview. *Comprehensive Physiology*

Diversity among different members of the potassium channels family is related mainly to the various ways in which potassium channels are activated and taken together with different topologies of potassium channel subunits, potassium channels are divided into four major classes: 1. Voltage gated potassium channels (Kv) that open or close in response to membrane potential that acts via a charged voltage sensor domain. 2. Inward rectifier potassium channels (K_{ir}) are either constitutively open or regulated by G-proteins or the ATP/ADP ration in the cell. 3. Ca^{2+} activated potassium channels (Kc_a), which are gated by the changes in the intracellular Ca^{2+} concentration. 4. K_{2P} channels that are activated by a variety of physiological stimuli such as pH, temperature, membrane tension, and certain signaling molecules.

One of the most striking properties of potassium channels is their remarkable ability to conduct K^+ ions with high selectivity and conduction rate. K^+ ions are necessary for the function of all living cells and consequently, potassium channels are involved in a multitude of physiological functions including cell metabolism, hormone secretion, and neuronal signaling regulation[2]. For example, K_{2P} channels underlie background potassium currents that contribute to stabilizing the resting membrane potential and counterbalance depolarization. In addition, the expression of TASK-3 channels, which belongs to the K_{2P} channel family, regulates granule neuron apoptosis during the early development of the cerebellum[13]. Similarly, TASK-3 channels are considered potentially to be involved in carcinogenesis and tumor progression[14]. In pancreatic β cells, K_{ATP} channels coassembled from the sulfonylurea receptor (SUR) and K_{ir} pore forming subunits regulate insulin secretion by sensing the changes of intracellular ATP levels[15,16]. In hippocampal CA1 pyramidal neurons, big conductance Ca^{2+}-activated potassium channels (BK channels) provide robust potassium currents that

contribute to repolarization of action potential (AP), give rise to a fast afterhyperpolarization (fAHP) and shape dendritic Ca^{2+} spikes[17,18,19]. In the same neurons, Kv4 voltage-gated channels are found mainly on distal portions of dendrites and in dendritic spines, modulating cell excitability and action potential waveforms[20,21,22].

II.1.3. Calcium activated potassium channels

Kc_a channels are widely expressed in neuronal and nonneuronal tissues including epithelia and smooth muscle cells, where they link excitability and intracellular Ca^{2+} concentration to modulate neuronal firing pattern or smooth muscle tone. Based on their conductance, Kc_a channels are divided into four subtypes: BK channels that exhibit big conductance (100-200 pS), IK channels that have intermediate conductance, SK channels that display small conductance (10-20 pS) and an as yet unidentified channel underlying the slow afterhyperpolarization (sAHP) that is responsible for spike-frequency adaptation in many central neurons. In 1991, the first Kc_a channel cDNA was cloned from *Drosophila*[23,24]. Subunits from the known Kc_a channel family have six transmembrane segments similar to the Kv subunits, except for BK channels in which the N-terminus makes a seventh pass across the membrane to end up outside the cell[25]. In addition, the BK channels are gated not only by intracellular Ca^{2+} concentration but also by action of membrane depolarization[26]. In fact, BK channels are really voltage-gated channels with an open probability that is modulated by Ca^{2+}.

II.2. Small-conductance Ca^{2+} activated K^+ channels

II.2.1. Identification of SK channels

In 1958, Gardos first described that the changes of internal Ca^{2+} either by adding ethylenediaminetetraacetate (EGTA) or $CaCl_2$ affects potassium outflow across membranes prepared from red blood cells[27]. In 1972, Meech and colleagues postulated the Ca^{2+} activated potassium conductance by observing that a microinjection of Ca^{2+} hyperpolarized the membrane potential of an *Aplysia* neuron because of a specific increase in potassium conductance[28]. With improved patch-clamp techniques, in 1981, Lux et al. described that single channel recordings from *Helix* neurons showed a 19 pS Ca^{2+}-activated potassium conductance[29]. Later, potassium channels with a similar small conductance were observed in cultured bovine adrenal chromaffin cells using patch-clamp techniques[30,31]. In 1986, SK channels were first identified as small conductance Kc_a channels in cultured rat muscle cells, with the single-channel conductance around 15 pS[32], and being blocked by peptide toxin apamin, which is an 18 amino acid peptide with two disulfide bridges and a C-terminal amide derived from bee venom[33].

II.2.2. History of apamin

Apamin is a remarkably selective toxin, blocking SK channels and having no other known targets. Thus, apamin selectivity is a fingerprint for SK channel activity. In 1978, Vladimirova et al. described the role of apamin as a specific blocker of

inhibitory postsynaptic potentials (IPSPs) and membrane hyperpolarization caused by nonadrenergic inhibitory nerve stimulations or exogenous ATP application to visceral smooth muscle cells[34]. A year later, Banks and Burgess et al. revealed that the inhibition of hyperpolarization caused by apamin was due to block of increased potassium permeability induced by agent such as ATP[35]. In 1981, Burgess et al. reported that apamin blocks potassium efflux through Ca^{2+}-dependent potassium channels in guinea pig and rabbit liver cells[36]. By radiolabelling iodo-apamin, Hugues et al. in 1982 confirmed apamin inhibition of Ca^{2+}-dependent potassium channels and identified a putative protein component of the Kc_a channel that interacts with apamin[37,38]. After identifying the SK channels by applying apamin in 1986[32], subsequent structural modeling and mutagenesis studies of the binding site of apamin to SK channel revealed that, unlike traditional potassium channel blockers, such as tetraethylammonium (TEA) which binds deep within channel pore to physically exclude potassium ions permeability, apamin would bind to the outer vestibule of the pore[39,40] as well as the S3-S4 extracellular loop[41,42] of the SK channels, suggesting an allosteric blockage of channel activity.

II.2.3. Cloning and structure of SK channels

In 1996, the SK channels were first cloned[43]. The amino acid sequences revealed that SK channel subunits share similar transmembrane topology with Kv channels, having six transmembrane segments and cytosolic N- and C-termini. Among three cDNA clones (SK1-3) that encode SK channel[43], SK1 and SK2 are predominantly expressed

in neurons in neurons while SK3 is expressed both neuronal and nonneuronal cells such as endothelial and smooth muscle cells[44,45,46]. In addition, Gardos' description of a Ca^{2+}-activated potassium flux in 1958 provided a prototypic member of a intermediate conductance Ca^{2+}-activated potassium channel with a conductance of 20-80 pS[27,47]. In 1997, sequence homology screens from pancreas[48] and placenta[49] identified the fourth member of the family, IK1 (SK4). The IK channels are mainly expressed in blood cell, epithelial and smooth muscle cells[30,49,50], and in some peripheral neurons such as dorsal root ganglia[51]. Recent reports suggest there may be some IK1 expression in central nervous system (CNS).

Although the overall architecture of SK subunits is conserved with voltage-gated potassium channels, the S4 segment, which confers voltage sensitivity to the Kv channel, shows a reduced number and disrupted array of positively charged amino acids in SK channels[4,6,43]. The SK channels retain only two of the seven positively charged amino acids that are found in the S4 segment of Kv channels, and only one of these residues corresponds to the four arginine residues that carry the gating chargers in Kv channels. The primary sequence difference explains the observed voltage independence of SK channels in the molecular level. Despite the highly conserved pore regions among different potassium channels, the most conserved domain among SK channel subunits is the intracellular C terminus immediately following the sixth transmembrane segment. Subsequent studies revealed an important role of this region for Ca^{2+} gating[52,53].

Heterologous expression of rodent SK2 or SK3 subunits results in functional homomeric apamin-sensitive SK channels[43,54]. In contrast, rat SK1 does not form

functional channels in the plasma membrane. Instead, the SK1 proteins remain largely at intracellular locations[55]. Several studies have shown that SK channels can also form heretomeric chennels. Co-assembly of rat SK1 potassium channel subunit with rat SK2 results in a large current with a reduced sensitivity for apamin compared with rat SK2 alone[55]. Ishii et all showed heteromeric SK channels composed of human SK1 and rat SK2 subunits in *Xenopus* oocytes have an intermediate sensitivity for apamin compared with homomeric human SK1 or rat SK2 channels[39]. Immunoprecipitation from heterologously expressed subunits or from rat brain suggest heteromeric assembly of SK2 and Sk3[56]. Surprisingly, human SK1 subunits reduced the functional expression of rat SK3 channels in a heterologous expression system, which might be explained by the retention of heteromeric hSK1/rSK3 channels in intracellular locations[57].

II.2.4. SK channel activation, Ca^{2+} gating and modulation

SK channels are gated directly by submicromolar concentrations of intracellular Ca^{2+} ions (IC_{50}= 300-700 nM)[32,58,59], and the Hill coefficients greater than 1 suggesting that multiple Ca^{2+} ions are involved in a cooperative gating process[43]. The time constant of SK channel activation is ~ 5 ms, while the time constant for channel deactivation ranges from 15-60 ms[60].

Site-directed mutagenesis studies of predicted intracellular negatively charged Ca^{2+}-binding residues indicated that their pore-forming subunits do not contain an intrinsic Ca^{2+} binding domain. Instead, each subunit of SK channels displays a highly

conserved domain, the 'calmodulin-binding domain' (CaMBD), which is located immediately following the sixth transmembrane segment and stretches over approximately 90 amino acids[52]. Yeast two-hybrid analysis and in vitro binding experiments revealed that the CaMBD is responsible for both Ca^{2+}-dependent and Ca^{2+}-independent interactions with calmodulin (CaM). CaM is a small acidic protein ubiquitously expressed in eukaryotic cells, which has four approximately symmetrical E-F hand motifs, two at either end of the protein, that bind Ca^{2+} ions. The E-F hand containing N- and C-terminal lobes are separated by a flexible linker region[53,61]. Therefore, SK channels use CaM as a Ca^{2+} sensor to trigger the channel gating.

The crystal structure of the CaMBD in complex with CaM and in the absence or presence of Ca^{2+} ions showed that in the absence of Ca^{2+}, the CaMBD-CaM complex is monomeric. In contrast, in the presence of Ca^{2+}, the structure becomes a dimer – 2 CaMs and 2 CaMBDs. The components are arranged such that the CaMs bridge the CaMBDs that are themselves antiparallel; each CaM touches each CaMBD but the CaMBDs do not interact with each other. In addition, the N-lobe E-F hands are Ca^{2+} loaded while the C-lobe E-F hands are vacant. Further examination shows that the C-lobe E-F hands are 'warped' – their planar geometry is disrupted due to multiple strong interactions with the CaMBDs, rendering them unable to chelate Ca^{2+} ions[53].

Comparison of Ca^{2+}-bound and -free forms of the complex suggests that Ca^{2+} binding to the CaM N-lobe leads to folding and dimerization of the complex, the ultimate outcome of which are large conformational changes in CaMBD residues 430-440, which is directly attached to the inner S6 pore gating helix, by more than 90° rotation[62]. In consequence, the SK channel changes its conformation from a tetramer

of monomers to a folded dimer of dimers, yielding a mechanical opening of the channel gate[53,62].

Further study of the SK channel and CaM complex by Lee et al. showed that heterologous expression of double charge reversal in SK2, SK2 R464E/K467E, which interrupts the electrostatic interaction with CaM, did not yield detectable surface expression or channel activity in whole cell or inside-out patching recordings, indicating the SK channel surface expression requires constitutive interaction with CaM[63]. However, co-expression of SK2 R464E/K467E with CaM E84R/E87K produced functional channels. Also, co-expression of SK2 R464E/K467E with 'extra' CaM rescued surface expression and transient channel activity right after inside-out patch excision exposed to Ca^{2+}. After channel activity had ceased, it could be reconstituted by application of CaM to the inside face of the patch. Taken together, these results show that constitutive interaction of SK2 with CaM is required for surface expression and Ca^{2+} gating[63].

Subsequent studies by Li et al. showed that the EF hands at the CaM N-lobe, other than binding Ca^{2+} ions for SK channels gating, are also required for stable SK-CaM interaction[64]. They studied two different SK2 splice variants, SK2-a and SK2-b whose primary amino acid sequences are virtually identical with the exception that SK2-b has three addition amino acid residues-A463, R464, and K465-in its CaBMD, which reduces SK2-b channel Ca^{2+} sensitivity. Recent structural analysis showed that the additional three amino acid residues rotate the downstream residues of CaMBD in SK2-b channel subunits by ~ 300°, which effectively changes the relative spatial orientations of the two fragments in CaMBD that interact with CaM, and allows

substantial conformational changes of CaM C-lobe, resulting in the overall reduced Ca^{2+} sensitivity in SK2-b channels[65]. Thus, SK channels use a unique, constitutive interaction with the ubiquitous Ca^{2+} sensor, CaM to drive Ca^{2+} gating.

Proteomics analysis revealed that in addition to the CaM, SK2 and SK3 have additional association with protein kinase CK2 and protein phosphatase 2A (PP2A), that alter Ca^{2+} sensitivity[66,67]. In complex with the SK channels, CK2 does not phosphorylate the channel, but rather phosphorylates CaM at T80, reducing Ca^{2+} sensitivity ~ 3-fold, while PP2A dephosphorylates T80 and increases the Ca^{2+} sensitivity ~ 3-fold. Remarkably, the actions of CK2 and PP2A on SK-bound CaM are strictly state-dependent, representing the only known instance of state dependent ion channels modulation by a protein kinase/phosphatase. CK2 works only when the SK channels are in the closed state, resulting in a reduced Ca^{2+}-sensitivity of the channels. The effect is counterbalanced by PP2A dephosphorylation of the same residue when the channels are open[66,67]. This exquisite state dependence is endowed by the relative conformation of a single lysine residue (K121) in the N-terminal domain of SK2 channels. Therefore, the state dependent CK2 and PP2A modulations endow the SK channels with dynamic Ca^{2+}-sensitivities.

The relevance of CK2/PP2A modulation has been revealed in several studies. In one study, in superior cervical ganglion neurons, instead of decreasing the Ca^{2+} source for SK channels, noradrenaline and somatostatin decrease SK channel activity in a CK2-dependent manner. They reduce the Ca^{2+} sensitivity of channel gating by promoting CK2 phosphorylation of CaM, therefore, reducing the AHP and spike-frequency adaption of the neurons[68]. In hippocampal CA1 pyramidal neurons, activation of M1

muscarinic acetylcholine receptors (mAChRs) increases excitatory postsynaptic potentials (EPSPs) and spine Ca^{2+} transients. However, using 2 photon glutamate uncaging onto single spines on apical dendrites of CA1 neurons, Giessle and Sabatini reported that M1 AChR activation does not work through direct modulation of N-methyl-D-aspartate receptors (NMDARs), but through CK2 to decreases the Ca^{2+} sensitivity of the SK channels, thereby increasing synaptic responses[69]. Interestingly, Buchanan et al. observed the same result of M1 activation decreasing SK channel activity by a theta burst pairing protocol and Shaffer collateral stimulations. However, they found no evidence that this occurs through CK2, but rather involves the protein kinase C modulation of SK[70]. Also, in hypothalamic pre-sympathetic neurons, Pachuau et al. found that CK2 phosphorylation of CaM leads to diminished SK channel function, which is important in regulating the activities of pre-sympathetic neurons involved in hypertension[71]. Thus, CK2/PP2A play important role regulating SK channel activity.

II.2.5. SK channel pharmacology

SK channels are potently and selectively blocked by apamin, a 18-amino-acid peptide derived from the *Apis melllifera* venom[32,33]. Apamin had proved to be extremely valuable as a highly specific blocker for which the only known receptors are the SK channels, with the binding sites of the outer vestibule of the pore[39,40] as well as the S3-S4 extracellular loop[41,42] of the SK channels. Interestingly, the SK channel subtypes present different sensitivity to this toxin, with SK2 channels being the most

sensitive (IC_{50} = 27-140 pM), SK3 channels displaying an intermediate sensitivity to apamin (IC_{50} = 0.6-4.0 nM), and human SK1 channels being the least sensitive (IC_{50} = 0.7-12.0 nM) whereas the rat SK1 is apamin insensitive. IK (SK4) channels are insensitive to apamin, but are blocked by clotrimazole/Tram34 and the scorpion toxin charybdotoxin.

Besides apamin, several scorpion toxins specifically target SK channels. These include tamapin from the *Mesobuthus tamulus*, leiurotoxin-I from scorpion *Leiurus quinquestriatus* and P05 from *Androctonus mauretanicus.* All of these scorpion toxins and apamin contain an RXCQ motif, which is crucial for binding to SK2 channels[72,73]. Tamapin binds with a higher affinity to SK2 than SK3 channels (~70-fold difference), and it binds deep within the pore to cause block by pore occlusion. As with tamapin, leiurotoxin-I binds deep within the channel pore to occlude ion conduction, but it blocks both SK2 and SK3 with lower affinity than tamapin, and with only ~ 5-fold discrimination between channel subtypes[74]. Other less selective compounds such as D-tubocurarine and 2-aminobenzimizoles also block SK channels. The amino acids identified in the outer pore region that influence the sensitivity of SK channels to apamin also affected the sensitivity for D-tubocurarine, indicating that D-tubocurarine is likely to bind to the outer pore region of the channel[39]. Unlike the pore block mechanism of scorpion toxins, the 2-aminobenzimizole is a negative gating modulator that decreases the sensitivity of the channels to Ca^{2+} ions[75].

A number of compounds, on the other hand, act as positive modulators to enhance SK channel activity. These compounds, including 1-Ethyl-2-benzimidazolinone (1-EBIO), 6,7-dichloro-1*H*-indole-2,3-dione 3-oxime (NS309), 4,5-dichloro-1,3-diethyl-1,3-

dihydro-benzoimidazol-2-one (NS4591) and *N*-cyclohexyl-*N*-[2-(3,4-dimethyl-pyrazol-1-yl)-6-methyl-4-pyrimidinamine] (CyPPA), target the association of CaM with CaMBD in SK channels. 1-EBIO was first shown to enhance IK channels in T84 epithelial cells[76]. Subsequently 1-EBIO was demonstrated to interact with the C terminal of SK2 channel subunit, slowing down deactivation of SK2 channels by almost 10-fold with no obvious effects on either activation kinetics or amplitude of SK2 currents in auditory outer hair cells and hippocampal pyramidal cells, therefore, shifting the Ca^{2+} sensitivity of SK2 channels toward lower concentration[77,78]. Application of the more potent NS309 enables recovery of rundown of SK channel activity from mutant CaM, suggesting it acts to stabilize the association of CaM and the SK channel subunit[64]. Similarly, CyPPA was developed with an improved selectivity profile, enhancing the Ca^{2+} sensitivity of SK2 and SK3 but not SK1 and IK channels[79].

II.2.6. SK channel distribution and localization

Over the past few decades, SK channels have been identified and studied in numerous neuronal and non-neuronal issues, such as the central nervous system[28,29,44,45,51,56,77], blood cells[27,30,36], muscle cells[32,34,50], adrenal chromaffin cells[31,59], T-lymphocytes[58], hepatocytes[36] and epithelia cells[76], indicating that SK channels are important for the function of many cell types, and even come with synergic physiological effects from different cell types. For example, in vascular endothelium, the activation of endothelial IK1 or SK3 channels hyperpolarizes endothelial cell membrane potential,

increases Ca^{2+} influx, and lead to the release of vasoactive factors, thereby impacting blood pressure[80]. While in hypothalamic pre-sympathetic neurons, the activation of SK3 channels affects the firing pattern of hypothalamic paraventricular nucleus, which plays an important role in regulating blood pressure[71].

In the mature rat CNS, *in situ* hybridization in accordance with immunohistochemical studies has shown that SK1-3 channel subunits have partially overlapping, but clearly distinct distribution patterns, with SK1 and SK2 showing extensive colocalization, and SK3 having a complementary distribution[44,45,81]. Expression at high levels of all three SK subunits in the same cell types could be detected in only a few brain regions, including the entorhinal cortex and the subiculum, the thalamic anterodorsal nucleus, and ambiguus and facial nuclei. Neurons showing the strongest labeling for both SK1 and SK2 were found in the subiculum, layer V of the neocortex, CA1-3 layers of the hippocampus, gigantocellular reticular nucleus, and facial nucleus. Additionally, labeling for the apamin-insensitive SK1 subunit was highest in the entorhinal cortex, lateral hypothalamic area, lateral mammillary nucleus, zona incerta, nuclei of the solitary tract and of the trapezoid body, and oculomotor, trochlear, parabigeminal, and red nuclei. The highly apamin-sensitive SK2 subunit showed maximal expression also in the hilar region of the hippocampus, tenia tecta, reticular thalamic nucleus, motor trigeminal, pontine, inferior olivary, and lateral reticular nuclei. Labeling for the low apamin-sensitive SK3 subunit was highest in the lateral septal and septohippocampal nuclei, substantia nigra, medial habenula, dorsal and central thalamic nuclei, dorsal raphe nucleus, locus coeruleus, ambiguus and dorsal motor nucleus of the vagus, and Golgi cells in the cerebellum. In addition, using confocal microscopy and SK3 specific antibodies, the SK3 channels are also localized presynaptically in the motor

nerve terminals, though the SK3 immunoreactivity is not found until postnatal day 35, indicating a developmental expression of SK3 channels in the motor neuron terminals[82]. Taken together, these studies suggest that specific SK subunits contribute to neuronal excitability and function in different brain regions.

Within the hippocampus, Stocker et al. showed that all SK1-3 mRNAs are present in the rat hippocampal CA1 to CA3 region, displaying different expression patterns and abundance. In particular, CA1 neurons express high levels of apamin sensitive SK2 transcript, moderate levels of apamin insensitive SK1 and low levels of SK3 subunits[83]. Patch-clamp recordings from transgenic knock-out mice revealed that in CA1 neurons, the amplitude of the apamin-sensitive tail current was not significantly different in mice lacking SK1 or SK3, but was not present in SK2 knock-out mice[84]. These results, taken together with the pharmacological profile of SK channel subtypes, indicate that SK2 channels are required for the SK currents in CA1 pyramidal neurons.

A close look at SK2 channel localization from live-cell immunostaining of a cultured hippocampal CA1 neuron expressing an external epitope tagged SK2 reveals that immunoreactivity was minimally detected in the soma. However, clusters of SK2 immunoreactivity were detected in the dendritic shafts and a recurrent axon[85]. Strikingly, each of the dendritic spines was decorated with SK2 immunoreactivity. Within the spine compartment, immunoelectron microscopy (iEM) for native SK2 demonstrated expression of SK2 in the postsynaptic density (PSD) where SK2 immunoparticles were co-distributed with immunoparticles for NMDARs[86]. The SK2 channel localization in dendrites and dendritic spines suggest an appropriate target for studying the role of SK2 channels in synaptic physiology.

Using iEM to study the temporal and spatial expression of SK2 in the developing mouse hippocampus, Ballesteros-Merino et al. showed that the SK2 protein increases with age, which is accompanied by a shift in subcellular localization[87]. In early development (P5), SK2 was predominantly localized to the endoplasmic reticulum in the pyramidal cell layer. By P30 SK2 was almost exclusively expressed in the dendrites and spines, with an increased expression level at the PSD. In consequence, electrophysiology recording displayed an increased apamin blockage of SK2 channels over time.

II.2.7. SK channel activity and the afterhyperpolarization

The SK channels are activated by a rise in intracellular Ca^{2+} ions, and, in some cells, they integrate Ca^{2+} signals over time to modulate repetitive electrical activity and firing pattern. For example, SK2 channels are found in the heart with a great abundance in the atrial myocytes. The SK2 channel activation contributes to the late phase of the cardiac action potential (repolarization), which is susceptible to aberrant excitation such as early after depolarization and arrhythmias[88,89]. Particularly in some CNS neurons, the resulting outflow of potassium currents from the SK channel activation contributes to the generation of an AHP of medium duration (mAHP) that follows single or bursts of action potentials[78,83]. During single action potentials, transient depolarization of the membrane opens Kv and K_{Ca} channels, the potassium channel mediated outward currents, especially from K_{Ca}, outlast the action potentials and tend to hyperpolarize the cells, consequently generating afterhyperpolarization.

The AHPs that follow a single spike or a spike train can mediate different forms of feedback regulation of excitability, for example, the increased potassium conductance underlies the AHP influences the voltage trajectory between APs, thus setting the cell firing frequency. In addition, repetitive firings result in summation of the AHP that gradually changes firing frequency from high to low or even stops firing in spite of the persistent input, termed spike frequency adaptation, which protects the neurons from the deleterious effects of continuous tetanic activity[2,90]. Consequently, in many different types of neurons such as dopaminergic neurons and cerebellar Purkinje neurons, blocking SK channels with apamin reduces the regularity of firing and promotes the transition towards burst firing[91,92,93,94]. Conversely, enhancing SK channel with 1-EBIO concerts burst firing into regular firing or stabilizes the spontaneous repetitive firing mode[78,91,92,95].

In the well-studied CA1 pyramidal neuron, the AHP may be divided into three overlapping kinetic components: fast (fAHP), medium (mAHP), and slow (sAHP). The fAHP overlaps the falling phase of the AP and contributes to spike repolarization and the initial component of the AHP, which lasts for 10-20 ms and whose underling channels are BK channels[17,18,19]. Following AP and fAHP, the mAHP activates rapidly and lasts from a few tens to a few hundreds of milliseconds[83,84], while sAHP can last for a few seconds[96,97]. Both mAHP and sAHP play a major role in successive slowing of the spike frequency[78,83,98].

Using a somatic whole cell voltage-clamp, depolarizing voltage steps generate an unclamped Ca^{2+} action current. Upon repolarization, the activity of Ca^{2+}-dependent and other voltage dependent K^+ currents are seen as a tail current[99]. The identity of the

underlying channels is determined by kinetic and pharmacological analysis. In doing so, at 50 nM, apamin selectively blocked medium component of AHP current in hippocampal pyramidal neurons that hyperpolarized the membranes away from spike threshold, resulting in repetitive firing[83]. In addition, the apamin-sensitive mAHP current (ImAHP) is absent in hippocampal CA1 neurons from SK2 channel knock-out mice[84]. These finding suggests that activation of SK channels, especially SK2 channels, contributes to the ImAHP in these neurons. The role of SK channels was confirmed by reports that 1-EBIO enhanced the AHP and terminated repetitive firing in hippocampal neurons[78,95]. In accordingly, apamin sensitive ImAHP has been recorded in many different brains areas, including spinal motoneurons, pyramidal neurons in the sensory cortex and so on (for a review, see ref. 99), which is largely in agreement with the widespread distribution of apamin-binding sites and SK channel mRNA[44,100].

When studying the contributions of different channels to the AHP, the recording technique used is an important contributor to date interpretation. In this regard, whether the SK channels determine the mAHP is still controversial. Even by using voltage-clamp recording, Lancaster and Nicoll in 1987, and Storm in 1989 reported that the muscarinic agonist carbachol at 40-50 μM or TEA at 1-10 mM partially reduced mAHP current in CA1 pyramidal neurons, suggesting voltage-dependent I_M, Ca^{2+} and voltage-dependent I_C are components of the mAHP[18,101]. When using a current-clamp recording to measure the AHP following APs, recent work by Gu et al. showed that blocking Kv7 M-channel with XE991 at 10 μM suppressed the mAHP and increased the number of APs and enhanced promoted bursting, while M-channel opener retigabine reduced excitability. In addition, application of H-channel blocker

ZD7288 fully suppressed the mAHP, indicating that M- and H-channels generate the somatic mAHP in hippocampal pyramidal cells, though the tail currents consistently show a pronounced apamin-sensitive component[102,103]. The possible explanation for this discrepancy is that under voltage-clamp condition, the depolarization commend last much longer (>10 ms) than action potentials (1-2 ms) in current-clamp recordings. This difference in depolarization duration can account for an increased Ca^{2+} influx in voltage-clamp experiment. In this context, it is possible that under low-frequency stimulation, M and H channels account for mAHP, while SK becomes relevant under higher frequencies where Ca^{2+} is bigger, or under Ca^{2+} spike. Indeed, most recent report from Chen et al. shows that although the SK channels can generate a mAHP current, they play only an auxiliary role in controlling the intrinsic excitability of pyramidal CA1 neurons, secondary to the M channels, as the SK channel activation significantly reduces spike output only when the M channel activity is compromised[104].

The channels underlying the sAHP have not been molecularly identified. It was originally thought to be a member of the SK family. In the 1980s, there are studies showing that Ca^{2+} dependent, voltage independent potassium channels underlie the sAHP[105], and that the sAHP is resistant to apamin[18,83,101]. Taken together with the fact that rat SK1 is insensitive to apamin, this makes the SK1 channels a prominent candidate for the channels underlying the sAHP. However, results from transgenic mice showed that the sAHP current remains intact in mice that lacking either SK1, SK2 or SK3, while the apamin-sensitive mAHP current was selectively abolished in CA1 pyramidal neurons from SK2 null mice[84]. These findings strongly confirm that SK1 channels are unlikely underlie sAHP.

II.2.8. SK channel and synaptic plasticity, learning and memory

Synaptic plasticity is the ability of synapses to strengthen or weaken depending upon patterns of activity. Historically, it was generally thought that the role of the synapse was to simply transfer information between one neuron and another neuron or a muscle cell, and that the connections were relatively fixed in their strength[1]. Not until the end of 19th century, when Spanish neuroanatomist Santiago Ramón y Cajal first suggested a mechanism of learning based upon the new formation of axonal collaterals and dendrites, and proposed that memories might be formed by strengthening the connections between existing neurons to improve the effectiveness of their communication[106]. In 1949, Donald Hebb introduced Hebbian theory, which describes a basic mechanism for synaptic plasticity, where an increase in synaptic efficacy arises from the presynaptic cell's repeated and persistent stimulation of the postsynaptic cell[107]. Using patch-clamp techniques, around 1970s, Bliss and Lømo conducted recordings in the hippocampal dentate granule neurons of adult cats and rabbits and found that brief repetitive activation of excitatory pathways resulted in a substantial increase in synaptic strength that lasts for many hours, even days[108,109,110]. Since its initial discovery, this synaptic enhancement, called long-term potentiation (LTP), has provided the most compelling model at the cellular level for learning and memory. Today, LTP is defined as an increase in synaptic responses following potentiating pulses of electrical stimuli that sustains at a level above the baseline responses for hours or longer. Conversely, brief activation of an excitatory pathway can also produce a long-term depression (LTD) of synaptic transmission, which is an

activity dependent reduction in the efficacy of neuronal synapses lasting for hours or longer. Both LTP and LTD are forms of long-term synaptic plasticity.

Since Bliss and Lømo's initial description of long-term synaptic enhancement, LTP in the CA1 region of the hippocampus has been the most extensively studied model. Initial efforts focused on the mechanism of the induction of LTP and found that the activation of NMDA receptors, the rise in postsynaptic Ca^{2+} and postsynaptic depolarization are required for LTP induction[111-119]. By taking advantage of pharmacology, Collingridge et al. in 1983 found that blocking NMDARs with D-2-amino-5-phosphonovalerate (APV) completely blocked LTP following tetanic stimulation at CA3-CA1 pathway in rat hippocampus, indicating that NMDAR activity is required for LTP[112]. In the same year, Lynch et al. reported that intracellular injections of the Ca^{2+} chelator EGTA blocked the development of LTP in hippocampus[113]. In 1986, a group of studies showed that injecting depolarizing current into the postsynaptic cell of hippocampal pyramidal neurons substituted for a strong tetanus and was sufficient to cause LTP when paired with a weak input[114,115,116]. In addition, the induction of LTP can be blocked by preventing the depolarization either by voltage clamping the cell or hyperpolarizing the membrane during a strong tetanic stimulation[116,117]. Taken together with the findings that NMDARs exhibit a voltage-dependent block by physiological levels of extracellular magnesium[180,181] and that NMDARs are permeable to Ca^{2+} ions[182,183], all of these studies suggest a NMDAR-dependent LTP mechanism in which Ca^{2+} influx through NMDARs depolarizes cells, increased intracellular Ca^{2+} leads to induction of LTP[111,118]. In 1992, NMDAR-dependent LTD was discovered in the hippocampus as well[119].

Subsequent studies revealed that the dynamic of α-amino-3-hydroxy-5-methyl-4-isoxazolepropionic acid receptors (AMPARs) also plays an important role in LTP and LTD. In 1995, Issac and Liao et al. first described silent synapses in hippocampal CA1 cells that express NMDARs but not AMPARs acquired AMPA-type responses following LTP, indicating that LTP may involve modification of AMPARs[120,121]. By expressing GFP-tagged receptors in organotypic hippocampal slices, Shi et al. in 1999 visualized that the AMPAR was recruited to synaptic spines after LTP induction and this recruitment paralleled synaptic strengthening[122]. Using single particle tracking techniques, Borgdorff et al. found that AMPARs were present in both PSD and extrasynaptic membranes, where they moved from extrasynaptic membrane into PSD after LTP induction[123]. These results show that AMPARs are dynamically trafficking and undergoing exocytosis and lateral diffusion during synaptic plasticity, which effectively increases the depolarizing drive upon excitatory synaptic transmission[124].

SK2 channels are expressed in the PSD of dendritic spines on CA1 pyramidal neurons and play important roles in synaptic physiology. In 2005, Ngo-Anh et al. showed that spine SK2-containing channels are activated by synaptically evoked Ca^{2+} influx that required NMDAR activity, and the SK-mediated repolarization activity provides a local shunting current to reduce the EPSP and promote rapid Mg^{2+} block of NMDARs, limiting the spine Ca^{2+} transient[85]. Thus, blocking synaptic SK2-containing channels with the highly selective blocker, apamin, boosts EPSPs and the spine Ca^{2+} transient by as much as 50%[85]. In the same year, Faber et al. reported the similar feedback loop in lateral amygdala pyramidal neurons[125]. Consistent with this, synaptic SK2 channel activity modulates the *induction* of synaptic plasticity. The first study that directly

linked SK channel activity to synaptic plasticity was reported by Behnisch and Reymann in 1998, in which blocking SK channels with apamin intensified LTP that was induced by a single 100 Hz tetanus in the CA1 region of rat hippocampal slices[126]. Later, Stackman et al. measured the frequency-response relationship for the induction of synaptic plasticity in area CA1. The results showed that apamin application shifted the modification threshold to reduced conditioning frequencies; therefore, apamin facilitated the induction of plasticity[127]. The role of SK2-containing channels was further substantiated by transgenic over-expression of SK2 or pharmacologically increasing SK2-containing channel activity; both manipulations impaired the induction of synaptic plasticity[128]. In addition to influencing induction, synaptic SK2-containing channel trafficking contributes to the *expression* of LTP. At Schaffer collateral-CA1 synapses, Lin et al. revealed that SK2-containing channel activity was abolished after LTP induction, and showed that this is due to SK2 internalization from the PSD into the spine, a process that requires a protein kinase A (PKA)[86]. Using a combination of electrophysiology and immunoelectron microscopy, Lin et al. later reported that LTP dependent endocytosis of SK2 is coupled with AMPAR exocytosis[129], suggesting that the increase in AMPARs and the decrease in SK2 channels combine to produce the increased EPSP, therefore engendering the expression of LTP.

Apamin crosses the blood-brain barrier; thus, it has been used in behavioral studies to investigate the role of SK channels in cognitive functions. Systemic apamin administration facilitates some forms of learning and improves the memory performance of mice and rats. The first such study, conducted by Messier et al., reported that systemic apamin injection accelerated the acquisition of a bar pressing

response in mice that was motivated by appetite[130]. In rats, apamin administration improved learning in an object-recognition task and the acquisition of information in a habituation task[131,132]. Consistently, apamin treated mice exhibit faster learning of the platform location during the initial training trials in the Morris water maze, suggesting blockage of SK channels facilitates an early stage of hippocampus dependent spatial memory encoding[127]. In contrast, SK2 overexpression mice cannot learn the platform location, and exhibit significantly less context dependent freezing[127,133]. Moreover, Blank et al. reported that the expression of SK3 increases with age in the hippocampal formation, thereby contributing to an age-related reduction in hippocampal LTP and impaired trace fear conditioning in older mice[134]. Thus, the expression of SK channels in the PSD is centrally important to normal neurotransmission, synaptic plasticity and memory encoding.

In summary, SK channels are multiprotein complexes of 7 transmembrane pore-forming subunits in complex with CaM which mediates Ca^{2+} gating, CK2 and PP2A, which modulate the Ca^{2+} sensitivity of the SK channels. SK channels are widely expressed in the brain, and in may principal neurons, SK channels are expressed in the postsynaptic membrane, where they modulate synaptic responses, influence the induction of synaptic plasticity, and affect learning. The study of the Ca^{2+} source for activating SK channels and how their activity contributes to synaptic plasticity in CA1 pyramidal neurons is of great interest in my thesis project.

SPECIFIC AIMS

***Aim 1**: Studying the role of SK2-L in synaptic plasticity in CA1 pyramidal neurons.*

The SK2 gene uses two promoters to encode two SK2 isoforms that differ only in the length of the intracellular N-terminal domain, with a long form (SK2-L) having an extra 207 amino acids at the N terminus than a short form (SK-S)[56]. The two isoforms are expressed in many of the same brain regions, including hippocampus[56]. When heterologously expressed separately, functional homomeric SK2-L channels and homomeric SK2-S channels yield similar Ca^{2+} sensitivity and amplitudes of whole-cell currents, but differ in currents from excised patches[56]. Preliminary results from the laboratory show that: 1. SK2-L directs the subcellular localization of synaptic SK2-containing channels and is important for normal synaptic signaling. 2. In transgenic mice that selectively lack SK2-L (SK2-S only mice), SK2-S-containing channels are expressed in the extrasynaptic spine plasma membrane, but are excluded from the PSD on CA1 pyramidal neurons. 3. The SK2 channel contribution to EPSP is abolished in SK2-S only mice and could be restored by SK2-L re-expression.

The SK2 channel expression in the PSD is important in synaptic plasticity, field potential recording in area CA1 in wild-type mice have shown that blocking SK channels facilitates the induction of synaptic plasticity[127]. To investigate the roles of SK2-L in synaptic plasticity in CA1 pyramidal neurons, we used SK2-S only mice to study the LTP induced in area CA1 in slices. We find that blocking SK channels with apamin increases LTP in wild-type mice but has no effect in SK2-S only mice. Therefore, SK2-L expression is important for normal synaptic plasticity.

***Aim 2**: Studying the Ca^{2+} source for SK channel activity in dendritic spines of CA1 pyramidal neurons.*

Ca^{2+} is a ubiquitous second messenger and the activation of Ca^{2+}-dependent ion channels is perhaps the most rapid response to discrete elevations of cytosolic Ca^{2+}. The SK channels are prime examples, being gated solely by intracellular Ca^{2+} ions with an EC_{50} of ~0.5μM. In spines of CA1 pyramidal neurons in hippocampus, synaptic stimulation activates synaptic SK2 channels and Ca^{2+} influx through NMDARs opens SK2 channels, which serve as an intrinsic feedback mechanism to limit NMDAR-dependent Ca^{2+} transients[85]. One central piece of evidence was that blocking NMDARs occluded the apamin effect on boosting the EPSP and Ca^{2+} transient. Subsequent work using 2-photon laser photoactivation of caged glutamate onto single spines showed that Ca^{2+} influx through SNX-sensitive R-type Ca^{2+} channels, which are activated secondary to NMDARs, opens SK2 channels[135,136]. Blocking R-type Ca^{2+} channels with SNX-482 occludes the apamin effect on boosting glutamate uncaging-evoked EPSP[135]. However, dialyzing CA1 pyramidal neurons with the fast Ca^{2+} buffer 1,2-bis(o-aminophenoxy)ethane-N'N'N'-tetraacetic acid (BAPTA) but not the slow buffer EGTA occluded the apamin effect on the EPSP, suggesting the SK2 channels and their Ca^{2+} source reside within 25-50 nm[85]. Immunoelectron microscopy (iEM) demonstrated expression of SK2 in the PSD where SK2 immunoparticles were codistributed with immunoparticles for NMDARs[86], whereas R-type Ca^{2+} channels are predominantly localized in extrasynaptic areas[137], indicating that synaptic SK2 channels and NMDARs are in close anatomical proximity. Here we tested whether SNX occludes synaptically evoked activation of apamin sensitive SK channels in spines. We find that synaptic stimulations reveal the

presence of two Ca^{2+} signaling pathways within the spine head, one that couples NMDARs with apamin-sensitive SK channels and another that couples SNX-sensitive R-type Ca^{2+} channels with 4-AP-sensitive $K_v4.2$ containing channels.

III.

The SK2-long Isoform Directs Synaptic Localization and Function of SK2-containing Channels

Allen D, Bond CT, Luján R, Ballesteros-Merino C, Lin MT, Wang K, Klett N, Watanabe M,

Shigemoto R, Stackman RW Jr, Maylie J, Adelman JP.

Nat Neurosci. 2011 Jun;14(6):744-9.

Contributions

D.A., M.T.L., K.W. and N.K. performed the electrophysiology. C.T.B. performed molecular biology and biochemistry. R.L., C.B.-M. and R.S. were responsible for iEM. M.W. provided the antibodies. R.W.S. was responsible for the behavioral testing. J.P.A. and J.M. wrote the manuscript.

K.W. performed the field EPSP recordings in figure 6 to study the effect of SK2 channel activity on LTP in WT and SK2-Short only mice.

ABSTRACT

SK2-containing channels are expressed in the postsynaptic density (PSD) of dendritic spines on mouse hippocampal area CA1 pyramidal neurons and influence synaptic responses, plasticity and learning. The *Sk2* gene (also known as *Kcnn2*) encodes two isoforms that differ only in the length of their N-terminal domains. SK2-long (SK2-L) and SK2-short (SK2-S) are coexpressed in CA1 pyramidal neurons and likely form heteromeric channels. In mice lacking SK2-L (SK2-S only mice), SK2-S–containing channels were expressed in the extrasynaptic membrane, but were excluded from the PSD. The SK channel contribution to excitatory postsynaptic potentials was absent in SK2-S only mice and was restored by SK2-L re-expression. Blocking SK channels increased the amount of long-term potentiation induced in area CA1 in slices from wild-type mice but had no effect in slices from SK2-S only mice. Furthermore, SK2-S only mice outperformed wild-type mice in the novel object recognition task. These results indicate that SK2-L directs synaptic SK2-containing channel expression and is important for normal synaptic signaling, plasticity and learning.

INTRODUCTION

Dendritic spines are specialized compartments that form the post- synaptic sites for excitatory neurotransmission. There are at least two anatomical and functional subdomains in the spine, the extra- synaptic membrane and the PSD, both of which contain AMPARs and NMDARs[1,2]. Proper and dynamic partitioning of AMPARs and NMDARs between the synaptic and extrasynaptic membranes is essen- tial for normal neurotransmission[3–5], and at many synapses, such as the Schaffer collateral to CA1 synapses in the hippocampus, changes in the number and subunit composition of AMPARs and NMDARs in the PSD contribute to the expression of synaptic plasticity[6–9].

SK channels are activated solely by intracellular Ca^{2+} ions and are selectively blocked by apamin[10]. SK2-containing channels are expressed in the PSD of dendritic spines on CA1 pyramidal neurons[11]. Spine SK2-containing channels are activated by synaptically driven Ca^{2+} influx and provide a repolarization that reduces the excitatory postsynaptic potential (EPSP), favoring Mg^{2+} re-block of NMDARs and reducing the spine Ca^{2+} transient that is crucial to the induction of synaptic plasticity[11–13]. Indeed, field potential recordings in area CA1 have shown that blocking SK channels facilitates the induction of synaptic plasticity, and administration of apamin to mice facilitates hippocampus-dependent memory encoding[14]. Moreover, transgenic overexpression of SK2 impairs the induction of synaptic plasticity and severely impairs hippocampus-dependent memory

encoding[15,16]. Similarly, administration of the SK channel agonist *N*-cyclohexyl-*N*-2-(3,5-dimethyl-pyrazol-1-yl)- 6-methyl-4-pyrimidinamine (CyPPA) impairs the encoding of hippocampus-dependent object memory[17]. In addition, protein kinase A-dependent endocytosis of synaptic SK2 contributes to the expression of long-term potentiation (LTP)[11,18]. Thus, the expression of SK2-containing channels in the PSD is important for synaptic signaling, plasticity and learning.

The *Sk2* gene directs expression of two isoforms that differ only in the length of the intracellular N-terminal domain, with SK2-L having an extra 207 amino acids at the N terminus. The two isoforms are expressed in many of the same brain regions, including hippocampus. SK2-L and SK2-S co-immunoprecipitate from brain and when coexpressed heterologously, suggesting that they co-assemble into hetero- meric channels[19]. When expressed separately, SK2-S and SK2-L form functional homomeric SK channels with similar Ca^{2+} sensitivities. Notably, homomeric SK2-S channels and homomeric SK2-L channels yield whole-cell currents of similar amplitudes, but SK2-L currents in excised patches are much smaller than SK2-S currents. The inconsistency between whole-cell and patch-current amplitudes for SK2-L reflects the markedly punctate surface expression of SK2-L compared with the more uniform expression of SK2-S[19]. These results suggest that SK2-L may be involved in the subcellular localization of native SK2-containing channels. To investigate the roles of SK2-L in CA1 pyramidal neurons, we engineered mice that selectively lack the SK2-L isoform.

RESULTS

SK2 expression in the PSD of CA1 neurons requires SK2-L

SK2-L is expressed in the dendrites in the stratum radiatum[19]. To determine the subcellular distribution of SK2-L, we carried out immunogold electron microscopy (iEM) on hippocampal sections with an antibody directed against an epitope in the unique intracellular N-terminal domain (**Supplementary Fig. 1**). We used pre-embedding immunogold labeling to examine the extrasynaptic localization of SK2-L and found that SK2-L was expressed in the plasma membrane of dendritic shafts and spines (**Fig. 1a**). Post-embedding immunogold labeling, to detect synaptic expression, revealed that SK2-L was expressed in the PSD (**Fig. 1b**). From 50 spines with a total of 133 gold particles, 29% (38) were in the extrasynaptic spine membrane and 71% (95) were in the PSD. This result was verified using double immunogold labeling SDS-digested freeze-fracture replica (SDS-FRL) iEM for SK2-L, together with PSD-95 to delineate the synaptic membrane. SDS-FRL visualizes the two-dimensional distribution of membrane proteins with resolution and sensitivity beyond thin-section electron microscopy. The SK2-L antibody is directed against an intracellular epitope and SK2-L was detected at the protoplasmic face of the spine plasma membrane, consistent with the results of pre- and post-embedding experiments. Double immunolabeling for SK2-L and PSD-95 revealed co-clustering of the immunoparticles in spines, indicating that SK2-L was expressed in the membrane at the PSD (**Fig. 1c**).

To investigate the physiological roles of the SK2-L isoform, we generated transgenic mice that selectively lack SK2-L expression. We have previously reported two

different SK2 transgenic alleles. One is a *cre-loxP* conditional allele (**Fig. 2a**) that was used to make *Sk2*$^{-/-}$ mice[20]. The other allele contains a tetracycline-regulated gene switch[21] that was inserted in a position 5′ to the translational initiator codon for SK2-S, but in the extended N-terminal coding sequence for SK2-L (*T* allele; **Fig. 2b**)[15]. To obtain mice selectively lacking SK2-L expression, we crossed *Sk2*$^{+/T}$ and *Sk2*$^{-/+}$ mice and identified *Sk2*$^{-/T}$ (SK2-S only) mice. In SK2-S only mice, the SK2 isoforms are not expressed from the null allele, SK2-L is not expressed from the *T* allele and SK2-S is overexpressed from the *T* allele[15]. Western blot analysis of brain proteins confirmed that SK2-S only mice lacked expression of SK2-L, whereas expression of SK2-S was increased fourfold (**Fig. 2c** and **Supplementary Fig. 2**).

To determine the distribution of SK2 in spines in the presence and absence of SK2-L, we carried out post-embedding iEM with a pan-SK2 antibody directed to the intracellular C-terminal domain[11]. In wild-type spines, SK2 was expressed in the extrasynaptic and synaptic membranes. From 71 spines with a total of 278 gold particles, 47% (130) were extrasynaptic and 53% (140) were at the PSD (**Fig. 3a**). In contrast, in SK2-S only mice, SK2-S was expressed in the extrasynaptic plasma membrane of dendritic spines, but was virtually absent from the PSD. From 82 spines with a total of 167 gold particles for SK2-S, 98% (164) were in the extrasynaptic spine membrane, whereas only 2% (3) of the gold particles were present at the PSD (**Fig. 3b**).

These results were confirmed and extended using SDS-FRL iEM. In contrast with the intermingled gold particles for PSD-95 and SK2-L (**Fig. 1c**) or PSD-95 and pan–SK2-

S (**Fig. 3c**) in wild-type spines, replicas from SK2-S only mice that were double-labeled for PSD-95 and for SK2 showed a segregation of the two populations of immunoparticles (**Fig. 3d**). The SDS-FRL results were quantified by measuring the distance from each SK2 gold particle to the nearest PSD-95 gold particle (**Fig. 3e**). Thus, in the absence of SK2-L expression, SK2-S–containing channels were excluded from the PSD.

Synaptic SK2-containing channel function requires SK2-L

These results suggest that SK2 synaptic function would be lost in the absence of SK2-L expression. To first determine whether SK2-S–containing channels are functionally expressed in the absence of SK2-L, we used somatic step depolarizations in whole-cell voltage clamp that activate an apamin-sensitive SK current in wild-type CA1 pyramidal neurons[14,20,22]. Following a depolarizing step to 20 mV to elicit an unclamped Ca^{2+} current, repolarizing the membrane to –55 mV evoked tail currents that were partially reduced by apamin (100 nM). Subtracting the traces recorded before and after apamin application yielded an apamin-sensitive current, I_{SK} (**Fig. 4a**). The apamin-sensitive tail current measured 100 ms after repolarization in SK2-S only mice (357 ± 127 pA, n = 7) was larger than the apamin-sensitive current recorded from wild-type littermates (95 ± 15 pA, n = 21, $P < 0.05$), reflecting SK2-S overexpression from the *T* allele in SK2-S only mice. To determine whether expression of SK2-L contributes further to the SK tail current, SK2-L was re-expressed in area CA1 of SK2-S only mice by transcranial delivery of a recombinant

adeno-associated virus (rAAV) directing separate expression of SK2-L and GFP (**Fig. 4b**). Apamin-sensitive tail currents were recorded from SK2-S only nonfluorescent cells or fluorescent cells as well as CA1 pyramidal neurons from wild-type littermates. The apamin-sensitive current was larger for SK2-S only injected cells, fluorescent or nonfluorescent, than for wild type ($P < 0.05$), reflecting SK2-S overexpression. However, the apamin-sensitive tail currents were not different than those from SK2-S only non-injected cells and were not different between SK2-S only fluorescent and nonfluorescent cells (nonfluorescent, 293 ± 106 pA, $n = 10$; fluorescent, 300 ± 68 pA, $n = 11$; **Fig. 4c**). Thus, re-expression of SK2-L in SK2-S only mice did not increase SK channel tail current amplitudes. These data are consistent with the previous finding that SK2 expression is necessary for the apamin-sensitive tail current in CA1 pyramidal neurons[20] and indicate that SK2-S–containing channels were sufficient for its expression.

To determine whether SK2 synaptic function is lost in the absence of SK2-L expression, we recorded synaptically evoked EPSPs from CA1 pyramidal neurons, before and after apamin application in brain slices prepared from rAAV-injected SK2-S only mice or wild-type littermates. EPSPs were evoked every 30 s by stimulation of Schaffer collateral axons. Following 10 min of stable baseline recordings, apamin (100 nM) was added and the EPSP amplitude was measured 18–20 min later. Apamin increased EPSPs in CA1 pyramidal neurons from wild-type mice by 58 ± 12% ($n = 8$), as previously reported[12]. In contrast, apamin did not affect EPSPs recorded from SK2-S only nonfluorescent CA1 pyramidal neurons (5 ± 6%, $n = 10$; **Fig. 5a**,**b**). However, apamin increased EPSPs from SK2-S only fluorescent CA1 pyramidal neurons to the

same extent as in wild-type CA1 pyramidal neurons (44 ± 14%, n = 10; **Fig. 5a**,**b**). These results indicate that SK2-L is necessary for SK channel synaptic function in CA1 pyramidal neurons.

SK channel activity does not affect LTP in SK2-S only mice

Apamin application to brain slices from wild-type mice facilitates the induction of synaptic plasticity in area CA1 in response to conditioning stimulations of the Schaffer collateral axons[14]. To determine whether apamin altered LTP in the absence of synaptic SK2-containing channels, theta-burst stimulation (TBS) was delivered to the Schaffer collateral axons with or without apamin application (100 nM) in hippocampal slices prepared from wild-type and SK2-S only mice.

For wild-type slices in control bath solution, TBS induced LTP, increasing the slope of the field EPSP (fEPSP) by 34 ± 4% (n = 12, P < 0.05). For wild-type slices in apamin, TBS-induced LTP was enhanced, increasing the fEPSP slope by 59 ± 4% (n = 7, P < 0.05; **Fig. 6a**). In SK2-S only slices, TBS also induced LTP to the same extent as in wild-type slices, increasing the fEPSP by 40 ± 3% (n = 8), but this was not different than the LTP induced in the presence of apamin (47 ± 3%, n = 7; **Fig. 6b**,**c**). Thus, the effects of apamin on LTP seen in wild-type mice are absent in SK2-S only mice.

Altered memory encoding in SK2-S only mice

Systemic apamin administration facilitates the encoding of object memory[14]. To test whether this is a consequence of blocking synaptic SK2-containing channels, we examined novel object recognition memory in a naive cohort of SK2-S only and wild-type littermate mice. The mice (n = 13 mice per group) were habituated to a novel high-walled arena for 10 min d^{-1} during day 1 and 2. Locomotor responding declined over the course of habituation in both groups. However, the SK2-S only mice exhibited higher levels of locomotor behavior. There was an effect of genotype on distance measures ($P < 0.001$) and a significant genotype × minutes interaction ($P < 0.009$; **Supplementary Fig. 3**). On day 3, each mouse was returned to the arena, which contained two identical novel objects (the sample session). Mice were removed from the arena after achieving 19 s of sample object exploration[14]. Wild-type and SK2-S only mice exhibited equivalent latencies to reach criterion, indicating no difference in the motivation to explore objects during the sample session (**Supplementary Fig. 4**). For the test session (day 4), each mouse was returned to the arena, which contained one familiar object and one novel object. The SK2-S only mice exhibited a significantly greater preference for exploring the novel object during the test session than the wild-type mice ($P < 0.005$; **Supplementary Fig. 4**). These data indicate that the absence of synaptic SK2-containing channels was associated with a robust enhancement of nonspatial memory. This is similar to the effects of systemic apamin administration in wild-type mice[14].

The same cohorts of mice received 24 training trials (4 per day) in the hidden platform Morris water-maze task. One SK2-S only mouse died before the start of water-maze training. Over the course of training, SK2-S only mice (n = 12) exhibited

poor spatial performance compared with wild-type mice (n = 13; **Fig. 7a**). The slopes of the acquisition curves were similar for wild-type and SK2-S only mice, indicating that spatial learning occurred at similar rates. However, the SK2-S only mice had longer latencies to find the submerged platform; there was an effect of genotype ($P <$ 0.002) and a genotype × trial block interaction ($P < 0.005$). SK2-S only mice also displayed poor retention of the platform location during 30-s platform-less probe tests imposed after the 4th, 12th and 20th training trials ($P < 0.003$; **Fig. 7b**). The paths taken during the probe test after the 20th training trial indicate that wild-type mice (**Fig. 7c**) were arriving at the platform location by a direct path from the release point and provide evidence of constrained search in the appropriate location of the maze. The paths taken by SK2-S only mice (**Fig. 7c**) were more circuitous and there was little evidence of appropriate search behavior. The mean percent dwell in the training quadrant during the last probe test for the wild-type and SK2-S only groups were 34.8 ± 2.8% and 22.4 ± 3.9%, respectively ($P < 0.05$). The wild-type and SK2-S only mice exhibited essentially equivalent learning in the visible platform version of the water maze. There was an effect of genotype on distance measures ($P < 0.001$), but a nonsignificant genotype × trial block interaction, ($P > 0.05$; **Supplementary Fig. 5**), suggesting that genotypic differences in sensorimotor function fail to explain the difference in spatial memory in the hidden platform task. The behavior of the SK2-S only mice in the Morris water-maze task was distinct from wild-type mice. The SK2-S only mice did not develop a spatial bias in their search for the platform and would often swim over the platform or fail to remain on the platform after finding it. Thus, the impairment in this task may reflect motivational or attention deficits that influence performance in the Morris water maze. These data indicate that the absence of SK2-L

was associated with an impairment of spatial learning and memory in the Morris water maze.

DISCUSSION

Our results indicate that the SK2-L isoform directs synaptic localization of SK2-containing channels that is necessary for their synaptic functions, including modulation of EPSPs and synaptic plasticity. Consistent with these synaptic roles, the SK2-L isoform was required for normal hippocampus-dependent learning. In the absence of SK2-L, SK2-S–containing channels were expressed on the extrasynaptic plasma membrane of dendritic spines, but they were selectively excluded from the PSD.

Northern blot analysis for SK2 mRNA detects a doublet of 2.2 and 2.4 kb[10]. However, these mRNA sizes are not sufficient to encode SK2-L, suggesting that SK2-S and SK2-L are translated from different mRNAs and that the SK2-L mRNA is in low steady-state abundance and may be rapidly turned over. The SK2-S mRNA cap site (data not shown) and the SK2-S promoter[23] are located in the SK2-L transcript. Mapping the 5′ untranslated sequences in the SK2-L mRNA onto the *Sk2* gene revealed that the promoter responsible for expression of the SK2-L mRNA must reside ~300-kb pairs 5′ of the promoter for SK2-S mRNA[23]. Thus, it appears that the SK2-L and SK2-S mRNAs are transcribed from independent promoters (**Fig. 2**). Indeed, 50–60% of human and mouse genes may use alternative promoters[24] that often result in expression of distinct protein isoforms. The SK2-L transcript is conserved between mouse and human and a cDNA from human hippocampus encoding the extended amino terminus of SK2-L has been identified (human EST DB636479.1), suggesting that the two SK2 isoforms, the molecular mechanisms that generate them, and their roles in synaptic localization and function, are conserved.

In mice lacking SK2-L, synaptic SK2-S–containing channels were absent. This could mean that, in wild-type CA1 pyramidal neurons, synaptic SK2-containing channels are homomeric assemblies of SK2-L. Using the SK2-L antibody, we found that SK2-L was expressed in the PSD of wild-type CA1 pyramidal neurons, but given that the SK2-S amino acid sequence is completely contained in SK2-L, we could not generate an SK2-S–specific antibody to independently examine SK2-S for synaptic expression. However, SK2-L and SK2-S subunits co-immunoprecipitate from brain, strongly suggesting that they form heteromeric channels[19]. In *SK2*$^{+/T}$ mice that overexpress SK2-S in the presence of SK2-L, apamin increases EPSPs more than in wild-type mice[15], suggesting that the excess SK2-S subunits contribute to synaptic SK2-containing channels. Thus, it is likely that synaptic SK2-containing channels are heteromeric assemblies of SK2-L and SK2-S subunits and that at least one SK2-L subunit is required for synaptic expression. Whether SK2-L is sufficient for synaptic expression and function awaits experiments in mice that express only SK2-L. The SK1 and SK3 mRNAs are also expressed in CA1 pyramidal neurons[25] and SK3 co-immunoprecipitates with SK2-L from brain[19]. The SK3 N-terminal domain is similar in length to SK2-L and contains several regions of homology. The functions of SK1 and SK3 in CA1 pyramidal neurons remain unknown. However, the lack of apamin sensitivity to EPSPs in SK2-S only CA1 pyramidal neurons suggests that SK2-L is necessary for synaptic function and that SK3 cannot substitute for SK2-L.

Recordings from CA1 pyramidal neurons revealed that, in the absence of SK2-L, synaptic SK channel activity was absent, but was re-instated by re-expression of SK2-L. However, SK2-L re-expression did not increase the amplitude of apamin-sensitive

tail currents in SK2-S only CA1 pyramidal neurons, suggesting that SK2-L may not increase surface expression *per se*, but may direct selective synaptic localization. Furthermore, in response to TBS, apamin increased LTP in brain slices from wild-type mice, but not SK2-S only mice, suggesting that blocking synaptic SK channel activity with apamin is responsible for the increased LTP. Notably, the amount of LTP induced in slices from SK2-S only mice was not significantly different from the LTP induced in wild-type slices in the absence of apamin ($P = 0.3$). This may reflect the overexpression of nonsynaptic SK2-S or compensatory changes in the SK2-S only mice.

Synaptic localization of SK2-containing channels is important for normal synaptic responses[12]. In contrast with glutamate receptors, SK2 does not contain a postsynaptic density protein, *Drosophila* disc large tumor suppressor or zonula occludens-1 protein (PDZ) ligand and must therefore employ a distinct molecular strategy for synaptic local- ization. Recent results have shown that a Ca^{2+}-calmodulin kinase II phosphorylation site in the first intracellular loop of the GluA1 subunit is critical for receptor targeting to synapses, but not for delivery of GluA1-containing AMPARs to the plasma membrane[26]. This PDZ-independent effect on trafficking of GluA1-containing AMPARs selectively to the synaptic membrane is similar to the synaptic localization endowed by the SK2-L subunit.

Previous studies have shown that SK channel activity affects learning and memory[14-16]. In the nonspatial object recognition task, the SK2-S only mice phenocopied wild-type mice treated with apamin, showing improved memory encoding. This indicates that SK2-L expression was required for normal performance in the object recognition

task and suggests that apamin and SK2-L deficiency both mediate their effects on object recognition through the loss of synaptic SK2-containing channel function. In contrast, SK2-S only mice were impaired in the spatial-learning Morris water-maze task, whereas apamin administration facilitated this task[14]. This might reflect compensatory alterations that are not observed with acute channel block by apamin. The Morris water-maze task requires several trials presented over several days and it is possible that experience-dependent endocytosis and subsequent repopulation of synaptic SK2-containing channels are necessary for normal acquisition of the Morris water-maze task. Notably, transgenic SK2 overexpression also results in impaired performance in the Morris water-maze task[15], and in both of these transgenic models, there are increased apamin-sensitive tail currents that might, in part, reflect dendritic SK2-containing channel activity. These channels may alter synaptic integration and could contribute to the deficits in water-maze performance. Taken together, the anatomical, electrophysiological and behavioral results from both tasks indicate that SK2-L expression is essential for normal synaptic responses, plasticity and learning.

MATERIAL AND METHODS

Animal care. All procedures were performed in accordance with the guidelines of the Oregon Health and Science University, the University of Castilla-La Mancha, and Florida Atlantic University, and the Animal Care and Use Committees of the respective institutions approved all of the experimental procedures.

Antibodies. Two affinity-purified polyclonal antibodies to SK2 were raised in rabbit and guinea pig, respectively. The specificity of the guinea pig pan-SK2 antibody has been previously described[11]. The mouse monoclonal antibody to PSD-95 was obtained from Abcam.

iEM. Immunohistochemical reactions for pre- and post-embedding electron microscopy were performed as previously described[27]. Ultrastructural analyses were performed in a Jeol-1010 electron microscope.

Pre-embedding immunogold. Briefly, free-floating sections were incubated in 10% normal goat serum (NGS, vol/vol) diluted in Tris-buffered saline for 1 h at 22 °C Sections were then incubated for 48 h with pan SK2 or SK2-L antibodies (1–2 μg ml^{-1}) diluted in 1% NGS/Tris-buffered saline. After washes in Tris- buffered saline, sections were incubated for 3 h in goat antibody to rabbit IgG or goat antibody to guinea pig IgG coupled to colloidal gold particles (Nanoprobes) diluted 1:100 in 1% NGS/Tris-buffered saline. After washes in phosphate-buffered saline (PBS), the sections were postfixed in 1% glutaraldehyde (vol/vol) diluted in the same buffer for 10 min, washed in double-distilled water, followed by silver enhancement of the gold particles with a HQ Silver kit (Nanoprobes). Sections were then treated with osmium

tetraoxide (1% in 0.1 M phosphate buffer, vol/vol), block-stained with uranyl acetate, dehydrated in graded series of ethanol and flat-embedded on glass slides in Durcupan (Fluka) resin. Regions of interest were cut at 70–90 nm on an ultramicrotome (Reichert Ultracut E) and collected on 200-mesh nickel grids. Staining was performed on drops of 1% aqueous uranyl acetate (wt/vol) followed by Reynolds' lead citrate.

Post-embedding immunogold. Ultrathin sections 80 nm thick from Lowicryl-embedded blocks of hippocampus were picked up on coated nickel grids and incubated for 45 min on drops of a blocking solution consisting of 2% human serum albumin (HSA, wt/vol) in 0.05 M Tris-buffered saline and 0.03% Triton X-100 (TBST, wt/vol). The grids were incubated with pan-SK2 or SK2-L antibodies (10 μg ml^{-1}) in TBST with 2% HSA at 28 °C overnight. After washing, the grids were incubated for 3 h on drops of goat antibody to guinea pig IgG or goat antibody to guinea pig IgG conjugated to colloidal gold particles (Nanoprobes) diluted 1:80 in 2% HSA and 0.5% polyethylene glycol in TBST. The grids were then washed in Tris-buffered saline for 30 min and counterstained for electron microscopy with saturated aqueous uranyl acetate followed by lead citrate.

SDS-FRl. SDS-FRL was performed as described previously[28] with some modifications. Animals were anesthetized with sodium pentobarbital and killed by transcardiac perfusion with formaldehyde (0.5%, wt/vol, freshly depolymerized from paraformaldehyde) in 0.1 M sodium phosphate buffer. After perfusion, brains were removed. The hippocampi were cut into 120-μm-thick sections using a Microslicer (Dosaka) and cryoprotected with 32% glycerol (vol/vol) in PBS for 12–16 h. The sections were then frozen by a high-pressure freezing machine (HPM 010, Bal-Tec)

and fractured by the double replica method in a freeze etching system (BAF 060, Bal-Tec). The fractured faces were replicated by carbon (5 nm) with an electron beam gun from overhead and shadowed by platinum/carbon positioned at a 25° angle with rotating (2.5 nm) or at a 45° angle (2 nm) unidirectionally, followed by carbon (20 nm) applied from overhead. We applied 5 nm of carbon before platinum to increase the detection efficiency. The pieces of replica were transferred to 2.5% SDS (vol/vol) containing 62.5 mM Tris and 10% glycerol, pH 6.8. SDS treatment was performed for 15 min at 105 °C with autoclaving, 16 h at 80 °C with shaking, or 16 h at 30 °C with vigorous stirring. After the treatment with SDS, replicas were washed with three times with 0.1% bovine serum albumin (BSA, wt/vol) in Tris-buffered saline, blocked for 1 h, and washed twice with 5% BSA/Tris-buffered saline. The replicas were then reacted with a mixture of pan-SK2 or SK2-L antibody and monoclonal antibody for PSD-95 at 22 °C for 1 h, followed by 4 °C for 36–48 h. Following three washes with 0.1% BSA in Tris-buffered saline and blocking in 5% BSA/Tris-buffered saline, replicas were incubated in a mixture of secondary antibodies (goat antibody to guinea pig IgG and goat antibody to mouse IgG coupled to gold particles; British Biocell International) for 1 h at 22 °C, and then for 12–16 h at 4 °C. When one of the primary antibodies was omitted, no immunoreactivity for the omitted primary antibody was observed. After immunogold labeling, the replicas were immediately rinsed three times with 0.1% BSA/Tris-buffered saline, washed twice with distilled water, and picked up onto grids coated with pioloform (Agar Scientific).

Western blots. Hippocampal membranes were prepared from adult wild-type, SK2-S only and *Sk2*$^{-/-}$ mice as previously reported[19]. We separated 40 μg of protein by SDS-

PAGE and transferred to nitrocellulose membranes. The membranes were probed with pan-SK2 (3 μg ml^{-1}) or with SK2-L (1 μg ml^{-1}) antibody. Protein bands were visualized after application of secondary antibody to rabbit conjugated to horseradish peroxidase (Promega) at 1:20,000 using Supersignal West Pico Chemoluminescent ECL (Thermo Scientific).

Virus injections. We anesthetized 3–4-week-old mice with isoflurane, immobilized them in a Kopf Stereotaxic Alignment System and injected with them 0.2 μl of virus solution (2×10^{10} viral genomes per ml) at two to six sites targeting the hippocampus with the Quintessential Stereotaxic Injector (Stoelting). Recordings were performed more than 14 d after surgery.

Slice preparation. Hippocampal slices were prepared from 6–10-week-old C57BL/6J mice as previously described[11,12]. Slices were transferred into a holding chamber containing artificial cerebrospinal fluid (aCSF; 125 mM NaCl, 2.5 mM KCl, 21.5 mM $NaHCO_3$, 1.25 mM NaH_2PO_4, 2.0 mM $CaCl_2$, 1.0 mM $MgCl_2$, 15 mM glucose, equilibrated with carbogen). Slices were incubated at 34 °C for 30 min and then at room temperature for ≥1–4 h before recordings were performed.

Electrophysiology. Whole-cell patch-clamp recordings were obtained from CA1 pyramidal cells as previously described[11,12]. Patch pipettes (open pipette resistance, 2–4 MΩ) were filled with a solution containing 130 mM potassium gluconate, 8 mM NaCl, 1 mM $MgCl_2$, 10 mM HEPES, 4 mM ATP, 0.3 mM GTP, and 10 mM phosphocreatine (pH 7.26). In voltage clamp, series resistance was compensated to >80%. For current clamp, series resistance was not electronically compensated and

recordings with series resistance that changed more than 20% during the experiment were discarded. All recordings were from cells with a resting membrane potential between −70 and −50 mV, and a stable input resistance. A bias current was applied to maintain the membrane potential at −60 mV in current clamp. All whole-cell recordings were performed at 20–21 °C.

Field recordings. Extracellular fEPSPs were recorded as previously described[14,15]. LTP was induced by a TBS protocol consisting of 10 theta bursts at 5 Hz; each theta burst contained four to five pulses at 100 Hz. The initial slope of the fEPSP was measured to monitor the strength of synaptic transmission, minimizing contamination by voltage-dependent events. Summary graphs were obtained by normalizing each experiment according to the average value of all points on the 10-min baseline. Field recordings were performed at 30–32 °C.

Synaptic stimulations. Capillary glass pipettes filled with aCSF, with a tip diameter of 1–2 μm, connected to Model 2200 stimulus isolation unit (whole-cell recordings, A-M Systems) and a Digitimer DS3 stimulus isolation unit (field recordings, Automate Scientific). SR95531 (2 μM) and CGP55845 (1 μM) were present to reduce $GABA_A$ and $GABA_B$ contributions, respectively. To prevent epileptic discharges in the presence of GABAergic blockers, the CA3 region was microdissected out before recording.

Chemicals. CGP55845 and SR95531 were obtained from Tocris Cookson. Apamin was from Calbiochem.

Behavioral testing. All mice were acclimated to the laboratory before initiating

behavioral testing.

Spontaneous novel object recognition. As described previously[14], during the sample session each mouse explored two novel toy objects in the familiar white ABS arena (37.5 cm × 37.5 cm × 50.8 cm tall). Mice were removed from the arena after accumulating 19 s of sample object exploration; any mice that failed to reach this encoding criterion in 10 min were removed from the study. During the test session 24 h later, each mouse was returned to the arena for a 5-min session and the arena contained one of the objects from the sample session and a novel object. Object exploration was recorded with digital stopwatches for the sample session and with the Ethovision XT manual event encoder for the test session. Exploration was defined as time spent with the head oriented toward the object and within 2–3 cm. Measures were 'latency to accumulate sample object exploration', defined as the amount of time (in seconds) each mouse took to reach the encoding criterion during the sample session; and 'novel object preference ratio', defined as the time spent exploring the novel object divided by the total time spent exploring both test session objects.

Morris water maze. Mouse behavior was recorded with the EthoVision XT video-tracking system. As described previously[14], mice received 6 d of hidden platform training (4 trials per day), to learn the location of a clear Plexiglas platform (8 cm diameter) submerged 1 cm below the surface of the pool (60 cm high, 109 cm diameter). Large visible cues were present around the pool. Mice remained on the platform for 30 s, and then were placed into a holding cage for a 45-s intertrial interval. To examine spatial memory retention, mice received a 30-s probe test 5 min after the 4th, 12th and 20th training trial during which the platform was removed from

the pool. Percent dwell in each pool quadrant was determined for each mouse and search ratio was calculated from probe test behavior as the number of crossings into a 23.8 cm diameter circular zone around the platform location, divided by the total number of crossings into four equivalent zones (in each of the four pool quadrants). During visible platform training (six trials per day), each mouse swam to a black Plexiglas platform (13 cm diameter) located just above the water's surface at a position that was randomized each trial.

Data analysis. Data were analyzed using IGOR (WaveMetrics). A nonparametric Wilcoxon-Mann-Whitney two-sample rank test or a paired two-sample *t* test was used to determine significance; $P < 0.05$ was considered significant.

The Morris water-maze data were analyzed with two-factor, repeated-measures (genotype, day or probe test) ANOVA with *post hoc* Student's *t* tests where appropriate. The novel object recognition data for latency to accumulate sample object exploration and the novel object preference ratio were analyzed with Student's *t* tests. $P < 0.05$ was considered significant.

REFERENCES

1. Bredt, D.S. & Nicoll, R.A.

AMPA receptor trafficking at excitatory synapses.

Neuron **40**, 361–379 (2003).

2. Petralia, R.S. & Wenthold, R.J.

Light and electron immunocytochemical localization of AMPA-selective glutamate receptors in the rat brain.

J. Comp. Neurol. **318**, 329–354 (1992).

3. Carroll, R.C. & Zukin, R.S.

NMDA-receptor trafficking and targeting: implications for synaptic transmission and plasticity.

Trends Neurosci. **25**, 571–577 (2002).

4. Adesnik, H., Nicoll, R.A. & England, P.M.

Photoinactivation of native AMPA receptors reveals their real-time trafficking.

Neuron **48**, 977–985 (2005).

5. Harris, A.Z. & Pettit, D.L.

Recruiting extrasynaptic NMDA receptors augments synaptic signaling.

J. Neurophysiol. **99**, 524–533 (2008).

6. Makino, H. & Malinow, R.

AMPA receptor incorporation into synapses during LTP: the role of lateral movement and exocytosis.

Neuron **64**, 381–390 (2009).

7. Derkach, V.A., Oh, M.C., Guire, E.S. & Soderling, T.R.

Regulatory mechanisms of AMPA receptors in synaptic plasticity.

Nat. Rev. Neurosci. **8**, 101–113 (2007).

8. van Zundert, B., Yoshii, A. & Constantine-Paton, M.

Receptor compartmentalization and trafficking at glutamate synapses: a developmental proposal.

Trends Neurosci. **27**, 428–437 (2004).

9. Bellone, C. & Nicoll, R.A.

Rapid bidirectional switching of synaptic NMDA receptors.

Neuron **55**, 779–785 (2007).

10. Köhler, M. *et al.*

Small-conductance, calcium-activated potassium channels from mammalian brain. *Science* **273**, 1709–1714 (1996).

11. Lin, M.T., Lujan, R., Watanabe, M., Adelman, J.P. & Maylie, J.

SK2 channel plasticity contributes to LTP at Schaffer collateral-CA1 synapses.

Nat. Neurosci. **11**, 170–177 (2008).

12.Ngo-Anh, T.J. *et al.*

SK channels and NMDA receptors form a Ca^{2+}-mediated feedback loop in dendritic spines.

Nat. Neurosci. **8**, 642–649 (2005).

13. Bloodgood, B.L. & Sabatini, B.L.

Nonlinear regulation of unitary synaptic signals by $Ca_V(2.3)$ voltage-sensitive calcium channels located in dendritic spines.

Neuron **53**, 249–260 (2007).

14. Stackman, R.W. *et al.*

Small conductance Ca^{2+}-activated K^+ channels modulate synaptic plasticity and memory encoding.

J. Neurosci. **22**, 10163–10171 (2002).

15. Hammond, R.S. *et al.*

Small-conductance Ca^{2+}-activated K^+ channel type 2 (SK2) modulates hippocampal learning, memory, and synaptic plasticity.

J. Neurosci. **26**, 1844–1853 (2006).

16. Stackman, R.W. Jr., Bond, C.T. & Adelman, J.P.

Contextual memory deficits observed in mice overexpressing small conductance Ca^{2+}-activated K^+ type 2 (KCa2.2, SK2) channels are caused by an encoding deficit.

Learn. Mem. **15**, 208–213 (2008).

17. Vick, K.A. IV, Guidi, M. & Stackman, R.W. Jr.

In vivo pharmacological manipulation of small conductance Ca^{2+}-activated K^+ channels influences motor behavior, object memory and fear conditioning.

Neuropharmacology **58**, 650–659 (2010).

18. Lin, M.T. *et al.*

Coupled activity-dependent trafficking of synaptic SK2 channels and AMPA receptors.

J. Neurosci. **30**, 11726–11734 (2010).

19. Strassmaier, T. *et al.*

A novel isoform of SK2 assembles with other SK subunits in mouse brain.

J. Biol. Chem. **280**, 21231–21236 (2005).

20. Bond, C.T. *et al.*

Small conductance Ca^{2+}-activated K^+ channel knock-out mice reveal the identity of calcium-dependent afterhyperpolarization currents.

J. Neurosci. **24**, 5301–5306 (2004).

21. Bond, C.T. *et al.*

Respiration and parturition affected by conditional overexpression of the Ca^{2+}-activated K^+ channel subunit, SK3.

Science **289**, 1942–1946 (2000).

22.Stocker, M., Krause, M. & Pedarzani, P.

An apamin-sensitive Ca^{2+}-activated K^+ current in hippocampal pyramidal neurons.

Proc. Natl. Acad. Sci. USA **96**, 4662–4667 (1999).

23. Kye, M.J., Spiess, J. & Blank, T.

Transcriptional regulation of intronic calcium-activated potassium channel SK2 promoters by nuclear factor-kappa B and glucocorticoids.

Mol. Cell. Biochem. **300**, 9–17 (2007).

24.Davuluri, R.V., Suzuki, Y., Sugano, S., Plass, C. & Huang, T.H.

The functional consequences of alternative promoter use in mammalian genomes.

Trends Genet. **24**, 167–177 (2008).

25.Stocker, M. & Pedarzani, P.

Differential distribution of three Ca^{2+}-activated K^+ channel subunits, SK1, SK2, and SK3, in

the adult rat central nervous system.

Mol. Cell. Neurosci. **15**, 476–493 (2000).

26. Lu, W., Isozaki, K., Roche, K.W. & Nicoll, R.A.

Synaptic targeting of AMPA receptors is regulated by a CaMKII site in the first intracellular loop of GluA1.

Proc. Natl. Acad. Sci. USA **107**, 22266–22271 (2010).

27. Luján, R., Nusser, Z., Roberts, J.D., Shigemoto, R. & Somogyi, P.

Perisynaptic location of metabotropic glutamate receptors mGluR1 and mGluR5 on dendrites and dendritic spines in the rat hippocampus.

Eur. J. Neurosci. **8**, 1488–1500 (1996).

28. Fujimoto, K.

Freeze-fracture replica electron microscopy combined with SDS digestion for cytochemical labeling of integral membrane proteins. Application to the immunogold labeling of intercellular junctional complexes.

J. Cell Sci. **108**, 3443–3449 (1995).

FIGURES AND LEGENDS

Figure 1

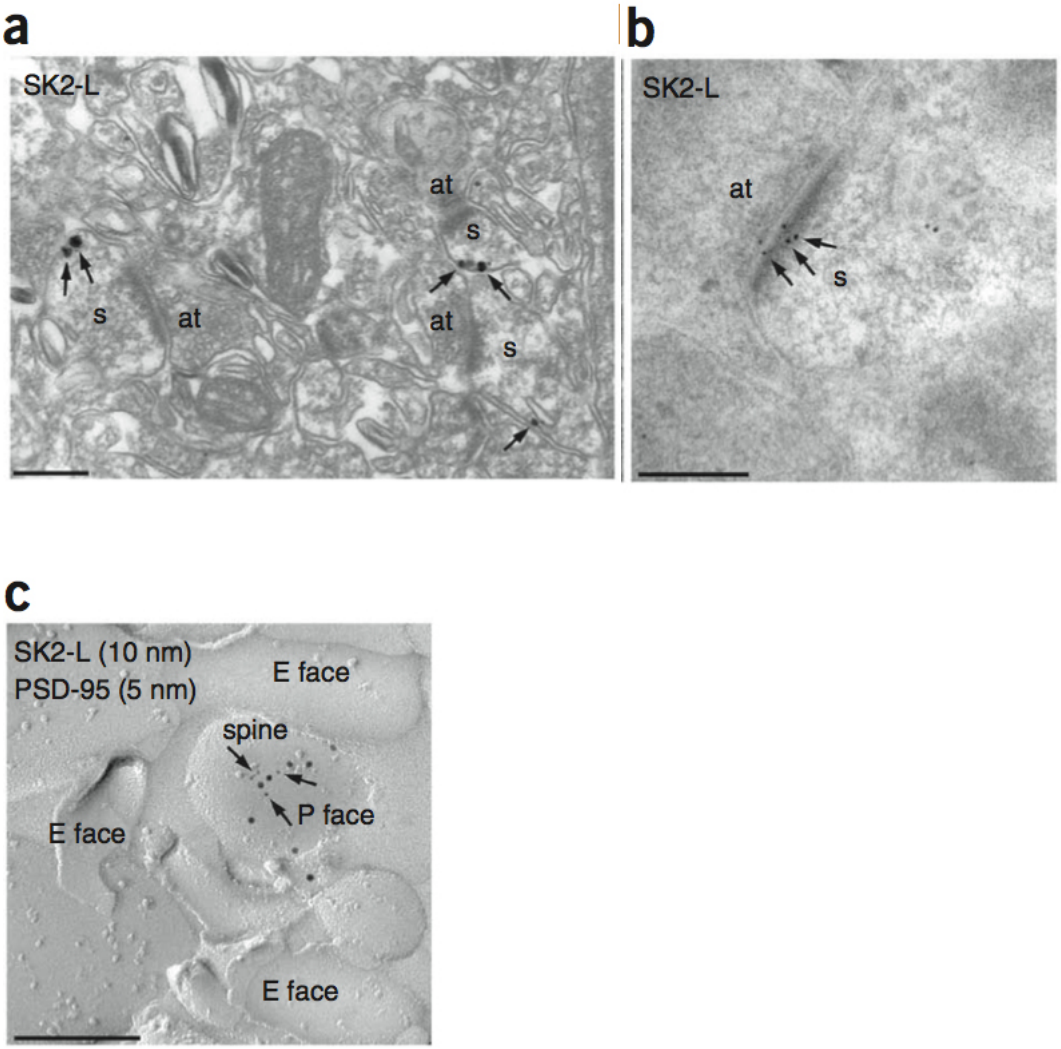

Figure 1

Subcellular localization of SK2-L in dendritic spines of wild-type CA1 pyramidal neurons. (**a**) Using the pre-embedding technique, immunoparticles for SK2-L were detected along the extrasynaptic plasma membrane (arrows) of dendritic spines (s). (**b**) Using the post-embedding technique, immunoparticles for SK2-L were detected along the PSD (arrows) of dendritic spines. (**c**) Using the SDS-FRL technique, the synaptic membrane was identified by immunoparticles for PSD-95 (arrows). SK2-L immunoparticles were detected in dendritic spines intermingled with immunoparticles for PSD-95. at: axon terminal; E face, exoplasmic face; P face, protoplasmic face. Scale bars represent 200 nm.

Figure 2

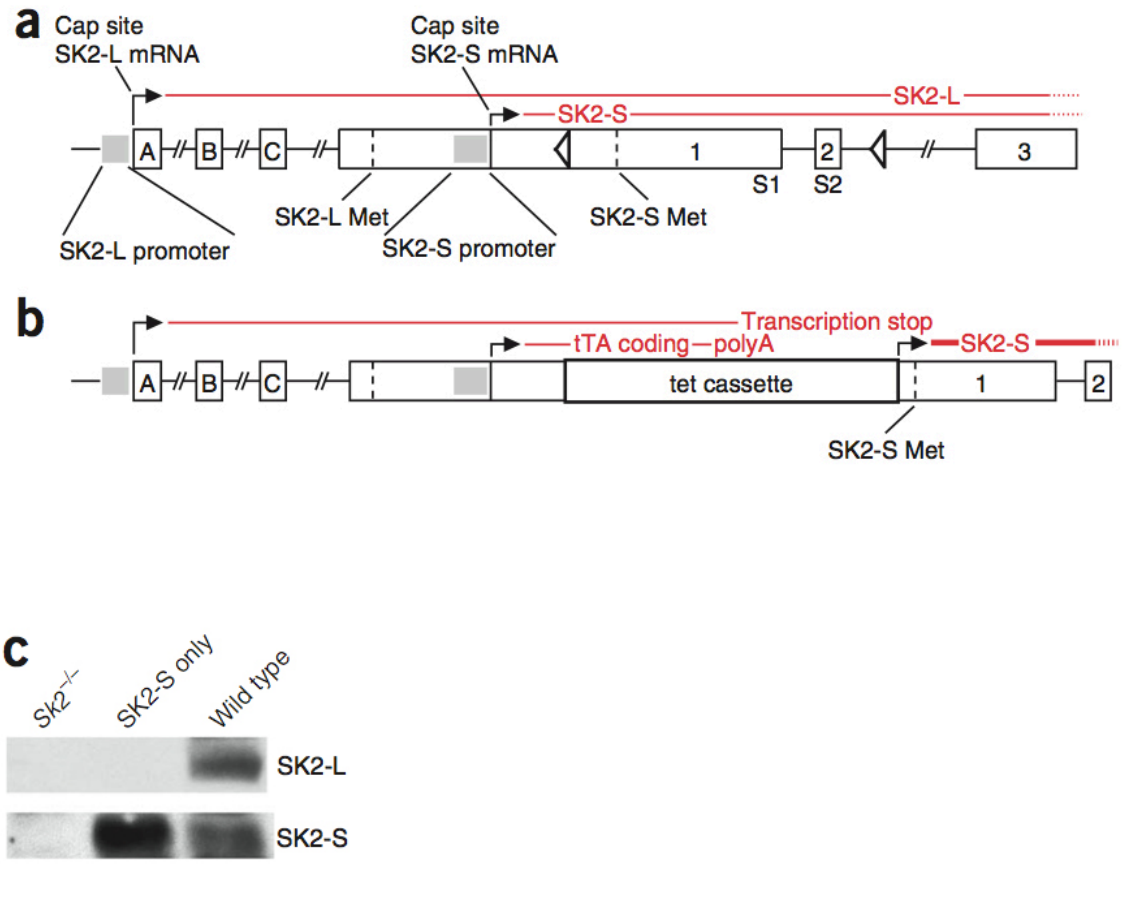
a
Cap site
SK2-L mRNA
Cap site
SK2-S mRNA
SK2-L
SK2-S
A
B
C
1
2
3
S1
S2
SK2-L Met
SK2-S Met
SK2-L promoter
SK2-S promoter
b
Transcription stop
tTA coding
polyA
SK2-S
tet cassette
1
2
SK2-S Met
c
Sk2−/−
SK2-S only
Wild type
SK2-L
SK2-S

Figure 2

Sk2 gene locus and western blot. (**a**) The 5′ region of the mouse *Sk2* gene. Boxes represent exons. The positions of the translational initiator methionine (Met) codons for SK2-L and SK2-S are shown as dotted lines. The 5′ end of the longest SK2-L mRNA resides in exon A, whereas the cap site for the SK2-S mRNA resides in exon 1. The shaded areas indicate the positions of the promoters that drive SK2-L and SK2-S expression. The lines above the exon-intron mosaic indicate the transcripts for SK2-L and SK2-S. The triangles show the positions of the *loxP* sites in the *loxP*-flanked *Sk2* allele. (**b**) The mouse *Sk2 T* allele. The position of the tetracycline gene switch is indicated in the SK2-S 5′ untranslated region, 5′ of the SK2-S initiator Met. The SK2-L transcript is terminated in the inserted tet cassette, abolishing SK2-L expression. The SK2-S promoter drives expression of the tetracycline transactivator (tTA) mRNA. The tTA protein binds to tet operator sequences at the 3′ end of the tet cassette and enables SK2-S overexpression from the minimal CMV promoter. (**c**) Western blots of hippocampal proteins probed for SK2 in wild-type, SK2-S only and *Sk2*$^{-/-}$ mice using the SK2-L antibody (top) and the pan-SK2 antibody (bottom).

Figure 3

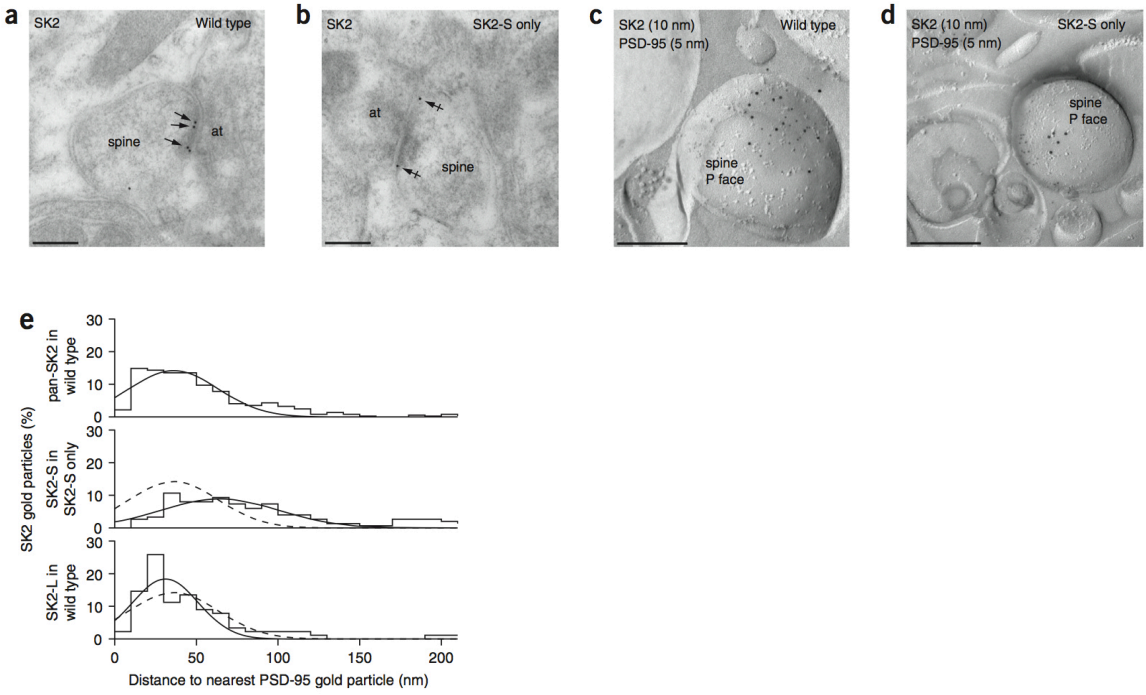
a
SK2
Wild type
spine
at
b
SK2
SK2-S only
at
spine
c
SK2 (10 nm)
PSD-95 (5 nm)
Wild type
spine
P face
d
SK2 (10 nm)
PSD-95 (5 nm)
SK2-S only
spine
P face
e
SK2 gold particles (%)
pan-SK2 in wild type
SK2-S in SK2-S only
SK2-L in wild type
0
10
20
30
0
50
100
150
200
Distance to nearest PSD-95 gold particle (nm)

Figure 3

Subcellular localization of SK2 in wild-type and SK2-S only CA1 pyramidal neurons. (**a**) Using the post-embedding technique in wild-type mice, immunoparticles for SK2 were detected along the PSD (arrows) of dendritic spines. (**b**) Using the post-embedding technique in SK2-S only mice, immunoparticles for SK2 were detected along the extrasynaptic membrane (arrows) of dendritic spines, but not along the PSD. (**c**) Using the SDS-FRL technique in wild-type mice, SK2 immunoparticles were detected in dendritic spines intermingled with immunoparticles for PSD-95. (**d**) Using the SDS-FRL technique in SK2-S only mice and double immunolabeling for SK2 and PSD-95, SK2 immunoparticles were detected in dendritic spines, but segregated from immunoparticles for PSD-95. Scale bars represent 200 nm. (**e**) For SDS-FRL immunolabeling, the percentage of SK2 immunoparticles was plotted as a function of distance from the nearest PSD-95 immunoparticle, and fit by Gaussians for the indicated groups. Dashed line in middle and bottom panels is the fit from wild type in the top panel.

Figure 4

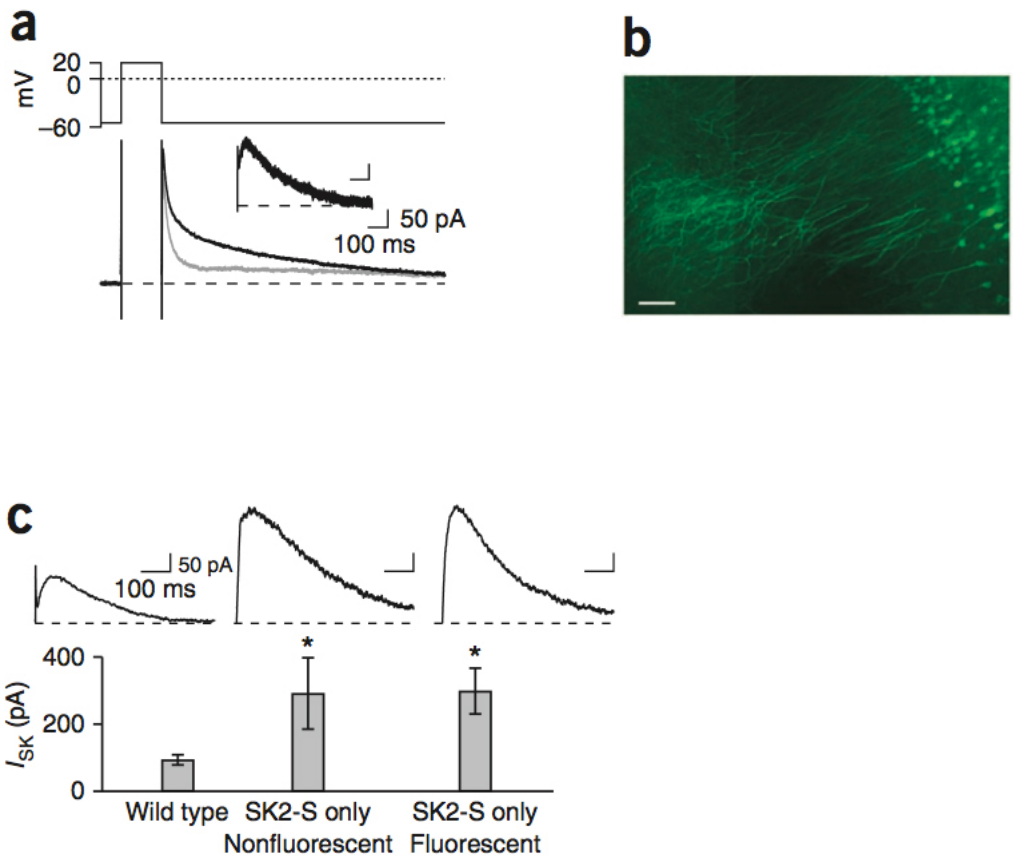
a
20
0
–60
mV
50 pA
100 ms
b
c
50 pA
100 ms
400
200
0
I_{SK} (pA)
*
*
Wild type
SK2-S only
Nonfluorescent
SK2-S only
Fluorescent

Figure 4

SK2-containing channels are expressed in the plasma membrane of SK2-S only CA1 pyramidal neurons. (**a**) Top, voltage protocol used to evoke tail currents. Cells were voltage clamped at −55 mV and tail currents were elicited after 200-ms depolarizing steps to 20 mV. Bottom, representative tail currents from a wild-type CA1 neuron before (black trace) and after (gray trace) apamin application. The inset shows the subtracted apamin-sensitive current. (**b**) Section through hippocampus from an SK2-S only mouse injected with rAAV directing separate expression of GFP and SK2-L. Scale bar represents 50 μm. (**c**) Left, representative apamin-sensitive currents from wild type (left), SK2-S only nonfluorescent (middle) and SK2-S only fluorescent (right) CA1 pyramidal neurons. Right, summary plot of the amplitude of apamin-sensitive currents (I_{SK}) for the three groups of neurons. Error bars indicate s.e.m. *P < 0.05 for wild type compared with SK2-S only nonfluorescent or SK2-S only fluorescent.

Figure 5

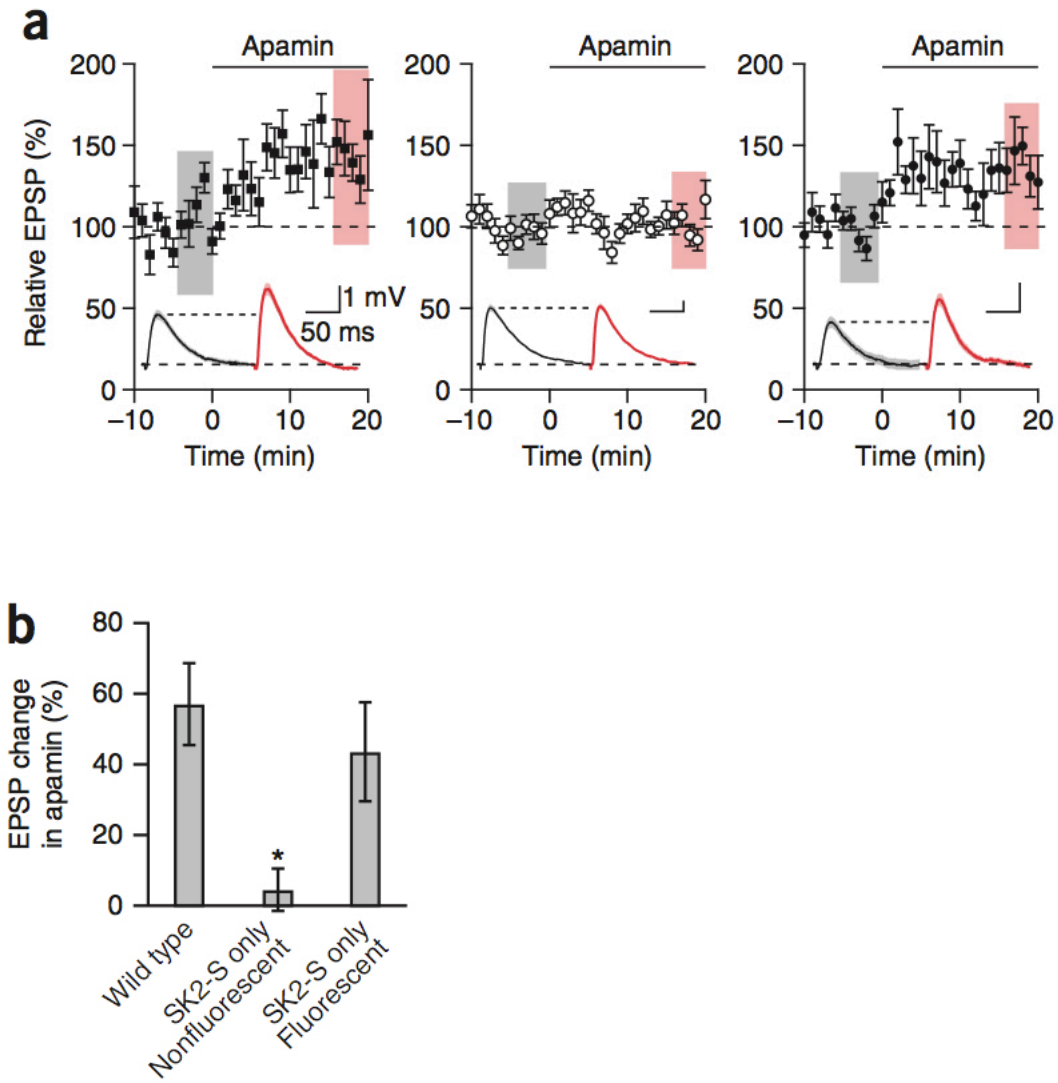
a
Apamin
Apamin
Apamin
Relative EPSP (%)
200
150
100
50
0
1 mV
50 ms
–10
0
10
20
Time (min)
b
EPSP change in apamin (%)
80
60
40
20
0
*
Wild type
SK2-S only Nonfluorescent
SK2-S only Fluorescent

Figure 5

SK2-L re-expression reinstates apamin sensitivity to synaptically evoked glutamatergic EPSPs. (**a**) Time course of the normalized EPSP amplitude (mean ± s.e.m.) before and after apamin application for wild type (left), SK2-S only nonfluorescent (middle) and SK2-S only fluorescent (right) CA1 pyramidal neurons. Insets show representative average of 20 EPSPs, mean ± s.e.m. (shaded area), taken from the indicated shaded time points in the control condition before (black line, left) and after (red line, right) apamin application. (**b**) Bar graph of the increase in EPSP following apamin application. Error bars indicate s.e.m. **P* < 0.05 for SK2-S only nonfluorescent and SK2-S only fluorescent compared to wild type.

Figure 6

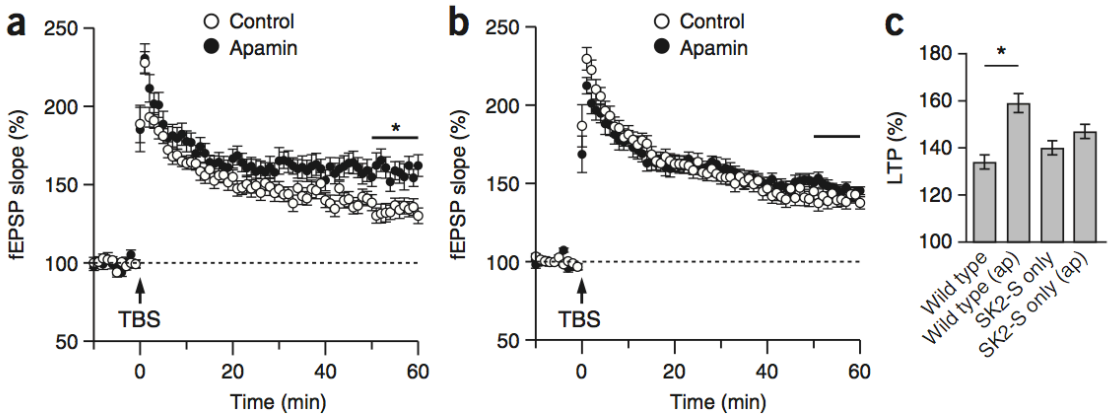
a
Control
Apamin
fEPSP slope (%)
250
200
150
100
50
TBS
0
20
40
60
Time (min)
*
b
Control
Apamin
fEPSP slope (%)
250
200
150
100
50
TBS
0
20
40
60
Time (min)
c
LTP (%)
180
160
140
120
100
*
Wild type
Wild type (ap)
SK2-S only
SK2-S only (ap)

Figure 6

SK channel activity affects LTP in wild-type, but not SK2-S only, mice. Field potentials were recorded from the CA1 region of hippocampal slices. (**a**) In wild-type stimulation of Schaffer collateral axons induced more LTP in the presence of apamin (filled circles) than in control bath solution (open circles). (**b**) LTP was not different with (filled circles) or without (open circles) apamin application in SK2-S only slices. LTP was measured 50–60 min after stimulation (black bars). (**c**) Summary plot of LTP from the indicated groups. Error bars indicate s.e.m. $*P < 0.05$.

Figure 7

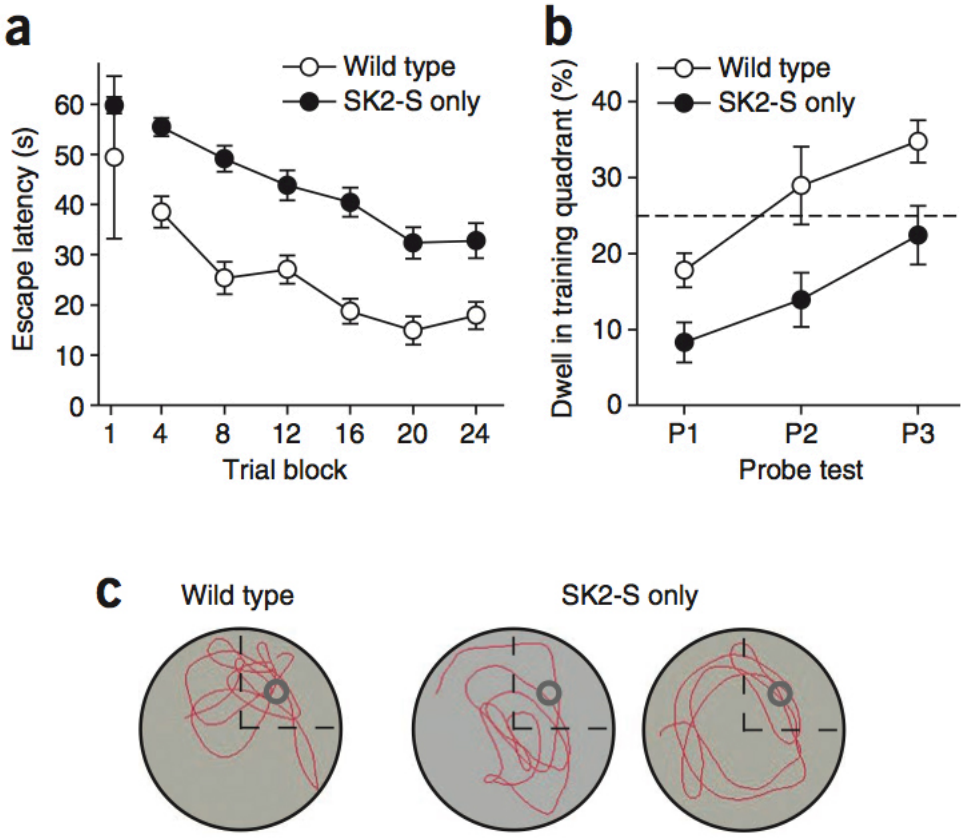
a
Wild type
SK2-S only
Escape latency (s)
60
50
40
30
20
10
0
1
4
8
12
16
20
24
Trial block
b
Wild type
SK2-S only
Dwell in training quadrant (%)
40
30
20
10
0
P1
P2
P3
Probe test
c
Wild type
SK2-S only

Figure 7

Spatial memory is impaired in SK2-S only mice. (**a**) The mean latency ± s.e.m. to escape on to the hidden platform was significantly different ($P < 0.002$) between wild-type (open circles) and SK2-S only mice (filled circles). There was no difference between genotypes in mean latency on trial 1, indicating that both groups exhibited nearly equivalent performance at the start of training. (**b**) The mean percentage dwell ± s.e.m. in the correct quadrant of the pool during the probe test of spatial memory retention imposed after the 4^{th} (P1), 12^{th} (P2) and the 20^{th} training trial (P3). The dashed line indicates chance performance. The SK2-S only mice (filled circles), but not wild-type mice (open circles), failed to exhibit a significant preference for searching ± s.e.m. in the correct quadrant of the pool ($P < 0.003$). (**c**) Representative paths taken by a wild-type mouse (left trace) and two SK2-S only mice (center and right traces) during the P3 probe test. The path of the wild-type mouse is direct to training quadrant and then characterized by repetitive passes through the precise location of the pool where the platform was placed during training (gray open circle). The paths of the SK2-S only mice are much less accurate and more circuitous than that of the wild-type mice.

Supplementary Figure 1

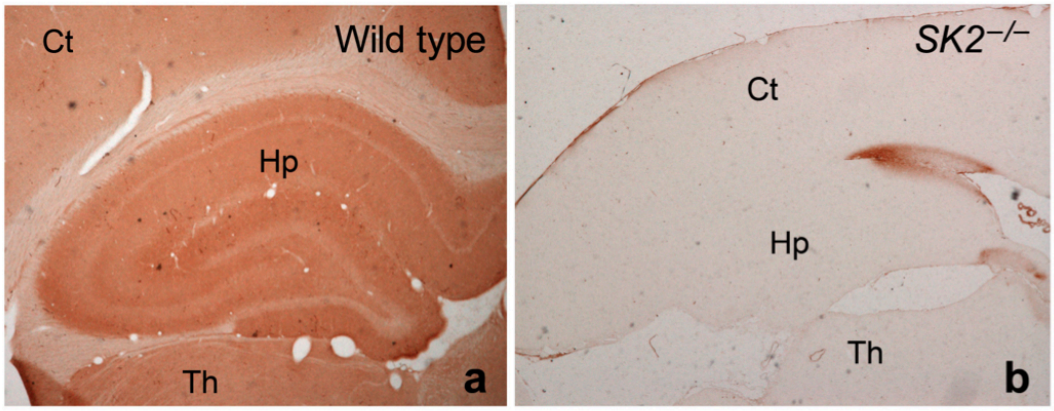

Immunoreactivity for SK2-L in the hippocampus and cortex of wild type and *SK2*$^{-/-}$ mice as revealed at the light microscopy level.

Staining for SK2 in the hippocampus, cortex, and thalamus from (**a**) a wild type mouse, while the section from an *SK2*$^{-/-}$ mouse (**b**), processed in parallel, showed a complete lack of staining.

Supplementary Figure 2

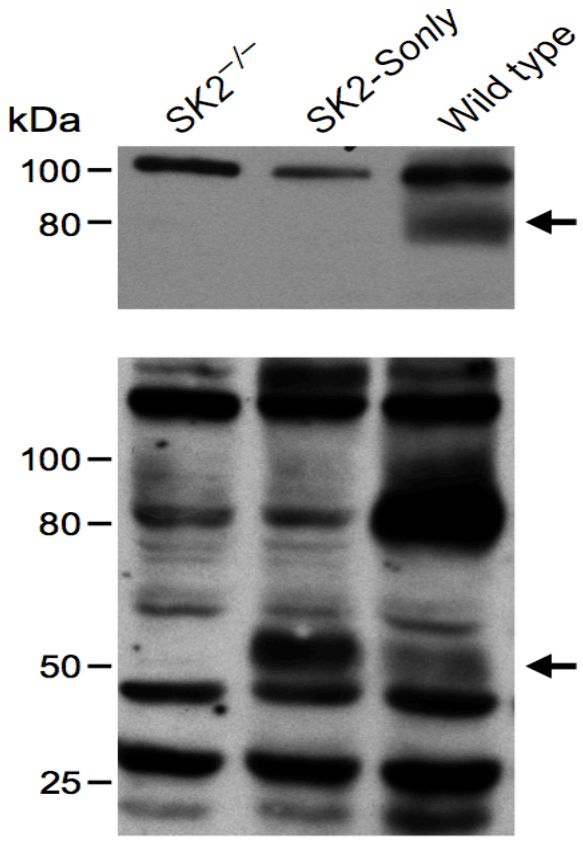

Western blot analysis of hippocampal membranes.

Crude membranes of hippocampus from wild type, *SK2-Sonly* and *SK2*$^{-/-}$ were probed as Western blots. The lower panel was probed with a rabbit polyclonal pan-SK2 antibody together with a rabbit polyclonal antibody against the N-terminus of SK2-L. Arrow marks the positions of SK2-S specific bands. Due to background bands that obscure the position of SK2-L, the top panel shows a blot of the same samples probed with the anti-SK-L antibody alone. Arrow marks the position of the SK2-L specific band. Molecular weight markers are indicated.

Supplementary Figure 3

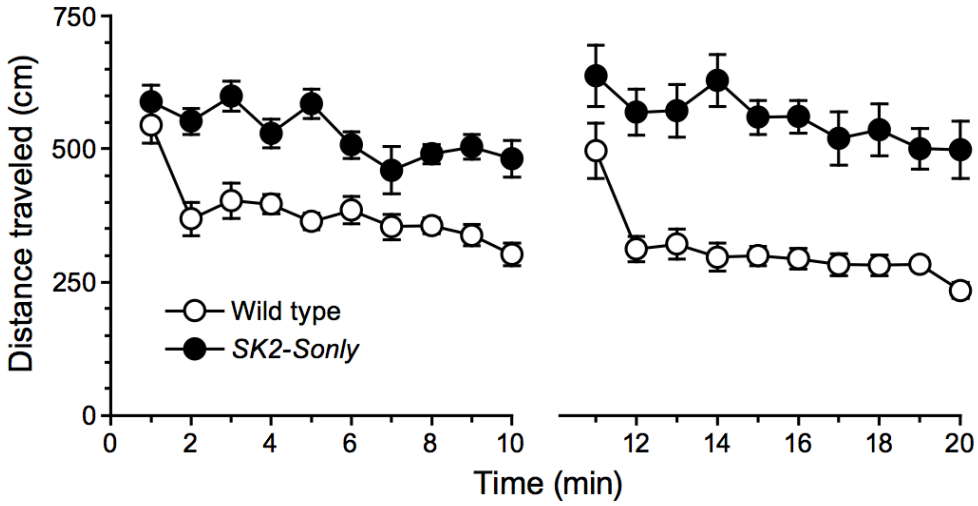

Locomotor activity is elevated in *SK2-Sonly* mice.

Mice were placed into a high-walled square arena and allowed to explore freely two 10-min sessions separated by 24 hours. These sessions served to habituate the wild type (open circles) and *SK2-Sonly* (filled circles) mice to the arena prior to novel object recognition testing. Graph depicts the average distance ± s.e.m. traveled in the open field as a function of minute.

Supplementary Figure 4

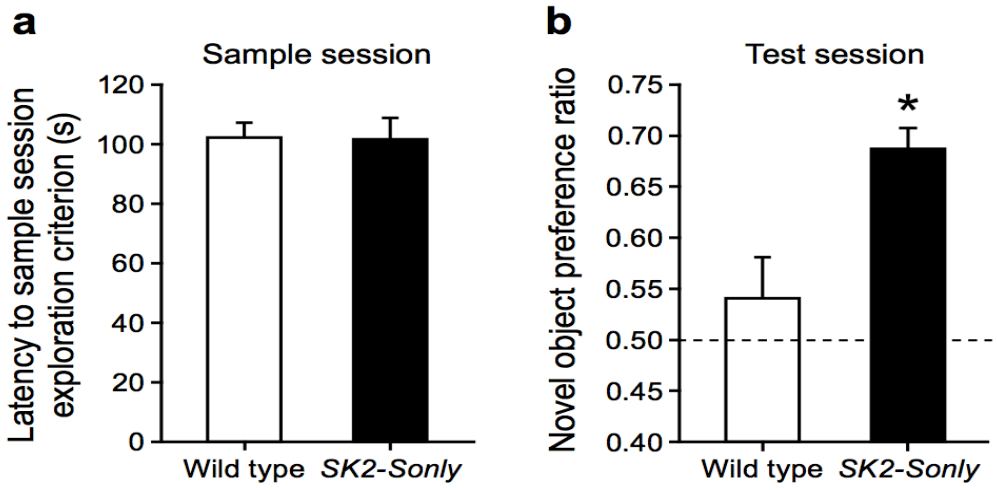

Encoding of object memory is enhanced in *SK2-Sonly* mice.

Object memory was examined in a spontaneous novel object recognition task. (**a**) The mean latency of mice to accumulate 19 sec of object exploration during the sample session did not differ between wild type (open circles) and *SK2-Sonly* mice (filled circles). (**b**) Preference for exploring the novel object was stronger in the *SK2-Sonly* mice (filled circles) compared to the wild type mice (open circles) during the test session presented 24 hours after the sample session. The degree of novel object preference observed by wild type mice is similar to that reported previously[14] and likely reflects insufficient exploration of the objects during the sample session. The *SK2-Sonly* mice exhibited novel object preference similar to that reported previ- ously for apamin-treated mice. Error bars indicate s.e.m. * $P < 0.005$.

Supplementary Figure 5

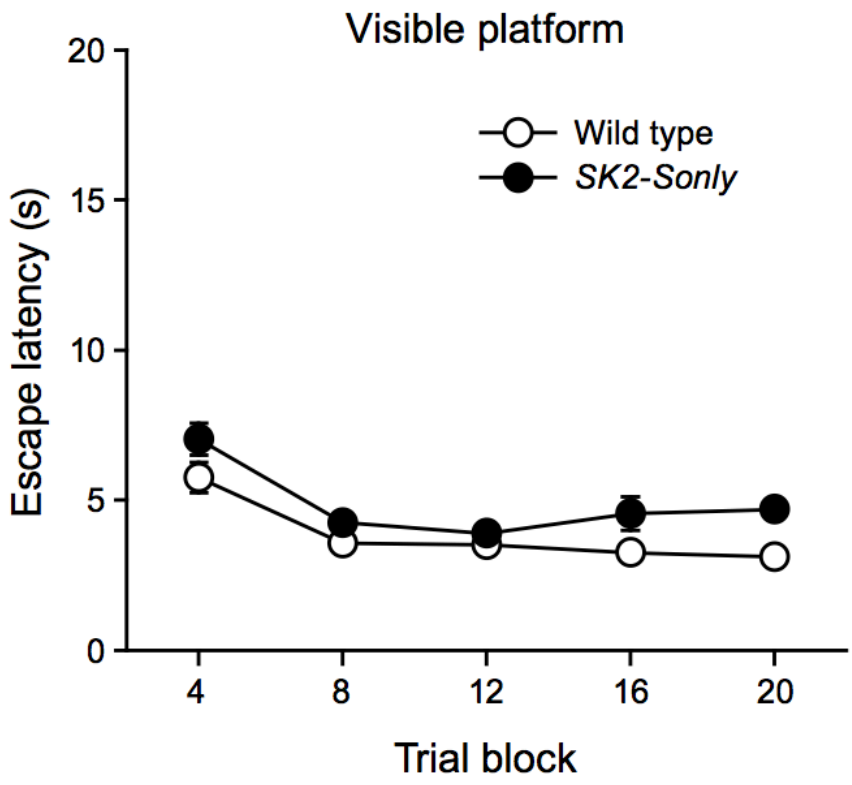

Acquisition of the visible platform water maze is comparable between wild type and *SK2-Sonly* mice.

Following completion of the hidden platform water maze training, each mouse was trained for 20 trials (4/day) to escape onto a platform that was visible and cued with a flag. This task served as a sensorimotor and motivational control task for the hidden platform water maze. Mean escape latencies ± s.e.m. in the visible platform water maze task were similar across wild type (open circles) and *SK2-Sonly* (filled circles) mice.

IV.

Distinct Ca^{2+} Sources in Dendritic Spines of Hippocampal CA1 Neurons Couple to SK and Kv4.2 Channels

Wang K, Lin MT, Adelman JP, Maylie J.

Neuron. 2014 Jan 22;81(2):379-87.

Contributions
M.T.L. performed preliminary study. K.W. performed all the figures. J.P.A. and J.M. wrote the manuscript.

ABSTRACT

Small conductance Ca^{2+}-activated K^+ (SK) channels and voltage-gated A-type K_V4 channels shape dendritic excitatory postsynaptic potentials (EPSPs) in hippocampal CA1 pyramidal neurons. Synaptically evoked Ca^{2+} influx through N-methyl-D-aspartate receptors (NMDARs) activates spine SK channels, reducing EPSPs and the associated spine head Ca^{2+} transient. However, results using glutamate uncaging implicated Ca^{2+} influx through SNX-482-sensitive (SNX-sensitive) $Ca_V2.3$ (R-type) Ca^{2+} channels as the Ca^{2+} source for SK channel activation. The present findings show that, using Schaffer collateral stimulation, the effects of SNX and apamin are not mutually exclusive and SNX increases EPSPs independent of SK channel activity. Dialysis with 1,2- bis(o-aminophenoxy)ethane-N'N'N'-tetraacetic acid (BAPTA), application of 4-Aminopyridine (4-AP), expression of a K 4.2 dominant negative subunit, and dialysis with a KChIPs antibody occluded the SNX-induced increase of EPSPs. The results suggest two distinct Ca^{2+} signaling pathways within dendritic spines that link Ca^{2+} influx through NMDARs to SK channels and Ca^{2+} influx through R-type Ca^{2+} channels to $K_V4.2$-containing channels.

INTRODUCTION

Excitatory postsynaptic responses are initiated primarily by the activation of ionotropic glutamate receptors that depolarize the spine membrane potential and mediate Ca^{2+} influx. These effects provide for the secondary activation of voltage- and Ca^{2+}-dependent channels that can modulate and shape the synaptic responses. One example is small conductance Ca^{2+}- activated K^+ (SK) channels in CA1 pyramidal neurons that are activated locally by synaptically evoked Ca^{2+} influx. Their repolarizing influence reduces excitatory postsynaptic potentials (EPSPs) and the associated spine head Ca^{2+} transient by promoting Mg^{2+} block of N-methyl-D-aspartate receptors (NMDARs). Therefore, blocking synaptic SK channels with apamin, a selective antagonist of SK channels, boosts EPSPs by as much as 50% and is reflected by an increase in the spine Ca^{2+} transient (Ngo-Anh et al., 2005). Immunoelectron microscopy (immuno-EM) demonstrated expression of one of the SK subunits, SK2, in the postsynaptic density (PSD) where SK2 immunoparticles were codistributed with immunoparticles for NMDARs (Lin et al., 2008). The colocalization of synaptic SK2-containing channels and NMDARs, taken together with the ability of either NMDAR blockers or dialysis with the Ca^{2+} buffer 1,2- bis(o-aminophenoxy)ethane-N'N'N'-tetraacetic acid (BAPTA) but not EGTA, in the patch pipette solution to occlude the effects of apamin, suggested that SK channels and their Ca^{2+} source reside within 25–50 nm and that synaptically evoked Ca^{2+} influx through NMDARs activates SK2-containing channels (Ngo-Anh et al., 2005).

Subsequent work demonstrated that voltage-dependent $K_V4.2$-containing channels (Kim et al., 2007) and voltage-dependent Ca^{2+} channels in spines are also activated

secondarily to ionotropic glutamate receptors. Among these channels are SNX-sensitive (peptide toxin SNX-482 derived from African tarantula *Hysterocrates gigas*), R-type Ca^{2+} channels (Bloodgood and Sabatini, 2007). Using 2-photon laser photoactivation of caged glutamate onto single spines, uncaging-evoked synaptic responses (uEPSPs) were measured at the soma. In addition, uncaging-evoked Ca^{2+} responses (Δ[Ca]uEPSPs) were measured with Fluo-5F in the pipette using 2-photon laser scanning microscopy. Under these conditions, in the presence of SNX to block $Ca_V2.3$ Ca^{2+} channels, the standard uncaging-evoked stimulation, adjusted in voltage clamp to give a 10–15 pA response, yielded a larger uEPSP and associated Δ[Ca]uEPSP compared to control cells. Importantly, in the presence of both apamin and SNX, the uEPSP and Δ[Ca]uEPSP measurements were the same as those recorded in either SNX or apamin alone, indicating that SNX-mediated blockade of R-type channels occludes the SK-mediated inhibition of the uEPSP and the Δ[Ca]uEPSP (Bloodgood and Sabatini, 2007). Taken together, the results suggested that Ca^{2+} entry through SNX-sensitive, R-type channels provides the Ca^{2+} for activating synaptic SK2-containing channels. In addition, the boosting effects of SNX on uncaging-evoked synaptic potentials and spine Ca^{2+} transients were absent in hippocampal pyramidal neurons from $Ca_V2.3$ null mice (Giessel and Sabatini, 2011). As previous results showed that synaptically evoked NMDAR activity is required to activate synaptic SK channels, we therefore tested whether SNX occludes synaptically evoked activation of apamin-sensitive SK channels in spines. We find that synaptic stimulations reveal the presence of two Ca^{2+} signaling pathways within the spine head, one that couples NMDARs with apamin-sensitive SK channels and another that couples SNX-sensitive, R-type Ca^{2+} channels with 4-Aminopyridine-

sensitive (4-AP-sensitive) $K_V4.2$-containing channels.

RESULTS

The Effects of Apamin and SNX Are Not Mutually Exclusive

Subthreshold EPSPs, evoked by stimulating the Schaffer collateral axons in stratum radiatum, were recorded in whole-cell current clamped CA1 neurons in acute slices from mouse hippocampus. To measure the effects of SK channels, EPSPs were recorded every 20 s before and after wash-in of apamin (100 nM). As previously reported (Ngo-Anh et al., 2005) and reproduced here, blocking SK channels with apamin increased the peak EPSP to 167% ± 12% ($n = 13$, $p < 0.001$) of the control baseline, and pretreatment of the cells with D(-)-2-Amino-5-phosphonovaleric acid (D-AP5) (50 μM) to block NMDARs occluded the effect of apamin (101% ± 8%, $n = 6$).

To determine whether the effects of apamin and SNX were mutually exclusive for synaptically evoked responses, SNX (0.3 μM) was bath applied prior to apamin coapplication. Pretreating cells with SNX did not occlude the effect of subsequent apamin application that increased the peak EPSP to 152% ± 6% ($n = 15$, $p < 0.001$; Figure 1A) compared to baseline in SNX alone. Also, in the presence of apamin, SNX application increased the EPSPs to 157% ± 8% compared to baseline in apamin alone ($n = 21$, $p < 0.001$; Figure 1C). The boosting of EPSPs by SNX does not require preblock of SK channels by apamin; SNX in the absence of apamin increased the EPSPs to 171.4% ± 10.9% compared to control ($n = 8$, $p < 0.001$), which was not different from that observed with apamin pretreatment ($p = 0.27$). Similar results were obtained when $NiCl_2$ (100 μM) was used, which at low concentrations blocks R-type channels (Myoga and Regehr, 2011; Soong et al., 1993). In cells pretreated with Ni^{2+},

apamin application increased EPSPs to 150% ± 13% (n = 10, $p < 0.05$), while Ni^{2+} application to cells pretreated with apamin increased EPSPs to 137% ± 10% (n = 6, $p < 0.05$). Therefore, using synaptic stimulations, SNX or low concentrations of Ni^{2+}, and apamin independently increased EPSPs, and their effects were not mutually exclusive.

Previously we showed that the apamin-induced enhancement of EPSPs was independent of the initial EPSP size from 1.1 to 7.9 mV (Lin et al., 2010b). To further examine whether apamin or SNX occlusion experiments were dependent on initial EPSP size, the enhancement of EPSPs by apamin or SNX was plotted against their initial EPSP amplitude (Figures 1B and 1D, respectively). The range of initial EPSP size for examining SNX occlusion of apamin in Figure 1A was from 0.8 to 3.8 mV. Fisher's r to z analysis of the EPSP increase by apamin in the presence of SNX compared to the initial EPSP size in SNX yielded no correlation. These results further demonstrate that SNX does not occlude the apamin response even for small initial EPSP sizes that are close to the average glutamate uncaging-evoked uEPSP of ~1 mV (Bloodgood and Sabatini, 2007). Additionally, the enhancement of EPSP amplitude by SNX in the presence of apamin was independent of initial EPSP size (Figure 1D).

Different from previous studies of postsynaptic R-type Ca^{2+} channels that used glutamate uncaging, responses to synaptic stimulation involve both presynaptic and postsynaptic components. In addition to postsynaptic localization, R-type channels may also be present in the presynaptic terminals (Parajuli et al., 2012), where they may influence glutamate release (Gasparini et al., 2001; Myoga and Regehr, 2011). To determine the effects of presynaptic R-type Ca^{2+} channels on glutamate release at

Schaffer collateral to CA1 synapses, evoked excitatory post-synaptic currents (EPSCs) were measured in voltage clamp at -60 mV using the K-gluconate-based internal solution. As control, the effect of apamin was also determined. Under these conditions, both SNX and apamin increased the peak EPSC by 37.4%±6.3%(n=9,p<0.001) and 33.2%±11.9% (n=12, $p < 0.05$), respectively (Figures 2A and 2C). Total charge transfer was similarly increased (Figures 2B and 2D).

Given that postsynaptic conductances may not be controlled using a K^+-based internal solution due to voltage escape in the dendrites, voltage clamp recordings of EPSCs were measured using a Cs^+-based internal solution. D600 (200 μM), QX-314 (3.35 mM), and BAPTA (5 mM) were added to the pipette solution to block postsynaptic Ca^{2+}, Na^+ channels, and Ca^{2+}-activated conductances, respectively, and D-AP5 was added to the bath solution to block NMDAR. Paired synaptic stimulations (50 ms interval) were delivered to monitor probability of release as measured by the peak and total charge transfer (area under the EPSC) of the EPSCs. Under these conditions, SNX (Figures 3A and 3B) reduced the amplitude to 79% ± 5% ($n = 10$, $p < 0.05$) but not the charge transfer of the first EPSC (88% ± 6%, $n = 10$, $p = 0.12$). The paired pulse ratios of EPSC peak and charge transfer were not significantly changed (117% ± 17% and 106% ± 10%, $n = 10$, respectively). In contrast, apamin had no effect on EPSC peak (93% ± 4%, $n = 5$) or charge transfer (Figures 3C and 3D). The paired pulse ratios of EPSC peak and charge transfer were also not affected by apamin (97% ± 6% and 98% ± 8%, $n = 5$, respectively).

These results confirm that glutamate release determined from EPSCs measured using the Cs^+-based internal solution with D600, QX-314, and BAPTA was not affected by

apamin (Stackman et al., 2002) and that SNX, if anything, modestly decreases release (Gasparini et al., 2001). Therefore, the increase in EPSPs by SNX is postsynaptic and is not occluded by apamin, and vice versa. Additionally, these results show that synaptic currents measured in voltage clamp with a K^+-based internal solution in the absence of channel blockers might be influenced by changes in postsynaptic conductances.

One difference between the recording conditions used here for evoked EPSP measurements and the previous work that examined synaptic responses to uncaged glutamate is that, in those previous experiments, cells were filled with Fluo-5F (300 μM), a BAPTA-based fluorescent Ca^{2+} indicator, as well as the Ca^{2+}-insensitive fluorescent dye Alexa 594 (10 μM) (Bloodgood and Sabatini, 2007). Therefore, it is possible that the presence of 300 μM Fluo-5F, which would serve as a mobile Ca^{2+} buffer (K_d = 2.3 μM), could alter the dynamics of Ca^{2+} signaling within the spine head. To test this, cells were loaded with the standard pipette solution containing Fluo-5F (300 μM) and Alexa Fluor 594 (10 μM), and synaptically evoked EPSPs were examined for the effects of apamin and SNX. Under these conditions, apamin still increased peak EPSPs (133% ± 14% of control; $n = 8$, $p < 0.05$). Moreover, the effects of apamin were not occluded by SNX in the presence of the indicators; apamin still increased EPSP peaks compared to baseline recorded in SNX (140% ± 6%; $n = 7$, $p < 0.05$). These results show that the relatively low concentration of the BAPTA-based Ca^{2+} indicator, Fluo-5F, did not markedly alter the independent boosting effects of apamin following SNX pretreatment.

The Boosting Effect of SNX Requires Ca^{2+} Influx

To determine whether Ca^{2+} influx through NMDARs is required for the boosting effect of SNX, baseline EPSPs were recorded in the presence of apamin and D-AP5 prior to application of SNX. Under these conditions, SNX increased EPSPs to 142% ± 17% ($n = 9$, $p < 0.05$) (Figures 4A and 4B), suggesting that Ca^{2+} influx through NMDARs is not necessary for SNX boosting of EPSPs and that Ca^{2+} influx through SNX-sensitive, R-type Ca^{2+} channels is required for the boosting effect of SNX on synaptically evoked EPSPs. To test whether an increase in Ca^{2+} mobilization is required for SNX boosting of EPSPs, BAPTA (5 mM) was included in the internal patch pipette solution. Under these conditions, SNX still increased the EPSPs to 142% ± 10% ($n = 9$, $p < 0.01$) in the presence of apamin. Increasing the concentration of BAPTA in the patch pipette solution to 10 mM blocked the increase in EPSP by SNX (EPSP peak: 110% ± 8% compared to baseline in apamin alone; $n = 10$) (Figures 4C and 4D). Therefore, an increase in Ca^{2+} mobilization is required for the boosting of EPSPs by SNX, suggesting that Ca^{2+} entry through SNX-sensitive, R-type Ca^{2+} channels is necessary and that Ca^{2+} flowing into the spine head through R-type channels works within a very short intermolecular distance.

SNX Boosting of Synaptic Responses Requires $K_V4.2$-Containing Channels

These results raise the question of how blockade of an inward, depolarizing Ca^{2+} current increases EPSPs. In principle, Ca^{2+} entry may activate a Ca^{2+}-dependent K^+ current that repolarizes the membrane potential, reducing EPSPs; blocking the Ca^{2+}

source would boost EPSPs. However, the results presented above argue against that being an apamin-sensitive SK channel. There are three other types of Ca^{2+}-dependent K^+ channels. Big conductance Ca^{2+}-activated K^+ (BK) channels, sensitive to Iberiotoxin (IbTx), are expressed in CA1 pyramidal neurons (Bloodgood and Sabatini, 2007), as are the as yet molecularly unidentified Ca^{2+}-dependent K^+ channels underlying the slow afterhyperpolarization (sAHP) (Gerlach et al., 2004; Madison and Nicoll, 1984). The third class is the intermediate conductance Ca^{2+}-activated K^+ channel, a member of the SK family that is not apamin sensitive but is blocked by the organic compound 1-[(2-Chlorophenyl) diphenylmethyl]-1*H*-pyrazole (TRAM- 34 [Wulff et al., 2000]) and has a very limited expression profile in central neurons. To test whether any of these channel types are coupled to Ca^{2+} entry through SNX-sensitive, R-type Ca^{2+} channels in CA1 pyramidal neurons, cells were pretreated with a cocktail of blockers (apamin, 100 nM; IbTx, 100 nM; carbachol, 5 μM; TRAM-34, 1 μM) to block SK, BK, sAHP, and IK channels, respectively. In the presence of this cocktail, SNX still increased EPSPs to 163% ± 15% of baseline ($n = 6$, $p < 0.05$) (Figures 5A and 5B).

How, then, does Ca^{2+} entry through SNX-sensitive, R-type Ca^{2+} channels boost EPSPs? The 4-AP-sensitive, A-type K^+ channels that contain $K_V4.2$ subunits are expressed in dendritic spines on CA1 pyramidal neurons and influence dendritic excitability and synaptic currents (Chen et al., 2006; Kim et al., 2007). Although these channels are intrinsically voltage dependent, native $K_V4.2$-containing channels are multiprotein complexes that include the Ca^{2+} binding proteins, K^+ channel interacting proteins (KChIPs), as auxiliary subunits (Rhodes et al., 2004). A recent report has

shown that in cerebellar stellate cells, Ca^{2+} entry through T-type Ca^{2+} channels acting via KChIPs shifts A-type channel availability to more negative potentials (Anderson et al., 2010). A similar shift in CA1 would increase the number of A-type channels available to open during an EPSP. Similarly, the activity-dependent trafficking of $K_V4.2$ in CA1 requires KChIPs (Lin et al., 2010a). To test whether SNX-sensitive, R-type Ca^{2+} channels boost EPSPs via effects on 4-AP-sensitive, A-type K^+ channels, we obtained baseline recordings in the presence of 4-AP (5 mM) and apamin prior to SNX application. In this case, SNX did not boost the EPSPs, being 90% ± 5% compared to baseline (n = 9; Figures 6A and 6B). These results suggest that the SNX boosting of EPSPs reveals an underlying coupling between R-type Ca^{2+} channels and activation of a 4-AP-sensitive current such as the A-type K^+ channel. Alternatively, it is possible that SNX has off-target effects at 0.3 µM and blocks 4-AP-sensitive, A-type channels. While this seems unlikely (Newcomb et al., 1998), we examined the effects of SNX (0.3 µM) on the 4-AP-sensitive, A-type transient outward current measured in voltage clamp in CA1 neurons. Although adequate voltage clamp control of CA1 neurons in slices is unlikely, the relative effects of SNX on the 4-AP-sensitive current can be used to qualitatively test whether SNX blocks the A-type current. For these experiments, Ca^{2+}-free artificial cerebrospinal fluid (aCSF) was supplemented with Mn^{2+} (2 mM) and tetrodotoxin (TTX; 1 µM) to block voltage-gated Ca^{2+} and Na^{2+} channels, respectively. Under these conditions, depolarization from -80 to 40 mV revealed an outward current that was partially blocked by 10 mM 4-AP (Figure 6C). Addition of SNX (0.3 µM) prior to addition of 4-AP had little effect on the total current and the 4-AP-sensitive component was not blocked by SNX (Figure 6C, inset). The average effect of SNX on the 4-AP-sensitive current was 96.8% ± 2.0% (n = 8, p

= 0.15; Figure 6D). Furthermore, SNX had no effect on the noninactivating, 4-AP-insensitive component (102.1% ± 2.2%, p = 0.9). Thus, SNX does not block the A-type current in CA1 pyramidal neurons. However, Kimm and Bean (2013, SFN, abstract) reported that SNX-482 blocks IA currents in cerebellar stellate cells (that contain primarily $K_V4.3$ channels) but not in cultured cerebellar granule cells (that contain primarily $K_V4.2$ channels). While we showed that SNX-482 does not block A-type current in hippocampal CA1 cells in voltage clamp and that dialysis with BAPTA occluded the SNX boosting of EPSPs, we cannot rule out an effect of SNX-482 on a subpopulation of Kv4 channels in CA1.

To determine whether the SNX boosting of EPSPs is mediated by an A-type channel that contains $K_V4.2$ subunits, a $K_V4.2$ dominant negative subunit, $K_V4.2$(W362F) (Kim et al., 2005), and enhanced GFP (eGFP) were expressed in CA1 pyramidal neurons using in utero electroporation of e16 embryos. Recordings were performed at 4–6 weeks of age. In eGFP-positive cells, SNX application did not affect peak EPSPs, being 99% ± 7% compared to baseline in apamin (n = 9; Figures 7A and 7B). As a control, non-eGFP-positive cells were studied, and SNX increased the EPSPs (159% ± 14%, n = 9, p < 0.01).

Finally, to test the hypothesis that KChIPs has an integral role in the SNX boosting of EPSPs, CA1 neurons were dialyzed with a pan-KChIPs antibody that has been shown to interrupt the coupling between T-type Ca^{2+} channels and A-type K^+ channels in cerebellar stellate cells (Anderson et al., 2010). Dialysis of CA1 pyramidal neurons with the pan-KChIPs antibody (20 µg/ml) occluded the boosting effect of SNX (105.7% ± 5.9%, n = 9, p = 0.37; Figure 8A, closed symbols, and Figure 8B). As a control,

SNX boosting of EPSPs in CA1 neurons dialyzed with a similar immunoglobulin G2a isotype antibody (lipoprotein-related protein 4 [LRP4]; 20 μg/ml) was 150.9% ± 13.6% ($n = 6$, $p < 0.01$; Figures 8A and 8C). Additionally, the pan-KChIPs antibody did not interfere with Ca^{2+} signaling for synaptic activation of SK channels, as apamin boosting of EPSPs was 143.4% ± 15.3% ($n = 8$, $p < 0.05$) in neurons dialyzed with the pan-KChIPs antibody.

DISCUSSION

The results presented here show that, in CA1 pyramidal neurons, blocking either apamin-sensitive SK channels or SNX-sensitive Ca^{2+} channels, presumably R-type, boosted synaptically evoked EPSPs, and the effects of apamin and SNX were not mutually exclusive. Preblocking NMDARs occluded the boosting of synaptic potentials by apamin, but not that of SNX, suggesting that Ca^{2+} entry through NMDARs is required for activation of synaptic SK channels but is not required for the effects of SNX. The boosting effect of SNX, on the other hand, required 4-AP-sensitive $K_V4.2$-containing channels and KChIPs, suggesting that Ca^{2+} influx through R-type Ca^{2+} channels is coupled to the availability of $K_V4.2$-containing channels.

The results are in contrast to those obtained by 2-photon laser uncaging of glutamate onto single spines, in which the increase in uEPSPs was not different when SNX was present with or without apamin in the bath (Bloodgood and Sabatini, 2007). One advantage of glutamate uncaging is that presynaptic effects on transmitter release are bypassed. It has been previously reported at mossy fiber and associative-commissural synapses on CA3 pyramidal neurons that Ca^{2+} channels sensitive to low concentrations of Ni^{2+} contribute to glutamate release during minimal synaptic stimulation (Gasparini et al., 2001). Similarly, using a Cs^{+}-based internal solution optimized to minimize K^{+}, Na^{+}, Ca^{2+}, and Ca^{2+} activated channels, SNX but not apamin decreased the EPSCs measured in voltage clamp. In contrast, if a K^{+}-based internal solution without pharmacological blockers of Na^{+} and Ca^{2+} channels is used, either apamin or SNX increased the EPSCs measured in voltage clamp by 33% and 37%, respectively. Similarly, it has been shown that, in cultured hippocampal neurons,

4-AP increased miniature EPSCs using a K^+-based internal solution and the increase was greater at a holding potential of -60 mV compared to -80 mV (Kim et al., 2007). These results suggest that the consequence of voltage clamp escape is considerably greater when using a K^+-based internal solution to measure EPSCs and that the EPSCs contain, in part, a postsynaptic outward current component. This may influence results obtained by glutamate uncaging when the uncaging laser power is adjusted to achieve a standard glutamate-evoked EPSC at -60 mV for different bath conditions using a K^+-based internal solution (Bloodgood and Sabatini, 2007). Consequently, a lower amount of glutamate uncaging may occur when SNX and/or apamin is in the bath, compared to control solutions. Therefore, it is possible that the discrepancy between our results and those of Bloodgood and Sabatini (2007) is the result of differences in glutamate uncaging due to adjusting the uncaging laser strength under different bath conditions where the neuron is not used as its own control. In contrast, synaptically evoked glutamate release in which the neuron is used as its own control for measuring the effects of apamin or SNX revealed that SNX does not occlude the apamin-mediated boosting of EPSPs.

Synaptic SK channel activity also has been shown to reduce EPSPs in cortical Layer 5 pyramidal neurons. In response to single synaptic stimulations, apamin boosted EPSPs and the apamin effect was occluded by blocking NMDAR, L-type Ca^{2+} channels, R-type Ca^{2+} channels, or Ca^{2+} release from intracellular stores, leading to the conclusion that all of these Ca^{2+} sources contributed to activating synaptic SK channels and blocking any one of them was sufficient to occlude synaptic SK channel activation. Interestingly, in the presence of nicardipine to block L-type Ca^{2+} channels and SNX to block R-type Ca^{2+} channels, synaptic SK channels were activated by a

train of stimuli, presumably due to increased Ca^{2+} influx through NMDARs, especially late in the train (Faber, 2010). Thus, spine Ca^{2+} dynamics may differ across different classes of synapses.

One central result from CA1 spines is that either by glutamate uncaging or synaptic stimulations, blocking SNX-sensitive, R-type Ca^{2+} channels boosts synaptic responses. The SNX effect did not require Ca^{2+} influx through NMDARs but did require a change in internal Ca^{2+}, as SNX did not increase synaptic responses when BAPTA was included in the internal pipette solution. Presumably, the source of Ca^{2+} is influx through R-type channels. The finding that blocking an inward, depolarizing Ca^{2+} current increased rather than decreased EPSPs suggested that the effect ultimately might be mediated by suppression of a Ca^{2+}-activated K current. Yet, applying a cocktail of blockers to eliminate the canonical Ca^{2+}-activated K channels (BK, SK, IK, and the sAHP channels) failed to occlude the SNX-induced increase in EPSPs. In contrast, application of 4-AP did occlude the SNX-induced increase of EPSPs, suggesting the involvement of an A-type, voltage-gated K^+ channel (I_A). $K_V4.2$ subunits are a major component of I_A in CA1 pyramidal neurons (Chen et al., 2006; Kim et al., 2005), and our results showing that expression of a $K_V4.2$ dominant negative abolishes the SNX boosting strongly support the model that SNX-sensitive Ca^{2+} channels are tightly coupled to regulation of availability of a $K_V4.2$-containing I_A channel.

$K_V4.2$ subunits are components of a multiprotein complex that includes the KChIPs (Rhodes et al., 2004), Ca^{2+} binding proteins that influence surface expression levels and biophysical attributes of K_V4-containing channels. Recently, it has been shown

that K_V4-containing channels in cerebellar stellate cells form a molecular complex with T-type Ca^{2+} channels; Ca^{2+} influx through mifebridil-sensitive, T-type Ca^{2+} channels maintains the voltage dependence of availability of K_V4-containing channels in the physiological range, in a KChIPs-dependent manner. Blocking T-type channels induced an ~10 mV hyperpolarizing shift in the voltage dependence of availability of I_A (Anderson et al., 2010). This shift was occluded by inclusion of 10 mM BAPTA or a pan-KChIPs antibody in the patch pipette internal solution, reflecting the close molecular proximity of K_V4-containing channels in complex with KChIPs and T-type channels. In CA1 pyramidal neurons, SNX-sensitive, R-type Ca^{2+} channels are primarily expressed in dendritic spines (Bloodgood and Sabatini, 2007) and, while the precise mechanism is not yet established, the present results are consistent with a similar tight coupling to K_V4-containing channels such that Ca^{2+} influx through R-type Ca^{2+} channels shifts the voltage dependence of availability of K_V4-containing channels, allowing them to be activated during synaptic transmission. Consistent with this assertion is that dialysis with a pan-KChIPs antibody abolished the boosting of EPSPs by SNX.

SK2-containing channels and $K_V4.2$-containing channels are both expressed in dendritic spines on CA1 pyramidal neurons and their activities limit synaptic responses. Both channel types also undergo long-term-potentiation-dependent (LTP-dependent) endocytosis, thereby contributing to the expression of LTP, and their trafficking is regulated by direct phosphorylation by protein kinase A (PKA; Cai et al., 2004; Kim et al., 2007; Lin et al., 2008; Marino et al., 1998). The LTP- and PKA-dependent endocytosis of $K_V4.2$-containing channels, but not their contribution to

basal synaptic responses, requires NMDAR activity. In this regard, it is interesting that immuno-EM studies demonstrate that SK2 is expressed in the PSD and shows a similar synaptic distribution as seen for NMDARs, suggesting a close anatomical arrangement (Lin et al., 2008). In contrast, $K_V4.2$ immunoparticles were detected in postsynaptic spines but not directly in the PSD (Kim et al., 2007). Indeed, this extrasynaptic localization of $K_V4.2$ is similar to the predominantly extrasynaptic localization of $Ca_V2.3$ (Parajuli et al., 2012). Taken together with the ability of 10 mM BAPTA in the pipette solution to block the effect of SNX, these results suggest that $K_V4.2$-containing channels and SNX-sensitive, R-type Ca^{2+} channels are closely coupled at extrasynaptic sites in spines. The colocalization of SK2-containing channels and NMDARs to the PSD and $K_V4.2$-containing channels and R-type Ca^{2+} channels to extrasynaptic sites therefore defines two Ca^{2+} signaling sources within spines. Interestingly, in the dendrites of CA1 pyramidal neurons, SK and K_V4-containing channels serve complementary roles in shaping the time course and extent of branch-specific dendritic excitability (Cai et al., 2004). Thus, SK channels and $K_V4.2$-containing channels may serve synergistic roles in regulating synaptic responses, the induction and expression of synaptic plasticity, and dendritic integration.

Many previous studies have concluded that fast excitatory transmission reflects glutamate receptor activation, as blocking a-amino-3-hydroxy-5-methyl-4-isozazolepropionic receptors and NMDARs abolished the excitatory postsynaptic response. However, the present results demonstrate a large contribution from two types of K^+ channels. Indeed, apamin and SNX each boosted synaptic responses, and

the lack of occlusion demonstrates that their combined contribution approximately doubles the EPSPs. Thus, together these two synaptic K^+ channels reduce the depolarizing component of EPSPs by at least 50%, suggesting that signaling cascades that alter their activities might potently regulate excitatory transmission. For example, cholinergic signaling in hippocampus by muscarinic acetylcholine receptors, previously thought to boost EPSPs and facilitate the induction of LTP by increasing NMDAR activity (Aramakis et al., 1999; Marino et al., 1998; Markram and Segal, 1990), has recently been shown instead to decrease SK channel activity, leading to increased excitatory responses and LTP (Buchanan et al., 2010; Giessel and Sabatini, 2010). It is also important to note that, in addition to the influence of repolarizing K^+ currents, Ca^{2+}-activated Cl^- channels (transmembrane protein 16B) that are closely coupled to NMDARs similarly dampen EPSPs (Huang et al., 2012), adding to the inhibitory repertoire that modulates synaptic signals.

MATERIAL AND METHODS

Slice Preparation All procedures were done in accordance with federal guidelines and were approved by the institutional review board at Oregon Health & Science University. Hippocampal slices were prepared from C57BL/6J mice from postnatal week 4–6. Animals were anesthetized by isofluorane and decapitated. The cerebral hemispheres were quickly removed and placed into cold aCSF equilibrated with 95% O_2/5% CO_2. Hippocampi were removed, placed onto an agar block, and transferred into a slicing chamber containing sucrose-aCSF. Transverse hippocampal slices (300 mm) were cut with a Leica VT1000s, transferred into a holding chamber containing regular aCSF (125 mM NaCl, 2.5 mM KCl, 21.4 mM $NaHCO_3$, 1.25 mM NaH_2PO_4, 2.0 mM $CaCl_2$, 1.0 mM $MgCl_2$, and 11.1 mM glucose), and equilibrated with 95% O_2/5% CO_2. Slices were incubated at 35 ^{o}C for 30–45 min and then recovered at room temperature (22 ^{o}C–24 ^{o}C) for ≥1 hr before recordings were performed.

In Utero Electroporation Timed-pregnant mice were anesthetized with isofluorane, their abdominal cavity was cut open, and the uterine horns/sac were exposed. Approximately 2 ml of DNA solution (~2 mg/ml) was injected into the lateral ventricle of e16 embryos, using a glass pipette pulled from thin-walled capillary glass (TW150F-4; World Precision Instruments) and a Picospritzer III microinjection system (Parker Hannifin). The head of each embryo within its uterine sac was positioned between tweezer-type electrodes (CUY650P10; Sonidel), and five square electric pulses (50 V; 100 ms; 1 s intervals) were passed using an electroporator (CUY21; Sonidel). After electroporation, the wall and skin of the abdominal cavity of the pregnant mouse were sutured closed and embryos were allowed to develop

normally.

Electrophysiology Slices were perfused with aCSF equilibrated with 95% O_2/5% CO_2 at a flow rate of 1 ml/min. All experiments were performed at room temperature (22 ^{o}C–24 ^{o}C). CA1 pyramidal cells were visualized with infrared-differential-interference contrast optics (Zeiss Axioskop 2FS) and a charge-coupled device camera (Sony). Whole-cell patch-clamp recordings were obtained from CA1 pyramidal cells using an Axopatch 1D (Axon Instruments) interfaced to an ITC-16 analog-to-digital converter (Heka Instruments) and transferred to a computer using Patchmaster software (Heka Instruments). Patch pipettes (open pipette resistance, 2.5–3.5 MU) for EPSPs were filled with either a K-gluconate internal solution containing 133 mM K-gluconate, 4 mM KCl, 4 mM NaCl, 1 mM $MgCl_2$, 10 mM 4-(2-hydroxyethyl)-1-piperazineethanesul-fonic acid (HEPES), 4 mM MgATP, 0.3 mM Na_3 guanosine triphosphate (Na_3GTP), and 10 mM K_2-phosphocreatine (pH 7.3) or a $KMeSO_4$ internal solution containing 140 mM $KMeSO_4$, 8 mM NaCl, 1 mM $MgCl_2$, 10 mM HEPES, 5 mM MgATP, 0.4 mM Na_3GTP, and 0.05 mM EGTA (pH 7.3). EPSPs were recorded in whole-cell current-clamp mode. Input and access resistances were monitored with a 25 pA hyperpolarizing step applied at the end of each trace. All current clamp recordings used cells with a stable input resistance (range: 130–300 MΩ) and access resistance (range: 15–25 MΩ) that did not change by more than 20%. All recordings were from cells with a resting membrane potential between -70 and -60 mV. A bias current was applied to maintain the membrane potential at -65 mV. Series resistance was not electronically compensated. For EPSC recordings in voltage clamp mode, patch pipettes were filled with a Cs^+-based solution containing 130 mM

$CsMeSO_4$, 10 mM CsCl, 10 mM HEPES, 0.4 mM Na_3GTP, 2 mM MgATP, 10 mM Tris-phosphocreatine, 3.35 mM QX-314, 0.2 mM D600, and 5 mM BAPTA (pH with CsOH to 7.2). Series resistance was not electronically compensated. Input resistance was monitored with a 5 mV hyperpolarizing step applied at the beginning of each trace. All voltage-clamp recordings used cells with a stable input and access resistances that did not change by more than 20%. For whole cell recording of A-type outward K^+ currents, patch pipettes were filed with 120 mM K-gluconate, 20 mM KCl, 10 mM HEPES, 0.2 mM EGTA, 8 mM NaCl, 4 mM MgATP, 0.3 mM Na_3GTP, and 14 mM Tris-phosphocreatine (pH 7.3). For whole-cell recording of A-type currents, the series resistance was ~80% compensated. Input resistance was monitored with a 5 mV hyperpolarizing step applied at the beginning of each trace. All voltage-clamp recordings used cells with a stable input and access resistances that did not change by more than 20%.

Synaptic Stimulation Presynaptic axons in stratum radiatum were stimulated using capillary glass pipettes filled with aCSF, with a tip diameter of ~5 μm, connected to an Iso-Flex stimulus isolation unit (A.M.P.I.). Stimulation electrodes were placed at ~100 μm from the soma and ~20 μm adjacent to the dendrite of the recorded cell. Gamma-aminobutyric acid (GABA)ergic blockers SR95531 (2 μM) and CGP55845 (1 μM) were present to reduce $GABA_A$ and $GABA_B$ contributions, respectively. To prevent epileptic discharges in the presence of GABAergic blockers, the CA3 region was microdissected out before recording. The input resistance was determined from a 25 pA hyperpolarizing current injection pulse given 500 ms after each synaptically evoked EPSP. Subthreshold EPSPs were elicited by 100 μs current injections that

were approximately one-third of the stimulus required for evoking an action potential. All recordings used cells with a resting membrane potential less than -60 mV that did not change by more than 2 mV during an experiment and with a stable input resistance that did not change by more than 20%.

Data Analysis Data were analyzed using IGOR (WaveMetrics). Data are expressed as mean ± SEM. Paired t tests or Wilcoxon-Mann-Whitney two-sample rank test was used to determine significance; $p < 0.05$ was considered significant.

Pharmacology Apamin was from Calbiochem; D-AP5, QX314, SR95531, and CGP55845 were from Tocris Cookson; SNX-482 was from Peptides International; IbTx and TRAM-34 were from Alomone; and carbachol and 4-AP were from Sigma. Pan-KChIPs (K55/82) and LRP4 (N207/27) antibodies were obtained from UC/Davis Neuromab Facility (Antibodies Incorporated).

REFERENCES

Anderson, D., Mehaffey, W.H., Iftinca, M., Rehak, R., Engbers, J.D., Hameed, S., Zamponi, G.W., and Turner, R.W. (2010).

Regulation of neuronal activity by Cav3-Kv4 channel signaling complexes.

Nat. Neurosci. *13*, 333–337.

Aramakis, V.B., Bandrowski, A.E., and Ashe, J.H. (1999).

Role of muscarinic receptors, G-proteins, and intracellular messengers in muscarinic modulation of NMDA receptor-mediated synaptic transmission.

Synapse *32*, 262–275.

Bloodgood, B.L., and Sabatini, B.L. (2007).

Nonlinear regulation of unitary synaptic signals by CaV(2.3) voltage-sensitive calcium channels located in dendritic spines.

Neuron *53*, 249–260.

Buchanan, K.A., Petrovic, M.M., Chamberlain, S.E., Marrion, N.V., and Mellor, J.R. (2010).

Facilitation of long-term potentiation by muscarinic M(1) receptors is mediated by inhibition of SK channels.

Neuron *68*, 948–963.

Cai, X., Liang, C.W., Muralidharan, S., Kao, J.P., Tang, C.M., and Thompson, S.M. (2004).

Unique roles of SK and Kv4.2 potassium channels in dendritic integration.

Neuron *44*, 351–364.

Chen, X., Yuan, L.L., Zhao, C., Birnbaum, S.G., Frick, A., Jung, W.E., Schwarz, T.L., Sweatt, J.D., and Johnston, D. (2006).

Deletion of Kv4.2 gene eliminates dendritic A-type K^+ current and enhances induction of long-term potentiation in hippocampal CA1 pyramidal neurons.

J. Neurosci. *26*, 12143–12151.

Faber, E.S. (2010).

Functional interplay between NMDA receptors, SK channels and voltage-gated Ca^{2+} channels regulates synaptic excitability in the medial prefrontal cortex.

J. Physiol. *588*, 1281–1292.

Gasparini, S., Kasyanov, A.M., Pietrobon, D., Voronin, L.L., and Cherubini, E. (2001).

Presynaptic R-type calcium channels contribute to fast excitatory synaptic transmission in the rat hippocampus.

J. Neurosci. *21*, 8715–8721.

Gerlach, A.C., Maylie, J., and Adelman, J.P. (2004).

Activation kinetics of the slow afterhyperpolarization in hippocampal CA1 neurons.

Pflugers Arch. *448*, 187–196.

Giessel, A.J., and Sabatini, B.L. (2010).

M1 muscarinic receptors boost synaptic potentials and calcium influx in dendritic spines by inhibiting postsynaptic SK channels.

Neuron *68*, 936–947.

Giessel, A.J., and Sabatini, B.L. (2011).

Boosting of synaptic potentials and spine Ca transients by the peptide toxin SNX-482 requires alpha-1E-encoded voltage-gated Ca channels.

PLoS ONE *6*, e20939.

Huang, W.C., Xiao, S., Huang, F., Harfe, B.D., Jan, Y.N., and Jan, L.Y. (2012).

Calcium-activated chloride channels (CaCCs) regulate action potential and synaptic response in hippocampal neurons.

Neuron *74*, 179–192.

Kim, J., Wei, D.S., and Hoffman, D.A. (2005).

Kv4 potassium channel subunits control action potential repolarization and frequency-dependent broadening in rat hippocampal CA1 pyramidal neurones.

J. Physiol. *569*, 41–57.

Kim, J., Jung, S.C., Clemens, A.M., Petralia, R.S., and Hoffman, D.A. (2007).

Regulation of dendritic excitability by activity-dependent trafficking of the A-type K^+ channel subunit Kv4.2 in hippocampal neurons.

Neuron *54*, 933–947.

Lin, M.T., Luja´ n, R., Watanabe, M., Adelman, J.P., and Maylie, J. (2008).

SK2 channel plasticity contributes to LTP at Schaffer collateral-CA1 synapses.

Nat. Neurosci. *11*, 170–177.

Lin, L., Sun, W., Wikenheiser, A.M., Kung, F., and Hoffman, D.A. (2010a).

KChIP4a regulates Kv4.2 channel trafficking through PKA phosphorylation.

Mol. Cell. Neurosci. *43*, 315–325.

Lin, M.T., Lujan, R., Watanabe, M., Frerking, M., Maylie, J., and Adelman, J.P. (2010b).

Coupled activity-dependent trafficking of synaptic SK2 channels and AMPA receptors.

J. Neurosci. *30*, 11726–11734.

Madison, D.V., and Nicoll, R.A. (1984).

Control of the repetitive discharge of rat CA 1 pyramidal neurones in vitro.

J. Physiol. *354*, 319–331.

Marino, M.J., Rouse, S.T., Levey, A.I., Potter, L.T., and Conn, P.J. (1998).

Activation of the genetically defined m1 muscarinic receptor potentiates N-methyl-D-aspartate (NMDA) receptor currents in hippocampal pyramidal cells.

Proc. Natl. Acad. Sci. USA *95*, 11465–11470.

Markram, H., and Segal, M. (1990).

Acetylcholine potentiates responses to N-methyl-D-aspartate in the rat hippocampus.

Neurosci. Lett. *113*, 62–65.

Myoga, M.H., and Regehr, W.G. (2011).

Calcium microdomains near R-type calcium channels control the induction of presynaptic long-term potentiation at parallel fiber to purkinje cell synapses.

J. Neurosci. *31*, 5235–5243.

Newcomb, R., Szoke, B., Palma, A., Wang, G., Chen, X., Hopkins, W., Cong, R., Miller, J., Urge, L., Tarczy-Hornoch, K., et al. (1998).

Selective peptide antagonist of the class E calcium channel from the venom of the tarantula Hysterocrates gigas.

Biochemistry *37*, 15353–15362.

Ngo-Anh, T.J., Bloodgood, B.L., Lin, M., Sabatini, B.L., Maylie, J., and Adelman, J.P. (2005).

SK channels and NMDA receptors form a Ca^{2+}-mediated feedback loop in dendritic spines.

Nat. Neurosci. *8*, 642–649.

Parajuli, L.K., Nakajima, C., Kulik, A., Matsui, K., Schneider, T., Shigemoto, R., and Fukazawa, Y. (2012).

Quantitative regional and ultrastructural localization of the Ca(v)2.3 subunit of R-type calcium channel in mouse brain.

J. Neurosci. *32*, 13555–13567.

Rhodes, K.J., Carroll, K.I., Sung, M.A., Doliveira, L.C., Monaghan, M.M., Burke, S.L., Strassle, B.W., Buchwalder, L., Menegola, M., Cao, J., et al. (2004).

KChIPs and Kv4 alpha subunits as integral components of A-type potassium channels in mammalian brain.

J. Neurosci. *24*, 7903–7915.

Soong, T.W., Stea, A., Hodson, C.D., Dubel, S.J., Vincent, S.R., and Snutch, T.P. (1993).

Structure and functional expression of a member of the low voltage-activated calcium channel family.

Science *260*, 1133–1136.

Stackman, R.W., Hammond, R.S., Linardatos, E., Gerlach, A., Maylie, J., Adelman, J.P., and Tzounopoulos, T. (2002).

Small conductance Ca^{2+}-activated K^{+} channels modulate synaptic plasticity and memory encoding.

J. Neurosci. *22*, 10163–10171.

Wulff, H., Miller, M.J., Hansel, W., Grissmer, S., Cahalan, M.D., and Chandy, K.G. (2000).

Design of a potent and selective inhibitor of the intermediate- conductance Ca^{2+}-activated K^{+} channel, IKCa1: a potential immunosuppressant.

Proc. Natl. Acad. Sci. USA *97*, 8151–8156.

FIGURES AND LEGENDS

Figure 1

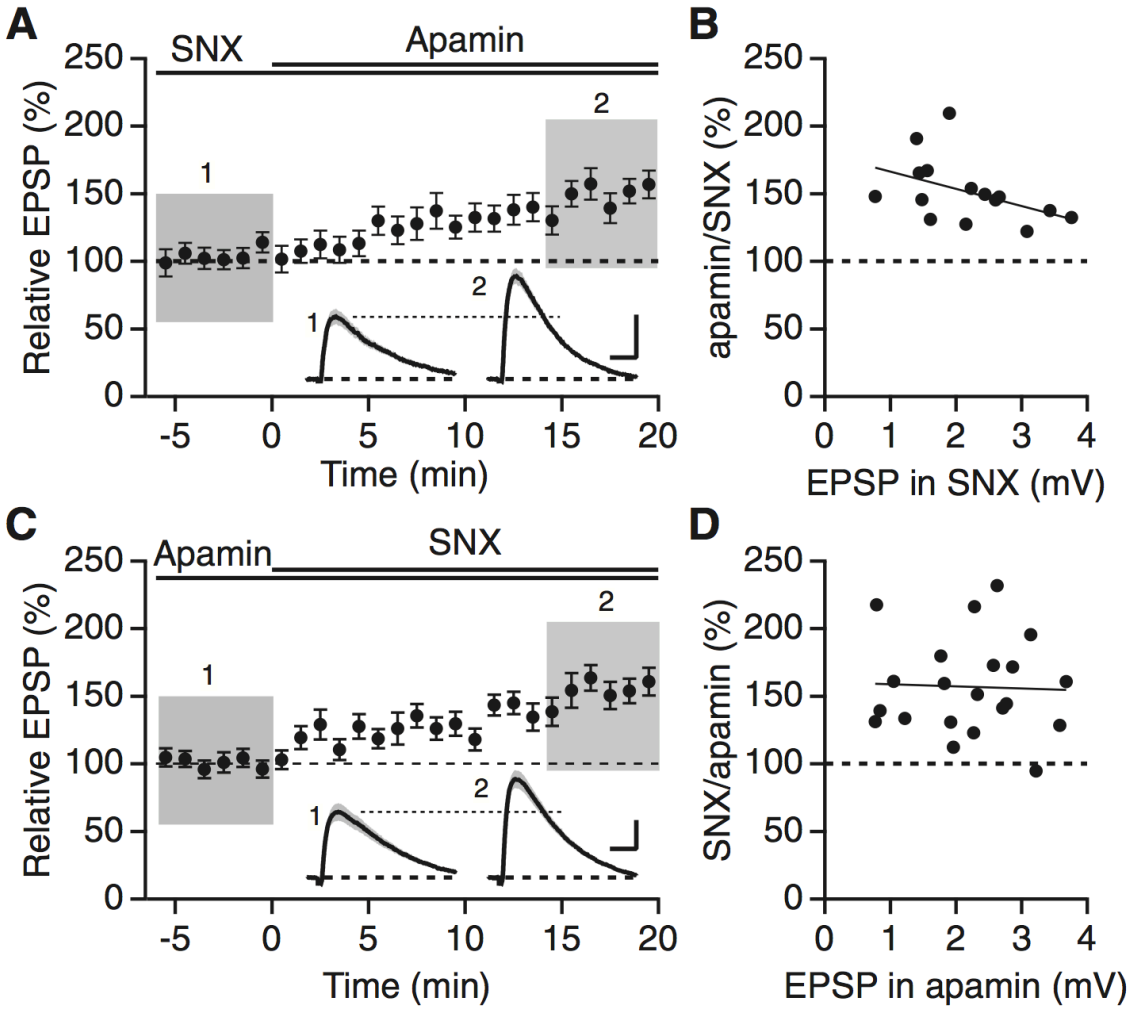

Figure 1

Boosting of EPSPs by SNX and Apamin Is Not Mutually Exclusive

(A) Time course of the normalized EPSP amplitude (mean ± SEM) for baseline in SNX and during wash-in of apamin as indicated above (n = 15). Inset shows the average of 18 EPSPs taken from indicated shaded time points in SNX (time point 1; 6 min baseline) and 14–20 min after coapplication of apamin (time point 2); shaded areas are mean ± SEM. Scale bars, 1 mV and 25 ms.

(B) Plot of relative boosting of EPSPs by apamin in the presence of SNX versus the initial EPSP in SNX. The line represents a least-square fit of the data to a liner function.

(C) Similar to (A), except baseline in apamin and during wash-in of SNX (n = 21). Insets: average EPSPs (±SEM, shaded areas) in apamin (time point 1) and after coapplication of SNX (time point 2). Scale bars, 1 mV and 25 ms.

(D) Plot of relative boosting of EPSPs by SNX in the presence of apamin versus the initial EPSP in apamin. The line represents a least-square fit of the data to a liner function.

Figure 2

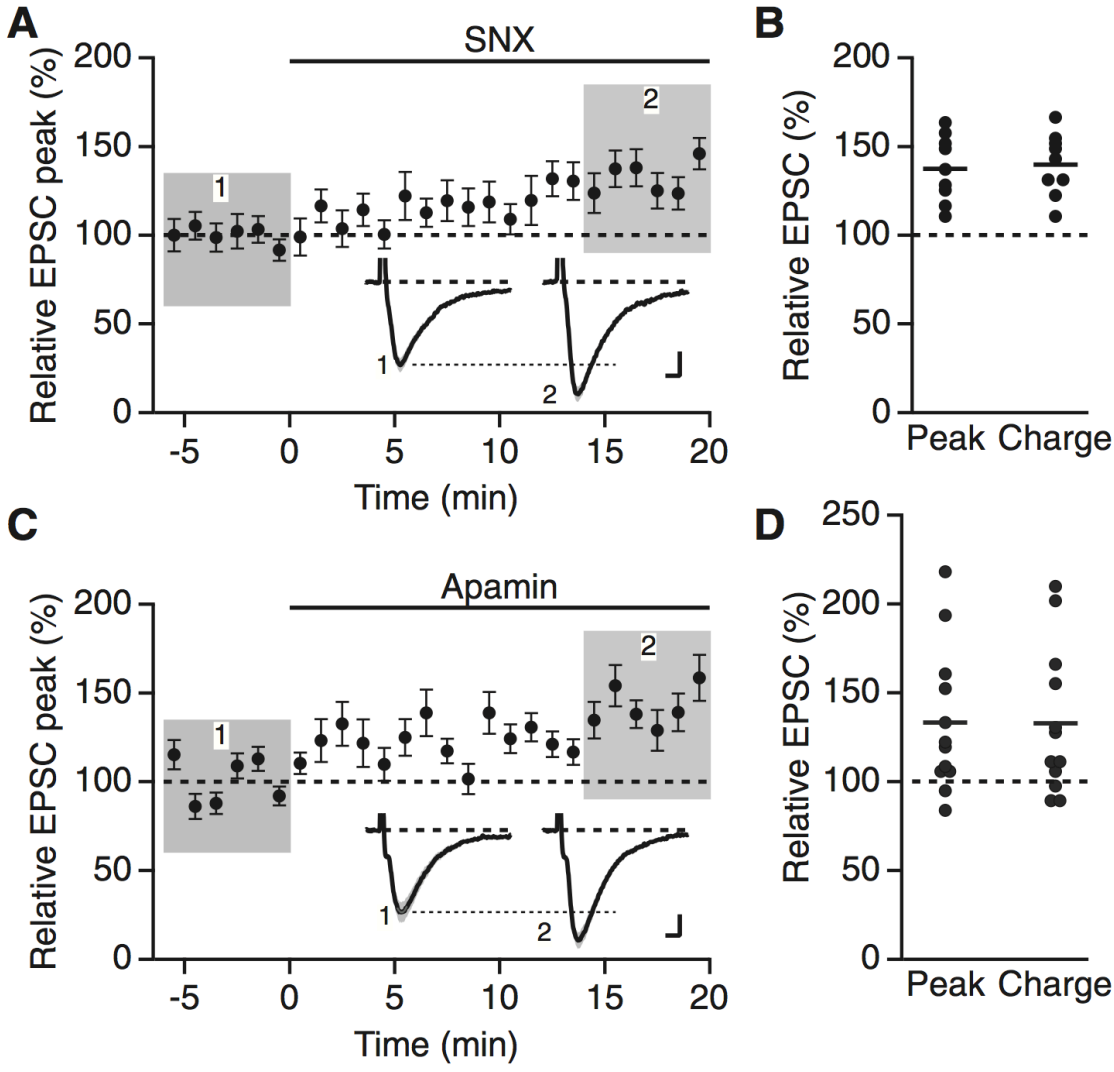
A
SNX
Relative EPSC peak (%)
200
150
100
50
0
1
2
-5
0
5
10
15
20
Time (min)
B
Relative EPSC (%)
Peak Charge
C
Apamin
D
250

Figure 2

SNX and Apamin Increase EPSCs Measured with a K^+- Based Internal Solution

(A) Time course of relative increase in peak EPSC by 0.3 μM SNX (mean ± SEM, n = 9). Insets: average of 18 EPSCs ± SEM (shaded areas) taken from indicated shaded time points for baseline (time point 1) and 14–20 min after wash-in of SNX (time point 2). Scale bars, 10 pA and 5 ms.

(B) Scatter plot of relative EPSC peak and charge in SNX compared to baseline from the individual slices in (A). Horizontal bar reflects mean response.

(C) Time course of relative increase in peak EPSC by 100 nM apamin (mean ± SEM, n = 12). Insets: average of 18 EPSCs ± SEM (shaded areas) taken from indicated shaded time points for baseline (time point 1) and 14–20 min after wash-in of apamin (time point 2). Scale bars, 10 pA and 5 ms.

(D) Scatter plot of relative EPSC peak and charge in apamin compared to baseline from the individual slices in (C). Horizontal bar reflects mean response.

Figure 3

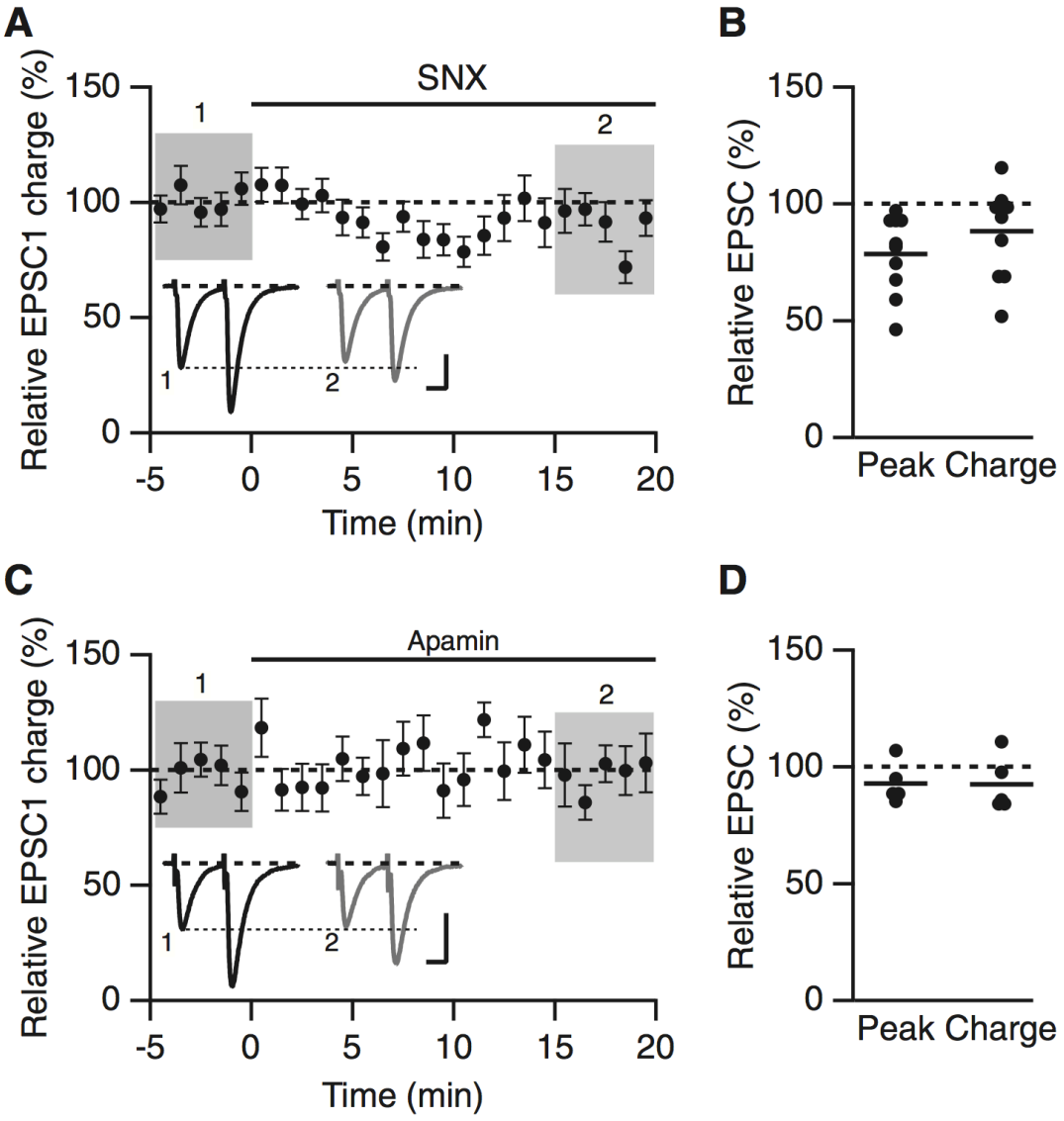
A
SNX
Relative EPSC1 charge (%)
150
100
50
0
1
2
-5
0
5
10
15
20
Time (min)
B
Relative EPSC (%)
Peak Charge
C
Apamin
D

Figure 3

Effect of SNX on Synaptic Transmission in Voltage Clamp

(A) Time course of the normalized charge transfer of the first EPSC (EPSC1; mean ± SEM) for baseline and during wash-in of SNX (n = 10). Insets: average of 15 paired EPSCs ± SEM (shaded areas) taken from indicated shaded time points for baseline (time point 1) and 15–20 min after wash-in of SNX (time point 2). Scale bars, 50 pA and 20 ms.

(B) Scatter plot of relative EPSC1 peak and charge in SNX compared to baseline from the individual slices in (A). Horizontal bar reflects mean response.

(C) Time course of the normalized charge transfer of the first EPSC (EPSC1; mean ± SEM) for baseline and during wash-in of apamin (n = 5). Insets: average of 15 paired EPSCs ± SEM (shaded areas) taken from indicated shaded time points for baseline (time point 1) and 15–20 min after wash-in of apamin (time point 2). Scale bars, 50 pA and 20 ms.

(D) Scatter plot of relative EPSC1 peak and charge in apamin compared to baseline from the individual slices in (A). Horizontal bar reflects mean response.

Figure 4

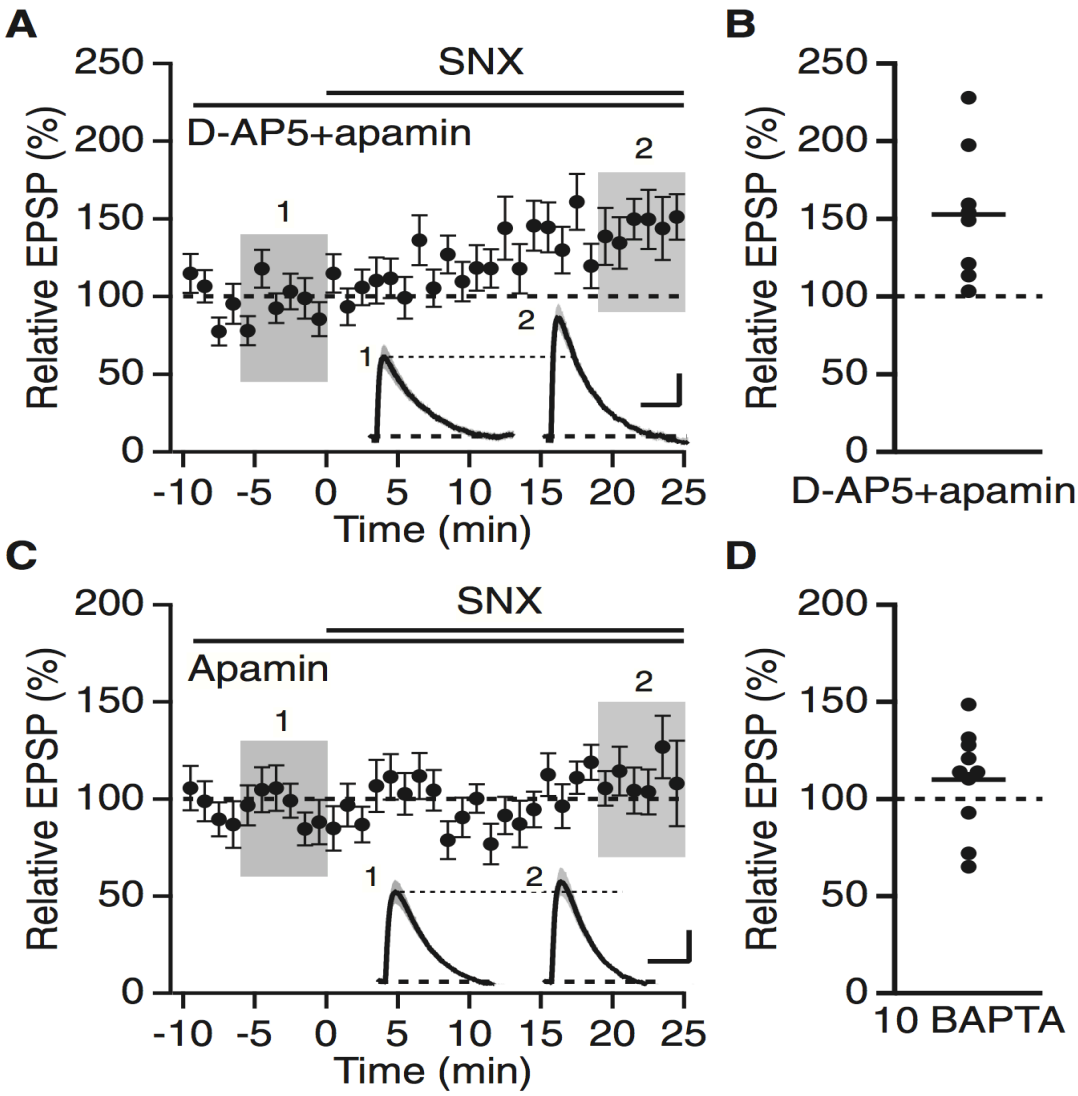
A
SNX
D-AP5+apamin
Relative EPSP (%)
250
200
150
100
50
0
1
2
-10 -5 0 5 10 15 20 25
Time (min)
B
Relative EPSP (%)
D-AP5+apamin
C
SNX
Apamin
Relative EPSP (%)
Time (min)
D
Relative EPSP (%)
10 BAPTA

Figure 4

Boosting of EPSPs by SNX Is NMDAR Independent and Ca^{2+} Dependent

(A) Time course of the normalized EPSP amplitude (mean ± SEM, n = 9) for baseline in D-AP5 and apamin and during wash-in of SNX (see Figure 1A). Inset: average of 18 EPSPs taken from indicated shaded time points in D-AP5 and apamin (time point 1) and 19–25 min after SNX wash-in (time point 2); shaded areas are ±SEM. Scale bars, 1 mV and 50 ms.

(B) Scatter plot of relative EPSP peak in SNX compared to baseline in D-AP5 and apamin from the individual slices in (A). Horizontal bar reflects mean response.

(C) Time course of the normalized EPSP amplitude (mean ± SEM, n = 10) re- corded with 10 mM BAPTA in the internal solution, for baseline in apamin and during wash-in of SNX (see Figure 1A). Inset: average of 18 EPSPs taken from indicated shaded time points in apamin (time point 1) and 19–25 min after SNX wash-in (time point 2); shaded areas are ±SEM. Scale bars, 0.5 mV and 50 ms.

(D) Scatter plot of relative EPSP peak in SNX compared to baseline in apamin from the individual slices in (C). Horizontal bar reflects mean response.

Figure 5

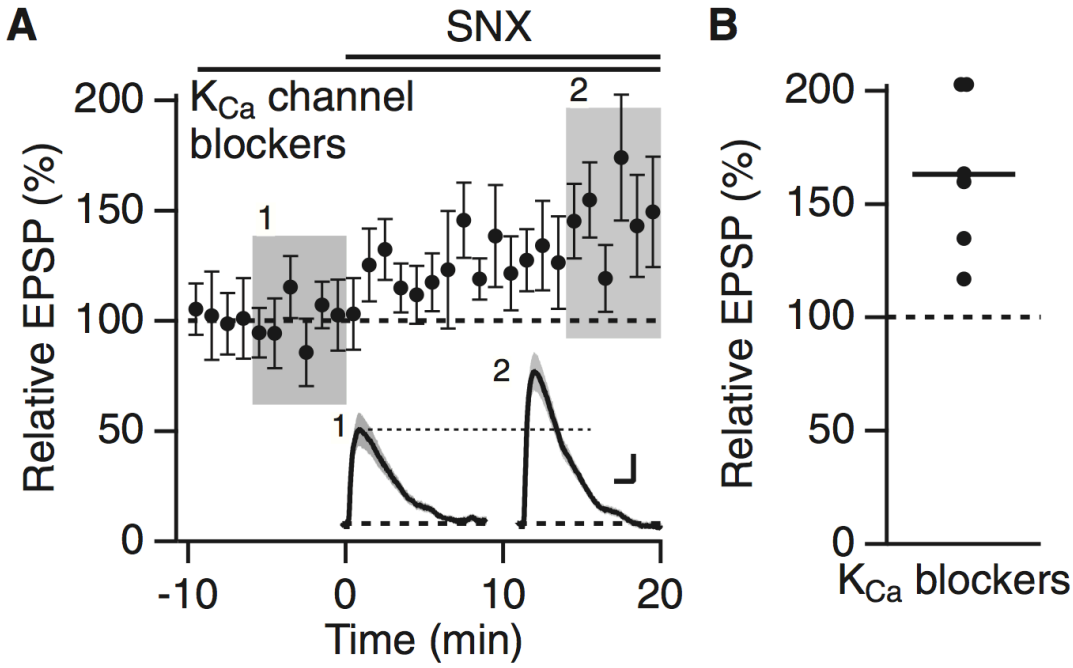
A
SNX
K_{Ca} channel blockers
1
2
200
150
100
50
0
Relative EPSP (%)
-10
0
10
20
Time (min)
B
200
150
100
50
0
Relative EPSP (%)
K_{Ca} blockers

Figure 5

Canonical K_{Ca} Channels Do Not Mediate the Boosting Effect of SNX

(A) Time course of the normalized EPSP amplitude (mean ± SEM, n = 6) for baseline in a cocktail of apamin, IbTx, TRAM-34, and carbachol, and during wash-in of SNX (see Figure 1A). Inset shows average of 18 EPSPs taken from indicated shaded time points in the cocktail of K_{Ca} blockers (time point 1) and 14–20 min after SNX wash-in (time point 2); shaded areas are ±SEM. Scale bars, 0.5 mV and 25 ms.

(B) Scatter plot of relative EPSP peak in SNX compared to baseline in the cocktail of K_{Ca} channel antagonists from the individual slices in (A). Horizontal bar reflects mean response.

Figure 6

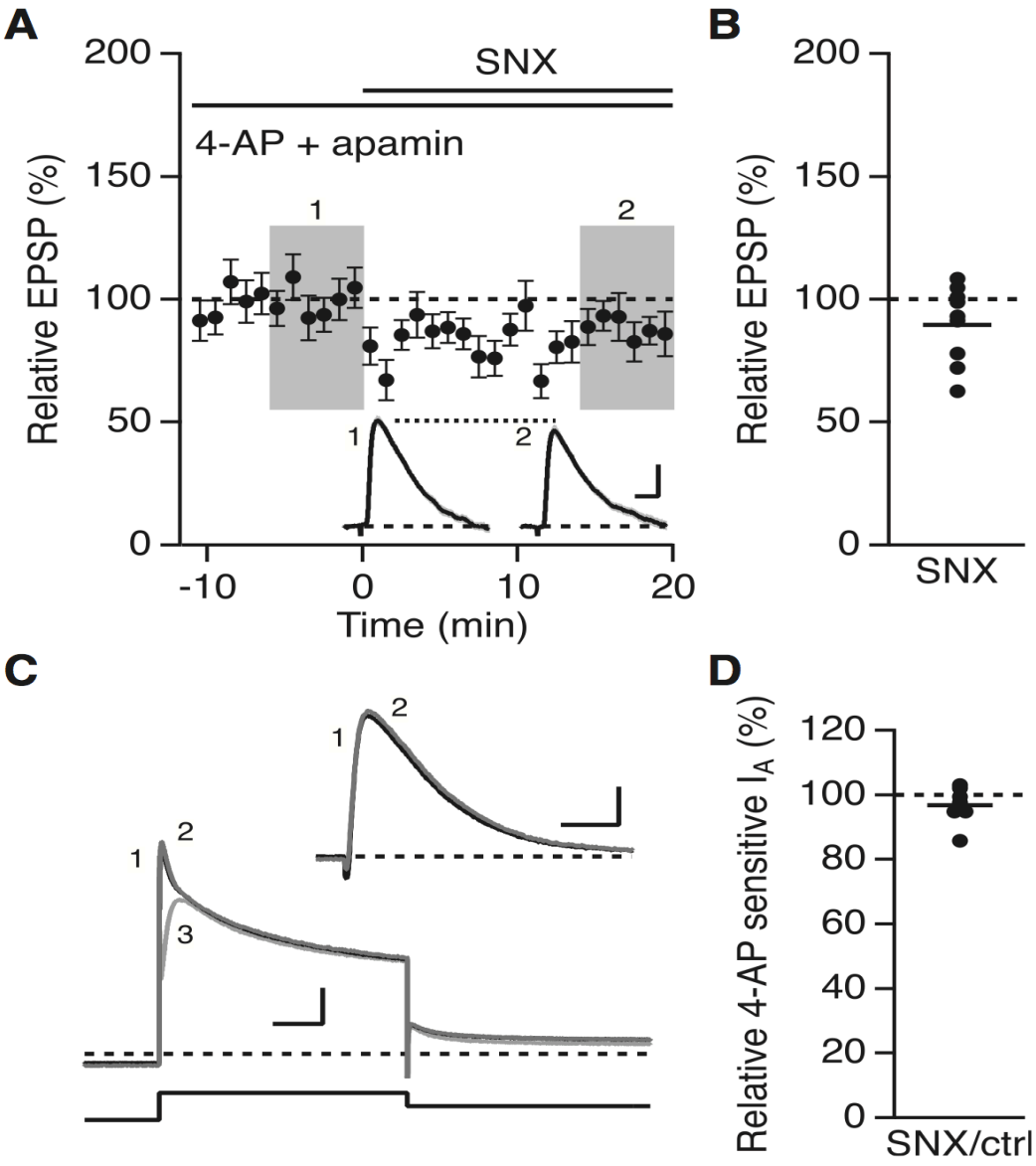
A
200
150
100
50
0
Relative EPSP (%)
SNX
4-AP + apamin
1
2
-10
0
10
20
Time (min)
B
SNX
C
3
D
120
100
80
60
40
20
0
Relative 4-AP sensitive I_A (%)
SNX/ctrl

Figure 6

4-AP Occludes the Boosting Effect of SNX

(A) Time course of the normalized EPSP amplitude (mean ± SEM, n = 9) for baseline in 4-AP and apamin and during wash-in of SNX (see Figure 1A). Inset shows average of 18 EPSPs taken from indicated shaded time points in 4-AP and apamin (time point 1) and 14–20 min after SNX wash-in (time point 2); shaded areas are ±SEM. Scale bars, 1.0 mV and 25 ms.

(B) Scatter plot of relative EPSP peak in SNX compared to baseline in 4-AP from the individual slices in (A). Horizontal bar reflects mean response.

(C) SNX does not block 4-AP-sensitive, A-type current (I_A) measured in voltage clamp. Slices were bathed in nominally Ca^{2+}-free aCSF containing TTX (1 μM) and Mn^{2+} (2 mM). In whole cell voltage clamp, A-type outward currents were elicited with 1 s depolarization to 40 mV from a holding potential of -80 mV followed by repolarization to -20 mV. Representative traces of outward current in control (trace 1), subsequent addition of SNX (trace 2), and SNX plus 4-AP (trace 3). Inset: 4-AP-sensitive current in control (trace 1) and SNX (trace 2). Scale bars, 1 nA and 20 ms.

(D) Scatter plot of individual slices for relative 4-AP-sensitive I_A current in SNX. Horizontal bar reflects mean response.

Figure 7

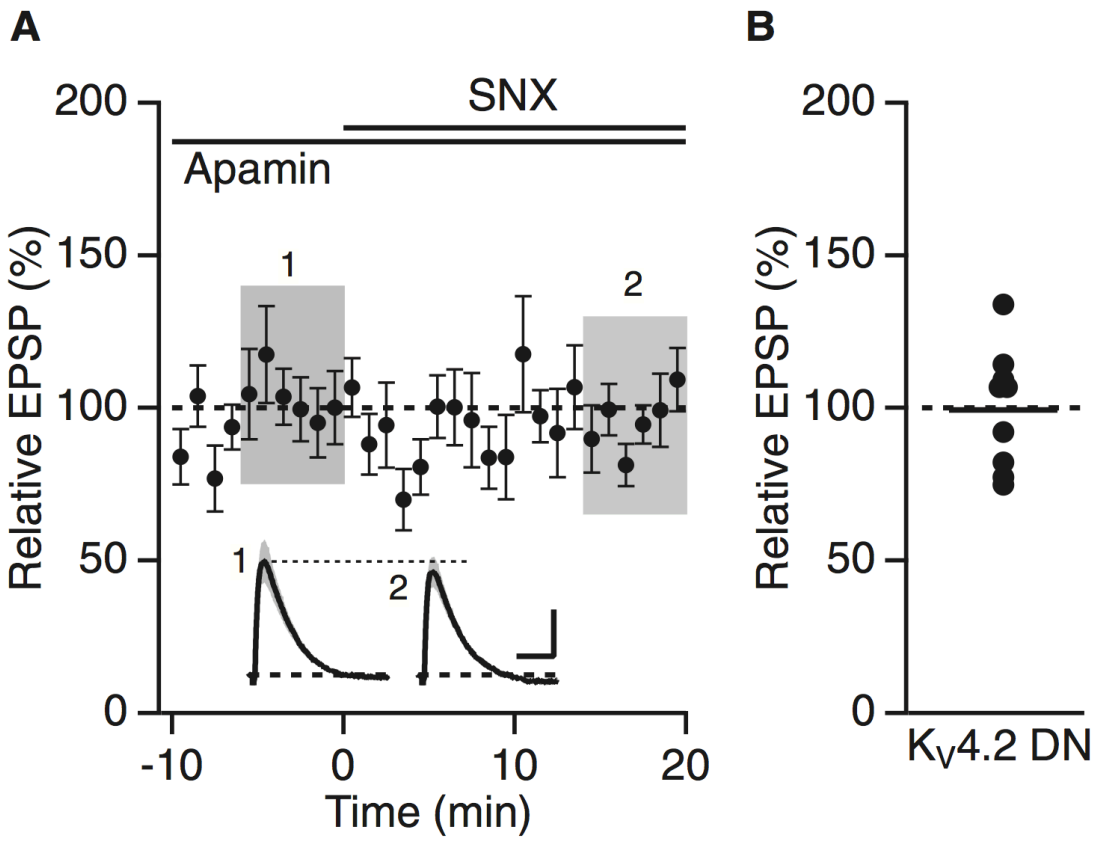
A
B
SNX
Apamin
200
150
100
50
0
Relative EPSP (%)
1
2
-10
0
10
20
Time (min)
K_V4.2 DN

Figure 7

Expression of K_V4.2(W362F) Abolishes the Boosting Effect of SNX

(A) Recordings from cells expressing K_V4.2(W362F). Time course of the normalized EPSP amplitude (mean ± SEM, n = 9) for baseline in apamin and during wash-in of SNX (see Figure 1A). Inset shows average of 18 EPSPs taken from indicated shaded time points in apamin (time point 1) and 14–20 min after SNX wash-in (time point 2); shaded areas are ±SEM. Scale bars, 1 mV and 50 ms.

(B) Scatter plot of relative EPSP peak in SNX compared to baseline in apamin from the individual slices in (A). Horizontal bar reflects mean response.

Figure 8

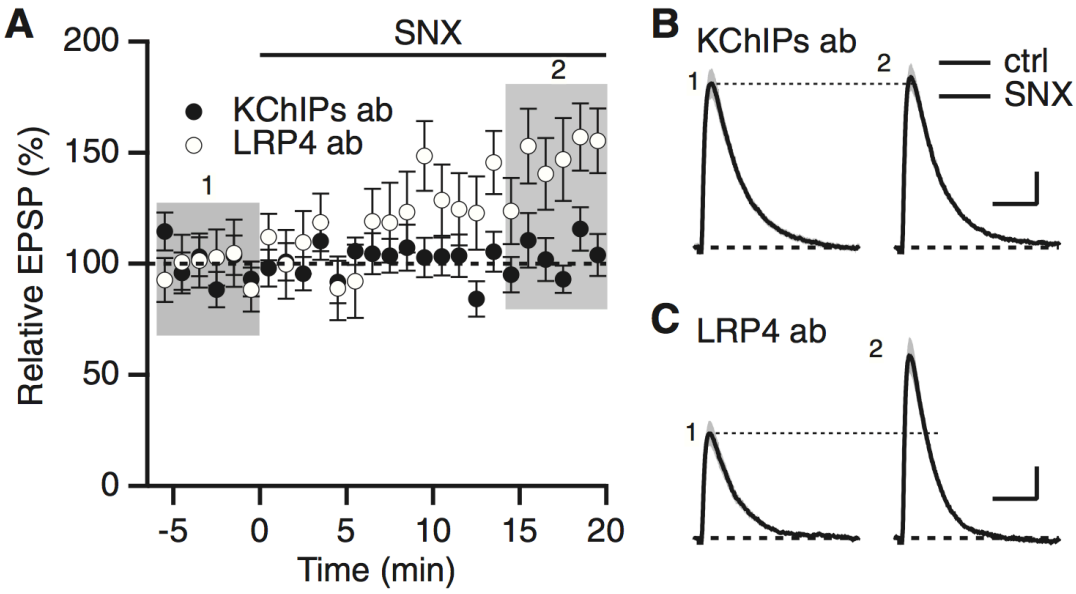
A
SNX
200
150
100
50
0
Relative EPSP (%)
KChIPs ab
LRP4 ab
1
2
-5
0
5
10
15
20
Time (min)
B
KChIPs ab
ctrl
SNX
C
LRP4 ab

Figure 8

SNX Boosting of EPSPs Requires Functional KChIPs

(A) Time course of normalized EPSP amplitude (mean ± SEM) for baseline in control aCSF and during wash-in of SNX in cells dialyzed with KChIPs antibody (closed symbols, n = 9) or LRP4 antibody (open symbols, n = 6).

(B) Representative average of 18 EPSPs dialyzed with KChIPs antibody taken from indicated shaded time points in (A) for control (time point 1) and 14–20 min after SNX wash-in (time point 2); shaded areas are ±SEM. Scale bars, 0.5 mV and 50 ms.

(C) Representative average of 18 EPSPs dialyzed with LRP4 antibody taken (1) from indicated shaded time points for control and (2) 14–20 min after SNX wash-in; shaded areas are ±SEM. Scale bars, 0.5 mV and 50 ms.

V. Synaptic EPSP Responses from R-type Knock-out Mice

Using 2-photon laser photoacitvation of caged glutamate onto single spines of CA1 pyramidal neurons, bloodgood and Sabatini showed that in the presence of SNX-482 to block R-type Ca^{2+} channels, the standard uncaging-evoked stimulation yielded a larger uEPSP compared to control cells, but had no difference to those uEPSPs generated in the condition where both apamin and SNX were present in the spine[135]. They concluded that R-type Ca^{2+} channels provide the Ca^{2+} for activating synaptic SK2-containing channels. In my study, in the presence of SNX-482 to block R-type channels, apamin still boosted synaptic evoked EPSP suggests that R-type Ca^{2+} channel does not provide Ca^{2+} for synaptic SK2-containing channel activation in hippocampal CA1 pyramidal neurons. A stronger control can be done by showing the effect of apamin on increasing EPSP in R-type knock-out mice. In this regard, synaptic stimulation evoked EPSPs were recorded in CA1 neurons from R-type null mice, addition of apamin boosted EPSPs to 149.7% from 18 cells tested, which is similar to the effect of apamin on boosting EPSPs to 151.5% in the presence of SNX-482 in wild-type mice (table 1).

Recent report from Kimm and Bean showed that native A-type current in midbrain dopamine neurons and cloned Kv4 channels are potentially inhibited by the toxin SNX-482[185]. In SNc dopamine neurons where native I_A is mediated by Kv4.3 channels, application of 250-500 nM SNX-482 completed inhibited I_A suggests SNX-482 effect on inhibit Kv4.3 channels. Furthermore, SNX-482 inhibited cloned Kv4.3 channels with an IC_{50} of <3 nM by shifting the voltage dependence of channel opening to more depolarized voltages and by reducing current elicited by maximal

depolarizations[185]. In addition, application of 500 nM SNX-482 also inhibited cloned Kv4.2 channels by shifting the voltage dependence of gating to depolarized voltage, although the effect was less potent than on Kv4.3 channels[185]. Even though in my study I have tested the SNX-482 effect on A-type current by voltage steps in CA1 neurons from acute brain slices, and found no significant SNX-482 effect on I_A. A stronger control experiment can be done by showing a lack of effect of SNX-482 in R-type knock-out mice. In this regard, synaptic stimulation evoked EPSPs were recorded in CA1 neurons from R-type null mice, application of SNX-482 has no significant effect on EPSPs (106.9%) in the presence of apamin (table 1), which is different from the effect of SNX-482 on boosting EPSPs to 157.0% in the presence of apamin in wild-type mice.

R-type null mice/EPSP	**Apamin/control**	**SNX/Apamin**	**Ni/control**	**Apamin/dAP5**
mean	149.7%	106.9%	86.8%	104.0%
sd	22.2%	22.7%	18.2%	17.5%
sem	5.2%	4.2%	6.4%	7.8%
n	18	29	8	5

Table 1.

To further test the presence of R-type Ca^{2+} channels in the R-type knock-out mice, 100 nM Ni was applied to the recording solution, which is thought to block R-type and T-type Ca^{2+} channels, in this condition, Ni has no effect on boosting synaptic evoked EPSP in R-type null mice. In contrast, Ni increased EPSPs to 134.4% in wild-type mice. Moreover, to test whether the NMDARs-SK2 coupling is still intact in R-type knock-out mice, apamin was applied in the presence of dAP5 that blocks NMDARs and no apamin effect on EPSP was detected in R-type null mice, similar to those recorded in wild-type mice.

In summary, apamin still increased synaptic evoked EPSP in R-type knock-out mice suggests that R-type Ca^{2+} channel does not provide Ca^{2+} for SK2 channel activation in hippocampal CA1 neurons. In contrast, dAP occludes the apamin effect on boosting EPSP in both wild-type and R-type null mice suggests that Ca^{2+} influx through NMDARs activate the SK2 channels. The lack of Ni and SNX-482 effect on boosting EPSPs in R-type knock-out mice further confirmed that SNX-482 inhibits R-type Ca^{2+} channels and those relevant effect studied in the project is indeed mediated by R-type channels.

VI. CONCLUSION AND DISCUSSION

Previous immunochemistry results showed that characteristic punctate staining seen in cells transfected with SK2-L but smoother distribution across cell surface seen in cells transfected with SK2-S[56]. In my first project, the immunoparticle staining and functional analysis of SK2-L and SK2-S isoforms of SK2 channels in hippocampal pyramidal neurons indicate that SK2-L isoform directs synaptic localization of SK2-containing channels. In the absence of SK2-L, SK2-S-containing channels were expressed on the extrasynaptic plasma membrane of dendritic spines, but they were selectively excluded from the PSD. In addition, the apamin effect on boosting EPSPs was abolished in SK2-S only mice but was rescued by SK2-L re-expression, suggesting that SK2-L-containing SK2 channels modulate EPSP in CA1 pyramidal cells. My experimental result of field EPSP recording from wild-type mice is consistent with previous report that SK2 channels contribute to the *induction* of LTP in terms of apamin application[127], whereas in SK-S only mice the LTP was not different with or without apamin application. Taken together with the animal behavioral test that memory encoding was altered in SK2-S only mice, these results suggest that the SK2-L isoform directs synaptic localization of SK2-containing channels that is necessary for their synaptic functions, including modulation of EPSPs, synaptic plasticity and learning and memory.

The finding that SK2-L isoform directs synaptic localization leads us to an as yet unresolved question: how are SK2 channels localized to the PSD of CA1 neurons? Given the fact that the originally identified SK2-S is completely contained within SK2-L and that SK2-L has an additional 209 N-terminal amino acids, it is possible

that there are heterologous proteins that interact with specific domains within the N-terminus of the SK2-L protein to engender synaptic SK2 expression. Therefore, as a future plan, we could identify the SK2-L N-terminal domains necessary for synaptic localization of functional SK2 channels, and identify the protein interactions that direct synaptic SK2 expression. Different fragments of N-terminal deletions from the additional 209 amino acids in SK2-L isoform will be expressed in CA1 neurons of SK2-S only mice and apamin sensitivity of CA1 EPSPs will be tested. When the sequence within the N-terminus of SK2-L is identified for synaptic SK2 localization, then biochemical analysis could be performed to identify the protein-protein interactions responsible for targeting SK2 to the PSD. Indeed, studies along these lines are ongoing in our laboratory. Gukhan Kim, another graduate student, has identified a synaptic scaffold that seems to be required for synaptic SK2 channel fuction.

In spines of CA1 pyramidal neurons in the hippocampus, synaptic stimulation promotes Ca^{2+} influx through NMDARs and opens SK2 channels[85]. Here I reconfirmed that by synaptic stimulation, blocking NMDARs with AP5 occluded the apamin effect of increasing EPSPs while blocking R-type Ca^{2+} channels with SNX-482 did not affect the apamin effect on EPSPs. These results are in contrast to Bloodgood and Sabatini's two-photon glutamate uncaging report, where they uncaged glutamate onto single spines to evoke uncaged EPSPs and found no difference in uEPSPs when SNX was present with or without apamin. One advantage of glutamate uncaging is that it bypasses the presynaptic effects of transmitter release, but one complication is that uncaged synapses cannot be used as their own control for measuring the effects of apamin or SNX. Furthermore, when using K^+ based internal

without manipulating postsynaptic conductance, I showed in my experiments that synaptically evoke EPSCs increased in the presence of either SNX or apamin, suggesting a postsynaptic outward current component in the EPSCs. This result is consistent with report from Kim et al. that 4-AP increased miniature EPSCs in cultured hippocampal neurons[138]. In addition, this result may explain the discrepancy between results obtained by synaptic stimulation and glutamate uncaging, likewise when switching from voltage clamp to current clamp to measure the SNX and/or apamin effect using the uncaging protocol, the actual glutamate released by uncaging may vary among spines treated with or without SNX and/or apamin.

A common feature from both glutamate uncaging and synaptic stimulation is that blocking R-type Ca^{2+} channels with SNX-482 increased EPSPs. My results here showed that the SNX effect requires intracellular Ca^{2+} ions but not via NMDARs opening, whereas blocking 4-AP sensitive A-type K^+ channels occluded the SNX effect, suggesting a possible connection between R-type Ca^{2+} channels and voltage gated A-type K^+ channels. Considering Kv4.2 subunits are the major component of A-type K^+ channels in CA1 pyramidal neurons[139,140] and that Kv4.2-containing K^+ channels form multiprotein complex with KChIPs[141], which endows calcium sensitivity to Kv4.2-containing K^+ channels, the introduction of a dominant negative Kv4.2 mutation and application of KChIP antibody both occluded the SNX effect on boosting EPSPs. These results suggest that Ca^{2+} influx through R-type Ca^{2+} channels actives Kv4.2-containing A-type K^+ channels rather than SK channels to increase synaptic responses. In summary, these results indicate that in dendritic spines, there are two distinct Ca^{2+} signaling pathways that link Ca^{2+} influx through NMDARs to

SK channels and that Ca^{2+} influx through R-type Ca^{2+} channels to Kv4.2-containing K^+ channels.

Although I tested whether the application of SNX blocks the Kv4.2-containing K^+ channels and showed that SNX does not affect Kv4.2-containing A-type current in acute slice preparation, recent work from Kimm and Bean showed that SNX-482 dramatically reduced the A-type potassium current in acutely dissociated dopamine neurons from mouse substantia nigra and in HEK-293 cells expressing cloned Kv4.3 channels[185]. In addition, 3 nM SNX produced a depolarizing shift in the voltage dependence of activation of cloned Kv4.3 channels, and a similar effect was seen on the gating of cloned Kv4.2 channels when treated with 500 nM SNX. Considering this result as a future plan of my project, a stronger control will be to show demonstrative a lack of effect of SNX on boosting EPSPs in R-type knock out mice.

Ca^{2+} sources for SK channel activation.

The SK channels are gated solely by intracellular Ca^{2+} ions with an EC_{50} of ~0.5μM. One of the purposes of this project was to revisit the Ca^{2+} sources for SK channel activation in hippocampal CA1 pyramidal spines. In fact, in different regions and cells, SK channels are activated by the elevation of cytosolic Ca^{2+} ions from several different sources.

In response to membrane depolarization, Ca^{2+} influx through voltage-gated Ca^{2+} channels (VGCCs) generates fast and large intracellular Ca^{2+} transients, which may provide a rapid Ca^{2+} source for SK channel activation. For example, in layer 2/3 and

layer 5 pyramidal neurons of the medial prefrontal cortex, applying the L-type Ca^{2+} channel antagonist nicardipine or the R-type Ca^{2+} channel antagonist SNX-482 blocked potentiation of EPSPs by apamin[142], indicating that Ca^{2+} influx through L- and R-type Ca^{2+} channels contributes to activation of synaptic SK channels. In immature mouse inner hair cells, blocking L-type Ca^{2+} channels with nifedipine blocked the outward current conducted by SK channels[143]. In hippocampal pyramidal neurons Tonini et al. showed that AP-induced Ca^{2+} influx through L-type Ca^{2+} channel activates the SK channels[184]. In addition, Cueni et al. reported that T-type Ca^{2+} channels and sarco/endoplasmic reticulum Ca^{2+}-ATPases (SERCAs) regulate the SK channel activity in neurons of the thalamic nucleus reticularis[144]. Womack et al. showed that in cerebellar Purkinje neurons, Ca^{2+} enters through P/Q-type Ca^{2+} channels and activates SK and BK channels, therefore, regulating spontaneous firing activity of Purkinje cells[145].

In addition, Ca^{2+} influx via transmitter-gated channels also provides a Ca^{2+} source for SK channel activation. Two Ca^{2+}-permeable ionotropic receptors that couple to SK channels are NMDARs[85,125,142] and α9-containig nAChRs[77,143,147]. In neurons of the hippocampus, amygdala and the medial prefrontal cortex, NMDARs are expressed in dendritic spines, and blockade of NMDARs by d-AP5 prevented enhancement of EPSPs by SK channel blockade, suggesting that NMDAR activation is required for activation of SK channels. In auditory hair cells, nicotinic acetylcholine receptors (nAChRs) contain the α9-subunit, which confers Ca^{2+} permeability to this type of channel[146]. SK channels driven by the opening of Ca^{2+}-permeable nAChRs give rise

to an inhibitory postsynaptic current (IPSC) carried by K^+ ions, and the time course of this IPSC is determined by the gating kinetics of the SK channels.

The Ca^{2+} sources for activating SK channels can also originate from intracellular stores. In neocortical layer 5 pyramidal neurons and basolateral amygdala projection neurons, the activation of muscarinic acetylcholine receptors (mAChRs) produces inositol 1,4,5-trisphosphate (IP3), inducing Ca^{2+} release from IP3-sensitive intracellular Ca^{2+} stores, which subsequently activate apamin-sensitive SK channels that conduct outward current to hyperpolarize cells[148,149]. In 1998, Fiorillo and Williams reported that in ventral midbrain dopamine neurons, the activation of metabotropic glutamate receptore (mGluR1) mobilized Ca^{2+} from caffeine/ryanodine-sensitive stores, which increased the opening of SK channels, conducting a unique class of IPSPs[150]. A subsequent study by Mirikawa et al. showed that photolytic release of IP3-induced Ca^{2+} release from IP3-sensitive store, which invoked Ca^{2+}-induced Ca^{2+} release (CICR) through ryanodine receptors, eliciting an outward SK current in the midbrain dopamine neurons[151]. In addition, in dopaminergic neurons from young animals, Ca^{2+} release from intracellular stores produces spontaneous miniature outward currents (SMOCs) through SK channels[152]. T-type Ca^{2+} channel blockers inhibit the large-SMOC current whil depletion of intracellular Ca^{2+} stores by ryanodine eliminates the SMOCs, suggesting that Ca^{2+} influx through T-type Ca^{2+} channels activates CICR, which in turn activates SK channels[153]. In rat medial preoptic neurons, Klement et al. showed that the SMOCs are carried through SK3 subtypes that are activated by Ca^{2+} release from intracellular store and affect impulse generation of medial preoptic neurons[154].

In non-neuronal cells such as urinary bladder myocytes, SK and BK are key regulators of excitability of urinary smooth muscle of guinea pig. Herrera and Nelson reported that blocking ryanodine receptors did not affect outward current conducted by SK channels but inhibited outward current conducted by BK channels, while inhibition of VGCCs significantly reduced both SK and BK current, suggesting that Ca^{2+} entry through VGCC activates both SK and BK channels, but CICR through ryanodine receptors activates only BK channels[155]. In human T lymphocyte and in Jurkat T cells, stimulation of T cell receptors initiates Ca^{2+} release from intracellular stores, which subsequently activates Ca^{2+} release-activated Ca^{2+} channels. The activation of SK2 channels in Jurkat T cells and SK4 (IK1) channels in mitogen-activated T cells through accumulation of intracellular Ca^{2+} ions conducts an outward potassium current, which in turn provides the electrochemical driving force for sustained Ca^{2+} influx required for normal T cell function[156].

There is not always only one Ca^{2+} source that contributes to SK channel activation. For example, Faber showed that in layer 2/3 and layer 5 pyramidal neurons of medial prefrontal cortex, blocking NMDARs, L- and R-type Ca^{2+} channels or Ca^{2+} release from ryanodine receptors-sensitive stores all blocked enhancement of EPSPs by apamin, indicating that there are multiple Ca^{2+} sources that regulate SK channels activation[142]. Likewise, in immature mouse inner hair cells, SK channels are significantly activated by Ca^{2+} influx through both L-type Ca^{2+} channels and nAChRs[143]. In summary, the SK channels are activated by elevation of cytosolic Ca^{2+} from several difference sources in different regions and cells.

Kv4.2-containing K^+ channels and KChIPs.

Another significant finding of my results is the coupling of voltage gated SNX-sensitive R-type Ca^{2+} channel to Kv4.2-containing potassium channel in hippocampal CA1 neurons. It was in 1987 when Papazian et al. first reported the isolation of cDNAs encoding the Kv channel α subunit encoded at the *Shaker* gene locus in *Drosophila melanogaster*[6,157]. A year later, by using the Shaker cDNAs as probes, Tempel et al. isolated the first mammalian Kv channels cDNA, Kv1.1[158]. In 1989, the cDNA encoding the rat brain Kv2.1 α subunit was isolated by expression cloning in Xenopus oocytes[159]. In 1991, McCormack et al. and Rudy et al. reported the isolation of cDNA encoding Kv3 α subunit in mammalian brain[160,161], and in the same year, Kv4 α subunit cDNAs were originally isolated by Baldwin et al. and Roberds and Tamkun[162,163]. Kv4 α subunits are divided into three subtypes; Kv4.1, Kv4.2 and Kv4.3. Kv4.1 expression is low in mammalian brain, whereas Kv4.2 and Kv4.3 are expressed at much higher levels and being able to form homomeric or heteromeric Kv4 channels.

One characteristic of Kv4.2-containing potassium channels is their exhibition of A-type inactivation, a process leading to the spontaneous closing of the channel upon sustaining depolarization. For example, after a sustained depolarizing voltage step, A-type potassium channels activate and then inactivate, producing a transient response. In 1990, Zagotta and Hoshi from the Aldrich laboratory first proposed a "N-type inactivation" mechanism for potassium channel inactivation, which occurs when a moveable 22-residue segment localized at the N-terminus of the channel blocks the

pore by binding to the internal entrance of the pore in the open conformation, acting as a tethered pore-blocked in a "ball-and-chain" mechanism. This mechanism was further confirmed by experiments showing that removal part of the N-terminus of the Shaker channel abolish N-type inactivation while the addition of the isolated 22-residue peptide back into the internal solution restores the inactivation in a dose-response manner[164,165].

Among those voltage gated potassium channels that rapidly inactivate, Kv1.4 and Kv4.2 channels conduct a very fast A-type inactivation that occurs within 100 ms after a sustained positive going voltage pulse, however, one difference between these two channels is that Kv4.2 channels recover within 100 ms giving a repolarized voltage step whereas it takes much longer for Kv1.4 channels recover from inactivation[140]. In spite of this difference, the very fast inactivation of Kv channel subtypes may play an important role in regulating action potential firing properties. Indeed, in different neuron types, Kv4 channels prolong the latency to the first spike in a train of action potentials, slow repetitive spike firing, shorten action potentials, and attenuate back-propagating action potentials[166]. For example, in hippocampal CA1 pyramidal neurons, dendritic transient A-type Kv4 channels, which are expressed in high densities in the distal dendrites, exert profound control over dendritic excitability by limiting dendritic depolarization[167]. By expressing a dominant negative Kv4.2(W362F) mutant in CA1 pyramidal neurons of organotypic slice cultures, Kim et al. found that neurons expressing the mutant Kv4.2 displayed broader action potentials with an increase in frequency-dependent AP broadening during a train. Conversely, neurons that with overexpressed Kv4.2 displayed narrow APs with less frequency-dependent broadening and decreased dendritic propagation[139].

By using Kv4.2 knockout mice, Chen et al. showed that deletion of the Kv4.2 gene and a loss of Kv4.2 protein resulted in a specific and near-complete elimination of A-type potassium currents from the apical dendrites of CA1 pyramidal neurons, which led to an increase of backpropagating AP amplitude and a lower threshold for LTP induction[140].

Another characteristic of Kv4.2-containing potassium channels is that they contain auxiliary subunits KChIPs, which are Ca^{2+}-binding proteins containing four EF hand domains. The KChIP family consists of four genes (KChIP1-4), and these genes yield at least 16 products through alternative splicing of KChIP mRNA[168]. Immunolocalization of Kv4 and KChIPs in rat brain revealed that immunoactivity for KChIP2 is concentrated in dendritic membranes, where their distribution corresponds closely with Kv4.2. In contrast, the distribution of KChIP1 closely matches the distribution of Kv4.3, particularly in the somatodendritic domain of neocortical, hippocampal, and striatal interneurons[168]. By using site-directed mutagenesis and deletion approaches, functional mapping of the Kv4 N-terminus and KChIP interaction has identified two N-terminal domains, the proximal N-terminal residues 7-11 and an internal region of 71-90 amino acids that are critical for the KChIP modulation[169]. Structural analysis of the KChIP1/Kv4.3 N-terminus complex revealed a clamping model whereby a single KChIP1 monomer laterally clamps two neighboring Kv4.3 N-termini in a 4:4 manner, with two contact interfaces being involved in the interaction[170,171]. The interaction of KChIPs with the N-terminal of Kv4 channels modulates the surface expression and gating of this class of ion channels. For example, when expressed alone in heterologous cells, Kv4.2 channels are not efficiently expressed on the cell surface, and the Kv4.2 channel protein is

misfolded, hypophosphorylated, and relatively unstable. In control, KChIP co-expression dramatically increases the density of surface Kv4.2 channels and slows their inactivation kinetics and accelerates the rate of recovery from inactivation, in addition to enhanced Kv4.2 protein folding, phosphorylation and stability[163,168]. Another study by Shibata et al. reported that the ER retention of Kv4 channels expressed in the absence of KChIPs appears to be the primary mechanism preventing surface expression[172]. Recently, Foeger et al. showed that target deletion of cytosolic KChIP2 resulted in a complete loss of the Kv4.2 protein in mouse heart, where it is critical for the generation of the ventricular fast transient outward potassium current that underlies the early phase of myocardial action potential repolarization[173]. Furthermore, Anderson et al. reported that Kv4-containing channels in cerebellar stellate cells form a molecular complex with T-type Ca^{2+} channels: Ca^{2+} influx through mifebridil-sensitive T-type Ca^{2+} channels maintains the voltage dependence of availability of Kv4-containing channels in the physiological range, and in a KChIPs dependent manner. Blocking T-type channels induced an ~10 mV hyperpolarizing shift in the voltage dependence of availability of A-type current. Intracellular applying 10 mM BAPTA or a pan-KChIPs antibody occludes this shift, suggesting KChIPs play an important role sensing Ca^{2+} ions for Kv4 channels and regulating Cav3-Kv4 signaling complex[174]. Their subsequent work showed that the Cav3-Kv4 complex expressed in stellate cells acts as a Ca^{2+} sensor, which adaptively regulates stellate cell output to maintain inhibitory charge transfer to *Purkinje* cells, therefore, modulating *Purkinje* cell excitability during fluctuations of extracellular Ca^{2+} concentration[175]. More recently, Heath et al. reported that blocking Cav3 channels with either 300 μM Ni^{2+} or 1 μM mibefradil leftward shifted the voltage-

inactivation relationship of Kv4 channels when expressed in tsA-201 cells or cerebellar granule cells, suggesting that Cav3 channels increase A-type Kv4 current availability through their influence on Kv4 voltage for inactivation[176].

Although there are not many other studies of direct interaction between Kv and Cav channels in the central nervous system, there are still many evidences suggesting a close localization of Kv and Cav channels. In the developing rat forebrain where pioneer axons navigate and pave the way for follower axons to establish the initial neuronal network, Huang et al. reported that A-type Kv3.4 channels are expressed in both pioneer axons and early follower axons, while L-type Cav1.2 channels are found in pioneer axons and early and late follower axons, and both Kv3.4 and Cav1.2 channels are spatially colocalized with markers of pioneer neurons and axons, suggesting that these two high voltage activated ion channels may act together to control Ca^{2+}-dependent electrical activity of pioneer axons during axon pathfinding[177]. In the dendritic spines of hippocampal CA1 pyramidal neurons, Kv4.2 immunoparticles were detected in postsynaptic spines but not directly in the PSD[138], which is similar to the predominantly extrasynaptic localization of Cav2.3 channels[137]. Taken together with the report from Anderson et al showing that 10 mM BAPTA shifted the Kv4 channels inactivation profile[174] and my result that 10 mM BAPTA in the pipet solution blocked the SNX effect on boosting EPSPs, these results suggest that Kv4.2-containing channels and SNX-sensitive Cav2.3 channels are closely coupled at extrasynaptic sites in spines.

Synaptic SK channels and Kv4.2-containing K^+ channels.

SK channels and Kv4 channels play important roles in regulating neuronal activity in central neurons. SK channels modulate neuron intrinsic excitability and firing patterns, while Kv4 channels modify the latency and frequency of spike output. In the dendrites of CA1 pyramidal neurons, SK and Kv4-containing channels serve complementary roles in shaping the time course and extent of branch-specific dendritic excitability[178]. Local apamin applied to distal dendrites increases plateau potential duration and Ca^{2+} influx but does not prevent compartmentalization, while Kv4 channels decrease the amplitude of plateau potentials, preventing their propagation to adjacent branches. Moreover, synaptic SK2 channels undergo endocytosis in a PKA dependent manner during LTP, which is coupled to the exocytosis of AMPRs in the spines[86,129]. Similarly, PKA phosphorylation mediates activity-dependent Kv4.2-containig channel internalization during LTP[138,179]. Therefore, both SK2 channels and Kv4.2-containing channels contribute to the expression of LTP. Taken together with the results of colocalized SK2 and NMDAR immunoparticles in PSD[86], and of Kv4.2 and Cav2.3 channel immunoparticles in extrasynaptic spines[137,138].

In summary, what I found lead to the following proposed model: in dendritic spine of CA1 pyramidal neurons, the SK2 channels and NMDARs are present in the PSD, while voltage gated Cav2.3 and Kv4.2 channels are expressed in extrasynaptically. The SK channels and Kv4.2-containing channels may serve synergistic roles in regulating synaptic responses, the induction and expression of synaptic plasticity, and dendritic integration.

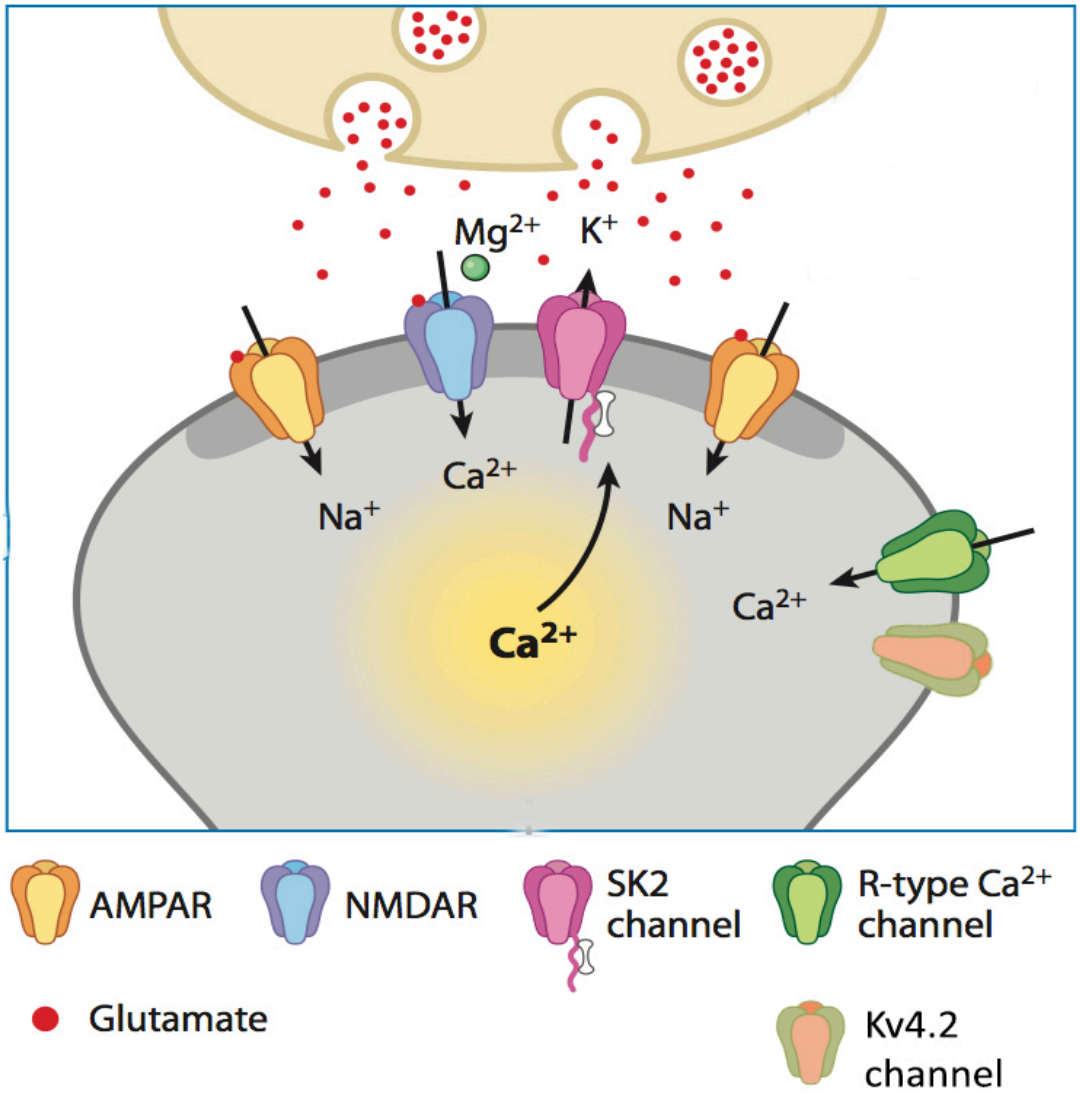

Adapted and modified from Adelman JP, Maylie J, Sah P. (2012) *Annu Rev Physiol.*

VII. LITERATURE

1. Alberts B, Johnson A, Lewis J, et al. (2002) in: Molecular Biology of the Cell, 4th Edn.. Garland Science, NY.
2. Hille, B. (2001) in: Ion Channels of Excitable Membrenes, 3rd Edn., Sinauer Associates, Sunderland, MA.
3. Heginbotham L, Lu Z, Abramson T, MacKinnon R. (1994) Mutations in the K^+ channel signature sequence. *Biophys J.* 66(4):1061-7
4. Doyle DA, Morais Cabral J, Pfuetzner RA, Kuo A, Gulbis JM, Cohen SL, Chait BT, MacKinnon R. (1998) The structure of the potassium channel: molecular basic of K^+ conduction and selectivity. *Science.* 280(5360):69-77
5. Zhou Y, Morais-Cabral JH, Kaufman A, MacKinnon R. (2001) Chemistry of ion coordination and hydration revealed by a K^+ channel-Fab complex at 2.0 A resolution. *Nature.* 414(6859):43-8
6. Papazian DM, Schwarz TL, Tempel BL, Jan YN, Jan LY. (1987) Cloning of genomic and complementary DNA from Shaker, a putative potassium channel gene from drosophila. *Science.* 237(4816):749-53
7. Pongs O, Kecskemethy N, Müller R, Krah-Jentgens I, Baumann A, Kiltz HH, Canal I, Llamazares S, Ferrus A. (1988) Shaker encodes a family of putative potassium channel proteins in the nervous system of Drosophila. *EMBO J.* 7(4):1087-96

8. French GC, VanDongen AM, Schuster G, Brown AM, John RH. (1989) A novel potassium channel with delayed rectifier properties isolated from rat brain by expression cloning. *Nature.* 340(6235):642-45
9. Ho K, Nichols CG, Lederer WJ, Lytton J, Vassilev PM, Kanazirska MV, Hebert SC. (1993) Cloning and expression of an inwardly rectifying ATP-regulated potassium channel. *Nature.* 362(6415):31-8
10. Kubo Y, Baldwin TJ, Jan YN, Jan LY. (1993) Primary structure and functional expression of a mouse inward rectifier potassium channel. *Nature.* 362(6416):127-33
11. Lesage F, Guillemare E, Fink M, Duprat F, Lazdunski M, Romey G, Barhanin J. (1996) TWIK-1, a ubiquitous human weekly inward rectifying K^+ channel with a novel structure. *EMBO J.* 15(5):1004-11
12. Goldstein SA, Wang KW, IIan N, Pausch MH. (1998) Sequence and function of the two P domain potassium channels: implications of an emerging superfamily. *J Mol Med (Berl).* 76(1):13-20
13. Lauritzen I, Zanzouri M, Honoré E, Duprat F, Ehrengruber MU, Lazdunski M, Patel AJ. (2003) K^+-dependent cerebellar granule neuron apoptosis. Role of task leak K^+ channels. *J Bio Chem.* 278(34):32068-76
14. Mu D, Chen L, Zhang X, See LH, Koch CM, Yen C, Tong JJ, Spiegel L, Nguyen KC, Servoss A, Peng Y, Pei L, Marks JR, Lowe S, Hoey T, Jan LY, McCombie WR, Wigler MH, Powers S. (2003) Genomic amplification and oncogenic properties of the KCNK9 potassium channel gene. *Cancer Cell.* 3(3):297-302
15. Aguilar-Bryan L, Nichols CG, Wechsler SW, Clement JP 4th, Boyd AE 3rd, González G, Herrera-Sosa H, Nguy K, Bryan J, Nelson DA. (1995) Cloning of the

beta cell high affinity sulfonylurea receptor: a regulator of insulin secretion. *Science.* 268(5209):423-6

16. Kieffer TJ, Heller RS, Leech CA, Holz GG, Habener JF. (1997) Leptin suppression of insulin secretion by the activation of ATP-sensitive K^+ channels in pancreatic beta-cells. *Diabetes.* 46(6):1087-93
17. Storm JF. (1987) Action potential repolarization and a fast after-hyperpolarization in rat hippocampal pyramidal cells. *J Physiol.* 385:733-59
18. Lancaster B, Nicoll RA. (1987) Properties of two calcium-activated hyperpolarizations in rat hippocampal neurons. *J Physiol.* 389:187-203
19. Golding NL, Jung HY, Mickus T, Spruston N. (1999) Dendritic calcium spike initiation and repolarization are controlled by distinct potassium channel subtypes in CA1 pyramidal neurons. *J Neurosci.* 19(20):8789-98
20. Maletic-Savatic M, Lenn NJ, Trimmer JS. (1995) Differential spatiotemporal expression of K^+ channel polypeptides in rat hippocampal neurons developing in situ and in vitro. *J Neurosci.* 15(5 Pt 2):3840-51
21. Serôdio P, Rudy B. (1998) Differential expression of Kv4 K^+ channel subunits mediating subthreshold transient K^+ (A-type) currents in rat brain. *J Neurophysiol*. 79(2):1081-91
22. Johnston D, Hoffman DA, Magee JC, Poolos NP, Watanabe S, Colbert CM, Migliore M. (2000) Dendritic potassium channels in hippocampal pyramidal neurons. *J Physiol.* 525 Pt 1:75-81
23. Atkinson NS, Robertson GA, Ganetzky B. (1991) A component of calcium-activated potassium channels encode by the Drosophila slo locus. *Science.* 253(5019):515-5

24. Adelman JP, Shen K-Z, Kavanaugh MP, Warren RA, Wu Y-N, Lagrutta A, Bond CT, North RA. (1992) Calcium-activated potassium channels expressed from cloned complementary DNAs. *Neuron.* 9(2):209-16

25. Meera P, Wallner M, Song M, Toro L. (1997) Large conductance voltage- and calcium-dependent K^+ channels with seven N-terminal transmembrane segments (S0-S6), and extracellular N terminus, and an intracellular (S9-S10) C terminus. *Proc Natl Acad Sci USA.* 94(25):14066-71

26. Stefani E, Ottolia M, Noceti F, Olcese R, Wallner M, Latorre R, Toro L. (1997) Voltage-controlled gating in a large conductance Ca^{2+}-sensitive K^+ channel (hslo). *Proc Natl Acad Sci USA.* 94(10):5427-31

27. Gardos G. (1958) The function of calcium in the potassium permeability of human erythrocytes. *Biochim Biophys Acta.* 30(3):653-4

28. Meech RW. (1972) Intracellular calcium injection causes increased potassium conductance in *Aplysia* nerve cells. *Comp Biochem Physiol A Comp Physiol.* 42(2):493-9

29. Lux HD, Neher E, Marty A. (1981) Single channel activity associated with the calcium dependent outward current in Helix pomatia. *Pfluger Arch.* 389(3):293-5

30. R Grygotczyk, W Schwarz, H Passow. (1984) Ca^{2+}-activated K^+ channels in human red cells. Comparison of single-channel currents with ion fluxes. *Biophys J.* 45(4):693-8

31. Marty A, Neher E. (1985) Potassium channels in cultured bovine adrenal chromaffin cells. *J Physiol.* 367:117-41

32. Blatz AL, Magleby KL. (1986) Single apamin-blocked Ca-activated K^+ channels of small conductance in cultured rat skeletal muscle. *Nature.* 323(6090):718-20

33. Habermann E. (1984) Apamin. *Pharmacol. Ther.* 25(2):255-70

34. Vladimirova IA, Shuba MF. (1978) Effect of strychnine, hydrastine and apamin on synaptic transmission in smooth muscle cells. *Neirofiziologiia.* 10(3):295-9

35. Banks BE, Brown C, Burgess GM, Burnstock G, Claret M, Cocks TM, Jenkinson DH. (1979) Apamin blocks certain neurotransmitter-induced increases in potassium permeability. *Nature.* 282(5737):415-7

36. Burgess GM, Claret M, Jenkinson DH. (1981) Effects of quinine and apamin on the calcium-dependent potassium permeability of mammalian hepatocytes and red cells. *J Physiol.* 317:67-90

37. Hugues M, Romey G, Duval D, Vincent JP, Lazdunski M. (1982) Apamin as a selective blocker of the calcium-dependent potassium channel in neuroblastoma cells: voltage-clamp and biochemical characterization of the toxin receptor. *Proc Natl Acad Sci.* 79(4)1308-12

38. Hugues M, Schmid H, Lazdunski M. (1982) Identification of a protein component of the Ca^{2+}-dependent K^{+} channel by affinity labeling with apamin. *Biophys Res Commun.* 107(4):1577-82

39. Ishii TM, Maylie J, Adelman JP. (1997) Determinants of apamin and d-tubocurarine block in SK potassium channels. *J Biol Chem.* 272(37):23195-200

40. Lamy C, Goodchild SJ, Weatherall KL, Jane DE, Liégeois JF, Seutin V, Marrion NV. (2010) Allosteric block of KCa2 channels by apamin. *J Biol Chem.* 285(35):27067-77

41. Nolting A, Ferraro T, D'hoedt D, Stock M. (2007) An amino acid outside the pore region influences apamin sensitivity in small conductance Ca^{2+}-activated K^{+} channels. J Biol Chem. 282(6):3478-86

42. Weatherall KL, Seutin V, Liégeois JF, Marrion NV. (2011) Crucial role of a shared extracellular loop in apamin sensitivity and maintenance of pore shape of small-conductance calcium-activated potassium (SK) channels. *Proc Natl Acad Sci U S A.* 108(45):18494-9

43. Köhler M, Hirschberg B, Bond CT, Kinzie JM, Marrion NV, Maylie J, Adelman JP. (1996) Small-conductance, calcium-activated potassium channels from mammalian brain. *Science.* 273(5282):1709-14

44. Stocker M, Pedarzani P. (2000) Differential distribution of three Ca^{2+}-activated K^{+} channel subunits, SK1, SK2, and SK3, in the adult rat central nervous system. *Mol. Cell. Neurosci.* 15(5):476-93

45. Sailer CA, Hu H, Kaufmann WA, Trieb M, Schwarzer C, Stom JF, Knaus HG. (2002) Regional differences in distribution and functional expression of small-conductance Ca^{2+}-activated K^{+} channels in rat brian. *J. Neurosci.* 22(22):9698-707

46. Stocker M. (2004) Ca^{2+}-activated K^{+} channels: molecular determinants and function of the SK family. *Nat Rev Neurosci.* 5(10):758-70

47. Latorre R, Oberhauser A, Labarca P, Alvarez O. (1989) Varieties of calcium-activated potassium channels. *Annu Rev Physiol.* 51:385-99

48. Ishii TM, Silvia C, Hirschberg B, Bond CT, Adelman JP, Maylie J. (1997) A human intermediate conductance calcium-activated potassium channel. *Proc Natl Acad Sci U S A.* 94(21):11651-6

49. Joiner WJ, Wang LY, Tang MD, Kaczmarek LK. (1997) hSK4, a member of a novel subfamily of calcium-activated potassium channels. *Proc Natl Acad Sci U S A.* 94(20):11013-8

50. Vogalis F, Zhang Y, Goyal RK. (1998) An intermediate conductance K^+ channel in the cell membrane of mouse intestinal smooth muscle. *Biochim Biophys Acta.* 1371(2):309-16

51. Boettger MK, Till S, Chen MX, Anand U, Otto WR, Plumpton C, Trezise DJ, Tate SN, Bountra C, Coward K, Birch R, Anand P. (2002) Calcium-activated potassium channel SK1-and IK1-like immunoreactivity in injured human sensory neurons and regulation by neurotrophic factors. *Brain.* 125(Pt 2):252-63

52. Xia XM, Fakler B, Rivard A, Wayman G, Johnson-Pais T, Keen JE, Ishii T, Hirschberg B, Bond CT, Lutsenko S, Maylie J, Adelman JP. (1998) Mechanism of calcium gating in small-conductance calcium-activated potassium channels. *Nature.* 395(6701):503-7

53. Schumacher MA1, Rivard AF, Bächinger HP, Adelman JP. (2001) Structure of the gating domain of a Ca^{2+}-activated K^+ channel complexed with Ca^{2+}/calmodulin. *Nature.* 410(6832):1120-4

54. Shah M, Haylett DG. (2000) The pharmacology of hSK1 Ca^{2+}-activated K^+ channels expressed in mammalian cell lines. *Br J Pharmacol.* 129(4):627-30

55. Benton DC, Monaghan AS, Hosseini R, Bahia PK, Haylett DG, Moss GW. (2003) Small conductance Ca^{2+}-activated K^+ channels formed by expression of rat SK1 and SK2 genes in HEK 293 cells. *J Physiol.* 553(Pt 1):13-9

56. Strassmaier T, Bond CT, Sailer CA, Knaus HG, Maylie J, Adelman JP. (2005) A novel isoform of SK2 assembles with other SK subunits in mouse brain. *J Biol Chem.* 280(22):21231-6

57. Monagha AS, Benton DC, Bahia PK, Hosseini R, Shah YA, Haylett DG, Moss GW. (2004) The SK3 subunit of small conductance Ca^{2+}-activated K^+ channels

interacts with both SK1 and SK2 subunits in a heterologous expression system. *J Biol Chem.* 279(2):1003-9

58. Grissmer S, Lewis RS, Cahalan MD. (1992) Ca^{2+}-activated K^+ channels in human leukemic T cells. *J Gen Physiol.* 99(1):63-84
59. Park YB. (1994) Ion selectivity and gating of small conductance Ca^{2+}-activated K^+ channels in cultured rat adrenal chromaffin cells. *J Physiol.* 481(Pt 3):555-70
60. Berkefeld H, Fakler B, Schulte U. (2010) Ca^{2+}-activated K^+ channels: from protein complexes to function. *Physiol Rev.* 90(4):1437-59
61. Keen JE, Khawaled R, Farrens DL, Neelands T, Ricard A, Bond CT, Janowsky A, Fakler B, Adelman JP, Maylie J. (1999) Domains responsible for constitutive and Ca^{2+}-dependent interactions between calmodulin and small conductance Ca^{2+}-activated potassium channels. *J Neurosci.* 19(20):8830-8
62. Schumacher MA, Crum M, Miller MC. (2004) Crystal structures of apocalmoduline and an apocalmodulin/SK potassium channel gating domain complex. *Structure.* 12(5):849-60
63. Lee WS, Ngo-Anh TJ, Bruening-Wright A, Maylie J, Adelman JP. (2003) Small conductance Ca^{2+}-activated K^+ channels and calmodulin: cell surface expression and gating. *J Biol Chem.* 278(28):25940-6
64. Li W, Halling DB, Hall AW, Aldrich RW. (2009) EF hands at the N-lobe of calmodulin are required for both SK channel gating and stable SK-calmodulin interaction. *J Gen Physiol.* 134(4):281-93
65. Zhang M, Abrams C, Wang L, Gizzi A, He L, Lin R, Chen Y, Loll PJ, Pascal JM, Zhang JF. (2012) Structural basis for calmodulin as a dynamic calcium sensor. *Structure.* 20(5):911-23

66. Bildl W, Strassmaier T, Thurm H, Andersen J, Eble S, Oliver D, Knipper M, Mann M, Schulte U, Adelman JP, Fakler B. (2004) Protein kinase CK2 is coassembled with small conductance Ca^{2+}-activated K^+ channels and regulates channel gating. *Neuron.* 43(6):847-58

67. Allen D, Fakler B, Maylie J, Adelman JP. (2007) Organization and regulation of small conductance Ca^{2+}-activated K^+ channel multiprotein complexes. *J Neurosci.* 27(9):2369-76

68. Maingret F, Coste B, Hao J, Giamarchi A, Allen D, Crest M, Lichfield DW, Adelman JP, Delmas P. (2008) Neurotransmitter modulation of small-conductance Ca^{2+}-activated K^+ channels by regulation of Ca^{2+} gating. *Neuron.* 59(3):439-49

69. Giessel AJ, Sabatini BL. (2010) M1 muscarinic receptors boost synaptic potentials and calcium influx in dendritic spines by inhibiting postsynaptic SK channels. *Neuron.* 68(5):936-47

70. Buchanan KA, Petrovic MM, Chamberlain SE, Marrion NV, Mellor JR. (2010) Facilitation of long-term potentiation by muscarinic M1 receptors is mediated by inhibition of SK channels. *Neuron.* 68(5):948-63

71. Pachuau J, Li DP, Chen SR, Lee HA, Pan HL. (2014) Protein kinase CK2 contributes to diminished small conductance Ca^{2+}-activated K^+ channel activity of hypothalamic pre-sympathetic neurons in hypertension. *J Neurochem.* doi: 10.1111/jnc.12758

72. Sabatier JM, Fremont V, Mabrouk K, Crest M, Darbon H, Rochat H, Van Rietschoten J, Martin-Eauclaire MF. (1994) Leiurotoxin I, a scorpion toxin specific for Ca^{2+}-activated K^+ channels. Structure-activity analysis using synthetic analogs. *Int. J Pept. Protein Res.* 43(5):486-95

73. Sabatier JM, Zerrouk H, Darbon H, Mabrouk K, Benslimane A, Rochat H, Martin-Eauclaire MF, Van Rietschoten J. (1993) P05, a new leiurotoxin I-like scorpion toxin: synthesis and structure-activity relationships of the alpha-amidated analog, a ligand of Ca^{2+}-activated K^+ channels with increased affinity. *Biochemistry.* 32(11):2763-70

74. Andreotti N, di Luccio E, Sampieri F, De Waard M, Sabatier JM. (2005) Molecular modeling and docking simulations of scorpion toxins and related analogs on human $SK_{Ca}2$ and $SK_{Ca}3$ channels. *Peptides.* 26(7):1095-108

75. Sorensen US, Strobaek D, Christophersen P, Hougaard C, Jensen ML, Nielsen EO, Peters D, Teuber L. (2008) Synthesis and structure-activity relationship studies of 2-(N-substituted)-aminobenzimidazoles as potent negative gating modulators of small conductance Ca^{2+}-activated K^+ channels. *J Med Chem.* 52(23):7625-34

76. Devor DC, Singh AK, Frizzell RA, Bridges RJ. (1996) Modulation of Cl-secretion by benzimidazolones. I. Direct activation of a Ca^{2+}-dependent K^+ channel. *Am J Physiol.* 271(5 Pt 1):L775-84

77. Oliver D, Klöcker N, Schuck J, Baukrowitz T, Ruppersberg JP, Fakler B. (2000) Gating of Ca^{2+}-activated K^+ channels controls fast inhibitory synaptic transmission at auditory outer hair cells. *Neuron.* 26(3):595-601

78. Pedarzani P, Mosbacher J, Rivard A, Cingolani LA, Oliver D, Stocker M, Adelman JP, Faker B. (2001) Control of electrical activity in central neurons by modulating the gating of small conductance Ca^{2+}-activated K^+ channels. *J Bio Chem.* 276(13):9762-9

79. Hougaard C, Eriksen BL, Jorgensen S, Johansen TH, Dyhring T, Madsen LS, Strobaek D, Christophersen P. (2007) Selective positive modulation of the SK3

and SK2 subtypes of small conductance Ca^{2+}-activated K^+ channels. *Br J Pharmacol.* 151(5):655-65

80. Lin MT, Adelman JP, Maylie J. (2012) Modulation of endothelial SK3 channel activity by Ca^{2+} dependent caveolar trafficking. *Am J Physiol Cell Physiol.* 303(3):C318-27
81. Tacconi S, Carletti R, Bunnemann B, Plumpton C, Merlo Pich E, Terstappen GC. (2001) Distribution of the messenger RNA for the small conductance calcium-activated potassium channel SK3 in the adult rat brain and correlation with immunoreactivity. *Neuroscience.* 102(1):209-15
82. Roncarati R, Di Chio M, Sava A, Terstappen GC, Fumagalli G. (2001) Presynaptic localization of the small conductance calcium-activated potassium channel SK3 at the neuromuscular junction. *Neuroscience.* 104(1):253-62
83. Stocker M, Krause M, Pedarzani P. (1999) An apamin-sensitive Ca^{2+}-activated K^+ current in hippocampal pyramidal neurons. *Proc Natl Acad Sci U S A.* 96(8):4662-7
84. Bond CT, Herson PS, Strassmaier T, Hammond R, Stackman R, Maylie J, Adelman JP. (2004) Small conductance Ca^{2+}-activated K^+ channel knock-out mice reveal the identity of calcium-dependent afterhyperpolarization currents. *J Neurosci.* 24(23):5301-6
85. Ngo-Anh TJ, Bloodgood BL, Lin M, Sabatini BL, Maylie J, Adelman JP. (2005) SK channels and NMDA receptors form a Ca^{2+}-mediated feedback loop in dendritic spines. *Nat Neurosci.* 8(5):642-9

86. Lin MT, Lujan R, Watanabe M, Adelman JP, Maylie J. (2008) SK2 channels plasticity contributes to LTP at Schaffer collateral-CA1 synapses. *Nat Neurosci.* 11(2):170-7

87. Ballesteros-Merino C, Lin M, Wu WW, Ferrandiz-Huertas C, Cabañero MJ, Watanabe M, Fukazawa Y, Shigemoto R, Maylie J, Adelman JP, Luján R. (2012) Developmental profile of SK2 channel expression and function in CA1 neurons. *Hippocampus.* 22(6):1467-80

88. Xu Y, Tuteja D, Zhang Z, Xu D, Zhang Y, Rodriguez J, Nie L, Tuxson HR, Young JN, Glatter KA, Vázquez AE, Yamoah EN, Chiamvimonvat N. (2003) Molecular identification and functional roles of a Ca^{2+}-activated K^+ channel in human and mouse hearts. *J Biol Chem.* 278(49):49085-94

89. Tuteja D, Xu D, Timofeyev V, Lu L, Sharma D, Zhang Z, Xu Y, Nie L, Vázquez AE, Young JN, Glatter KA, Chiamvimonvat N. (2005) Differential expression of small-conductance Ca^{2+}-activated K^+ channels SK1, SK2, and SK3 in mouse atrial and ventricular myocytes. *Am J Physiol Heart Circ Physiol.* 289(6):H2714-23

90. Madison DV, Nicoll RA. (1982) Noradrenaline blocks accommodation of pyramidal cell discharge in the hippocampus. *Nature.* 299(5884):636-8

91. Wolfart J, Neuhoff H, Franz O, Roeper J. (2001) Differential expression of the small-conductance, calcium activated potassium channel SK3 is critital for pacemaker control in dopaminergic midbrain neurons. *J Neurosci.* 21(10):3443-56

92. Cingolani LA, Gymnopoulos M, Boccaccio A, Stocker M, Pedarzani P. (2002) Developmental regulation of small-conductance Ca^{2+}-activated K^+ channel expression and function in rat Purkinje neurons. *J Neurosci.* 22(11):4456-67

93. Edgerton JR, Reinhart PH. (2003) Distinct contributions of small and large conductance Ca^{2+}-activated K^+ channels to rat Purkinje neuron function. *J Physiol.* 548(Pt 1):53-69

94. Hallworth NE, Wilson CJ, Bevan MD. (2003) Apamin-sensitive small conductance calcium-activated potassium channels, through their selective coupling to voltage-gated calcium channels, are critical determinants of the precision, pace, and pattern of action potential generation in rat subthalamic nucleus neurons in vitro. *J Neuronsci.* 23(20):7525-42

95. Pedarzani P, McCutcheon JE, Rogge G, Jensen BS, Christophersen P, Hougaard C, Strøbaek D, Stocker M. (2005) Specific enhancement of SK channel activity selectively potentiates the afterhyperpolarizing current I_{AHP} and modulates the firing properties of hippocampal pyramidal neurons. *J Biol Chem.* 280(50):41404-11

96. Hirst GD, Johnson SM, van Helden DF. (1985) The slow calcium-dependent potassium current in a myenteric neurone of the guinea-pig ileum. *J Physiol.* 361:315-37

97. Sah P, McLachlan EM. (1999) Ca^{2+}-activated K^+ currents underlying the afterhyperpolarization in guinea pig vagal neurons: a role for Ca^{2+}-activated Ca^{2+} release. *Neuron.* 7(2):257-64

98. Sah P. (1996) Ca^{2+}-activated K^+ currents in neurones: types, physiological roles and modulation. *Trends Neurosci.* 19(4):150-4

99. Adelman JP, Maylie J, Sah P. (2012) Small-conductance Ca^{2+}-activated K^+ channels: form and function. *Annu Rev Physiol.* 74:245-69

100. Gehlert DR, Gackenheimer SL. (1993) Comparison of the distribution of binding sites for the potassium channel ligands [^{125I}]apamin, [^{125I}]charybdotoxin and [^{125I}]iodoglyburide in the rat brain. *Neuroscience.* 52(1):191-205

101. Storm JF. (1989) An after-hyperpolarization of medium duration in rat hippocampal pyramidal cells. *J Physiol.* 409:171-90

102. Gu N, Vervaeke K, Storm JF. (2005) Kv7/KCNQ/M and HCN/h, but not $K_{Ca}2$/SK channels, contribute to the somatic medium after-hyperpolarization and excitability control in CA1 hippocampal pyramidal cells. *J Physiol.* 566(Pt 3):689-715

103. Gu N, Hu H, Vervaeke K, Storm JF. (2008) SK (K_{Ca2}) channels do not control somatic excitability in CA1 pyramidal neurons but can be activated by dendritic excitatory synapses and regulate their impact. *J Neurosci.* 100(5):2589-604

104. Chen S, Benninger F, Yaari Y. (2014) Role of small conductance Ca^{2+}-activated K^+ channels in controlling CA1 pyramidal cell excitability. *J Neurosci.* 34(24):8219-30

105. Alger BE, Nicoll RA. (1980) Epileptiform burst afterhyperolarization: calcium-dependent potassium potential in hippocampal CA1 pyramidal cells. *Science.* 210(4474):1122-4

106. Stahnisch FW, Nitsch R. (2002) Santiago Ramón y Cajal's concept of neuronal plasticity: the ambiguity lives on. *Trends Neurosci.* 25(11):589-91

107. Hebb DO. (1949) Organization of Behavior: a Neuropsychological Theory. New York: John Wiley

108. Lømo T. (2003) The discovery of long-term potentiation. *Philos Trans R Soc Lond B Biol Sci.* 358(1432):617-20

109. Andersen P, Lømo T. (1967) Control of hippocampal output by afferent volley frequency. *Prog Brain Res.* 27:400-12

110. Bliss TV, Lømo T. (1973) Long-lasting potentiation of synaptic transmission in the dentate area of the anaesthetized rabbit following stimulation of the perforant path. *J Physiol.* 232(2):331-56

111. Nicoll RA, Kauer JA, Malenka RC. (1988) The current excitement in long-term potentiation. *Neuron.* 1(2):97-103

112. Collingridge GL, Kehl SJ, McLennan H. (1983) Excitatory amino acids in synaptic transmission in the Schaffer collateral-commissural pathway of the rat hippocampus. *J Physiol.* 334:33-46

113. Lynch G, Larson J, Kelso S, Barrionuevo G, Schottler F. (1983) Intracellular injections of EGTA block induction of hippocampal long-term potentiation. *Nature.* 305(5936):719-21

114. Sastry BR, Goh JW, Auyeung A. (1986) Associative induction of posttetanic and long-term potentiation in CA1 neurons of rat hippocampus. *Science.* 232(4753):988-90

115. Wigström H, Gustafsson B, Huang YY, Abraham WC. (1986) Hippocampal long-term potentiation is induced by pairing single afferent volleys with intracellularly injected depolarizing current pulses. *Acta Physiol Scand.* 126(2):317-9

116. Kelso SR, Ganong AH, Brown TH. (1986) Hebbian synapses in hippocampus. *Proc Natl Acad Sci U S A.* 83(14):5326-30

117. Malinow R, Miller JP. (1986) Postsynaptic hyperpolarization during conditioning reversibly blocks induction of long-term potentiation. *Nature.* 320(6062):529-30

118. Bliss TV, Collingridge GL. (1993) A synaptic model of memory: long-term potentiation in the hippocampus. *Nature.* 361(6407):31-9

119. Dudek SM, Bear MF. (1992) Homosynaptic long-term depression in area CA1 of hippocampus and effects of N-methyl-D-aspartate receptor blockade. *Proc Natl Acad Sci U S A.* 89(10):4363-7

120. Issac JT, Nicoll RA, Malenka RC. (1995) Evidence for silent synapses: implications for the expression of LTP. *Neuron.* 15(2):427-34

121. Liao D, Hessler NA, Malinow R. (1995) Activation of postsynaptically silent synapses during pairing-induced LTP in CA1 region of hippocampal slice. *Nature.* 375(6530):400-4

122. Shi SH, Hayashi Y, Petralia RS, Zaman SH, Wenthold RJ, Svoboda K, Malinow R. (1999) Rapid spine delivery and redistribution of AMPA receptors after synaptic NMDA receptor activation. *Science.* 284(5421):1811-6

123. Borgdorff AJ, Choquet D. (2002) Regulation of AMPA receptor lateral movements. *Nature.* 417(6889):649-53

124. Opazo P, Choquet D. (2011) A three-step model for the synaptic recruitment of AMPA receptors. *Mol Cell Neurosci.* 46(1):1-8

125. Faber ES, Delaney AJ, Sah P. (2005) SK channels regulate excitatory synaptic transmission and plasticity in the lateral amygdala. *Nat Neurosci.* 8(5):635-41

126. Behnisch T, Reymann KG. (1998) Inhibition of apamin-sensitive calcium dependent potassium channels facilitate the induction of long-term potentiation in the CA1 region of rat hippocampus in vitro. *Neurosci Lett.* 253(2):91-4

127. Stackman RW, Hammond RS, Linardatos E, Gerlach A, Maylie J, Adelman JP, Tzounopoulos. (2002) Small conductance Ca^{2+}-activated K^+ channels modulate synaptic plasticity and memory encoding. *J Neurosci.* 22(23):10163-71

128. Hammond RS, Bond CT, Strassmaier T, Ngo-Anh TJ, Adelman JP, Maylie J, Stackman RW. (2006) Small-conductance Ca^{2+}-activated K^+ channel type 2 (SK2) modulates hippocampal learning, memory and synaptic plasticity. *J Neurosci.* 26(6):1844-53

129. Lin MT, Lujan R, Watanabe M, Frerking M, Maylie J, Adelman JP. (2010) Coupled activity-dependent trafficking of synaptic SK2 channels and AMPA receptors. *J Neurosci.* 30(35):11726-34

130. Messier C, Mourre C, Bontempi B, Sif J, Lazdunski M, Destrade C. (1991) Effect of apamin, a toxin that inhibits Ca^{2+}-activated K^+ channels, on learning and memory processes. *Brain Res.* 551(1-2):322-6

131. Deschaux O, Bizot JC, Goyffon M. (1997) Apamin improves learning in an object recognition task in rats. *Neurosci Lett.* 222(3):159-62

132. Deschaux O, Bizot JC. (1997) Effect of apamin, a selective Ca^{2+}-activated K^+ channel, on habituation and passive avoidance responses in rats. *Neurosci Lett.* 227(1):57-60

133. Stackman RW, Bond CT, Adelman JP. (2008) Contextual memory deficits observed in mice overexpressing small conductance Ca^{2+}-activated K^+ type

2($KCa_{2.2}$, SK2) channels are caused by an encoding deficit. *Learn Mem.* 15(4):208-13

134. Blank T, Nijholt I, Kye MJ, Radulovic J, Spiess J. (2003) Small-conductance, Ca^{2+}-activated K^+ channel SK3 generates age-related memory and LTP deficits. *Nat Neurosci.* 6(9):911-2

135. Bloodgood BL, Sabatini BL. (2007) Nonlinear Regulation of Unitary Synaptic Signals by $CaV_{2.3}$ Voltage-Sensitive Calcium Channels Located in Dendritic Spines. *Neuron.* 53(2):249-60

136. Giessel AJ, Sabatini BL. (2011) Boosting of synaptic potentials and spine Ca transients by the peptide toxin SNX-482 requires alpha-1E-encoded voltage-gated Ca channels. *PLoS One.* 6(6):e20939

137. Parajuli LK, Nakajima C, Kulik A, Matsui K, Schneider T, Shigemoto R, Fukazawa Y. (2012) Quantitative regional and ultrastructural localization of the Ca(v)2.3 subunit of R-type calcium channel in mouse brain. *J Neurosci.* 32(39):13555-67

138. Kim J, Jung SC, Clemens AM, Petralia RS, Hoffman DA. (2007) Regulation of dendritic excitability by activity-dependent trafficking of the A-type K^+ channel subunit Kv4.2 in hippocampal neurons. *Neuron.* 54(6):933-47

139. Kim J, Wei DS, Hoffman DA. (2005) Kv4 potassium channel subunits control action potential repolarization and frequency-dependent broadening in rat hippocampal CA1 pyramidal neurones. *J Physiol.* 569(Pt 1):41-57

140. Chen X, Yuan LL, Zhao C, Birnbaum SG, Frick A, Jung WE, Schwarz TL, Sweatt JD, Johnston D. (2006) Deletion of Kv4.2 gene eliminates dendritic A-type

K^+ current and enhances induction of long-term potentiation in hippocampal CA1 pyramidal neurons. *J Neurosci.* 26(47):12143-51

141. Rhodes KJ, Carroll KI, Sung MA, Doliveira LC, Monaghan MM, Burke SL, Strassle BW, Buchwalder L, Menegola M, Cao J, An WF, Trimmer JS. (2004) KChIPs and Kv4 alpha subunits as integral components of A-type potassium channels in mammalian brain. *J Neurosci.* 24(36):7903-15

142. Faber ES. (2010) Functional interplay between NMDA receptors, SK channels and voltage-gated Ca^{2+} channels regulates synaptic excitability in the medial prefrontal cortex. *J Physiol.* 588(pt 8):1281-92

143. Marcotti W, Johnson SL, Kros CJ. (2004) A transiently expressed SK current sustains and modulates action potential activity in immature mouse inner hair cells. *J Physiol.* 560(Pt 3):691-708

144. Cueni L, Canepari M, Luján R, Emmenegger Y, Watanabe M, Bond CT, Franken P, Adelman JP, Lüthi A. (2008) T-type Ca^{2+} channels, SK2 channels and SERCAs gate sleep-related oscillations in thalamic dendrites. *Nat Neurosci.* 11(6):683-92

145. Womack MD, Chevez C, Khodakhah K. (2004) Calcium-activated potassium channels are selectively coupled to P/Q-type calcium channels in cerebellar Purkinje neurons. *J Neurosci.* 24(40):8818-22

146. Elgoyhen AB, Johnson DS, Boulter J, Vetter DE, Heinemann S. (1994) Alpha 9: an acetylcholine receptor with novel pharmacological properties expressed in rat cochlear hair cells. *Cell.* 79(4):705-15

147. Glowatzki E, Fuchs PA. (2000) Cholinergic synaptic inhibition of inner hair cells in the neonatal mammalian cochlea. *Science.* 288(5475):2366-8

148. Gulledge AT, Stuart GJ. (2005) Cholinergic inhibition of neocortical pyramidal neurons. *J Neurosci.* 25(44):10308-20

149. Power JM, Sah P. (2008) Competition between calcium-activated K^+ channels determines cholinergic action on firing properties of basolateral amygdala projection neurons. *J Neurosci.* 28(12):3209-20

150. Fiorillo CD, Williams JT. (1998) Glutamate mediates an inhibitory postsynaptic potential in dopamine neurons. *Nature.* 394(6688):78-82

151. Morikawa H, Imani F, Khodakhah K, Williams JT. (2000) Inositol 1,4,5-triphosphate-evoked responses in midbrain dopamine neurons. *J Neurosci.* 20(20):RC103

152. Arima J, Matsumoto N, Kishimoto K, Akaike N. (2001) Spontaneous miniature outward currents in mechanically dissociated rat Meynert neurons. *J Physiol.* 534(Pt 1):99-107

153. Cui G, Okamoto T, Morikawa H. (2004) Spontaneous opening of T-type Ca^{2+} channels contributes to the irregular firing of dopamine neurons in neonatal rats. *J Neurosci.* 24(49):11079-87

154. Klement G, Druzin M, Haage D, Malinina E, Arhem P, Johansson S. (2010) Spontaneous ryanodine-receptor-dependent Ca^{2+}-activated K^+ currents and hyperpolarizations in rat medial preoptic neurons. *J Neurophysiol.* 103(5):2900-11

155. Herrera GM, Nelson MT. (2002) Differential regulation of SK and BK channels by Ca^{2+} signals from Ca^{2+} channels and ryanodine receptors in guinea-pig urinary bladder myocytes. *J Physiol.* 541(Pt 2):483-92

156. Fanger CM, Rauer H, Neben AL, Miller MJ, Rauer H, Wulff H, Rosa JC, Ganellin CR, Chandy KG, Cahalan MD. (2001) Calcium-activated potassium

channels sustain calcium signaling in T lymphocytes. Selective blockers and manipulated channel expression levels. *J Biol Chem.* 276(15):12249-56

157. Kamb A, Iverson LE, Tanouye MA. (1987) Molecular characterization of Shaker, a Drosophila gene that encodes a potassium channel. *Cell.* 50(3):405-13

158. Tempel BL, Jan YN, Jan LY. (1988) Cloning of a probable potassium channel gene from mouse brain. *Nature.* 332(6167):837-9

159. Frech GC, VanDongen AM, Schuster G, Brown AM, Joho RH. (1989) A novel potassium channel with delayed rectifier properties isolated from rat brain by expression cloning. *Nature.* 340(6235):642-5

160. McCormack T, Vega-Saenz de Miera EC, Rudy B. (1990/1991) Molecular cloning of a member of a third class of Shaker-family K^+ channel genes in mammals. *Proc Natl Acad Sci U S A.* 87(13):5227-31/88(9):4060

161. Rudy B, Sen K, Vega-Saenz de Miera E, Lau D, Ried T, Ward DC. (1991) Cloning of a human cDNA expressing a high voltage-activating, TEA-sensitive, type-A K^+ channel which maps to chromosome 1 band p21. *J Neurosci Res.* 29(3):401-12

162. Baldwin TJ, Tsaur ML, Lopez GA, Jan YN, Jan LY. (1991) Characterization of a mammalian cDNA for an inactivating voltage-sensitive K^+ channel. *Neuron.* 7(3):471-83

163. Roberds SL, Tamkun MM. (1991) Cloning and tissue-specific expression of five voltage-gated potassium channel cDNAs expressed in rat heart. *Proc Natl Acad Sci U S A.* 88(5):1798-802

164. Hoshi T, Zagotta WN, Aldrich RW. (1990) Biophysical and molecular mechanisms of Shaker potassium channel inactivation. *Science.* 250(4980):533-8

165. Zagotta WN, Hoshi , Aldrich RW. (1990) Restoration of inactivation in mutants of Shaker potassium channels by a peptide derived from ShB. *Science.* 250(4980):568-71

166. Covarrubias M, Bhattacharji A, De Santiago-Castillo JA, Dougherty K, Kaulin YA, Na-Phuket TR, Wang G. (2008) The neuronal Kv4 channel complex. *Neurochem Res.* 33(8):1558-67

167. Hoffman DA, Magee JC, Colbert CM, Johnston D. (1997) K^+ channel regulation of signal propagation in dendrites of hippocampal pyramidal neurons. *Nature.* 387(6636):869-75

168. An WF, Bowlby MR, Betty M, Cao J, Ling HP, Mendoza G, Hinson JW, Mattsson KI, Strassle BW, Trimmer JS, Rhodes KJ. (2000) Modulation of A-type potassium channels by a family of calcium sensors. *Nature.* 403(6769):553-6

169. Scannevin RH, Wang K, Jow F, Megules J, Kopsco DC, Edris W, Carroll KC, Lü Q, Xu W, Xu Z, Katz AH, Olland S, Lin L, Taylor M, Stahl M, Malakian K, Somers W, Mosyak L, Bowlby MR, Chanda P, Rhodes KJ. (2004) Two N-terminal domains of Kv4 K^+ channels regulate binding to and modulation by KChIP1. *Neuron.* 41(4):587-98

170. Pioletti M, Findeisen F, Hura GL, Minor DL Jr. (2006) Three-dimensional structure of the KChIP1-Kv4.3 T1 complex reveals a cross-shaped octamer. *Nat Struct Mol Biol.* 13(11):987-95

171. Wang H, Yan Y, Liu Q, Huang Y, Shen Y, Chen L, Chen Y, Yang Q, Hao Q, Wang K, Chai J. (2007) Structural basis for modulation of Kv4 K^+ channels by auxiliary KChIP subunits. *Nat Neurosci.* 10(1):32-9

172. Shibata R, Misonou H, Campomanes CR, Anderson AE, Schrader LA, Doliveira LC, Carroll KI, Sweatt JD, Rhodes KJ, Trimmer JS. (2003) A fundamental role for KChIPs in determining the molecular properties and trafficking of Kv4.2 potassium channels. *J Biol Chem.* 278(38):36445-54

173. Foeger NC, Wang W, Mellor RL, Nerbonne JM. (2013) Stabilization of Kv4 protein by the accessory K^+ channel interacting protein 2 (KChIP2) subunit is required for the generation of native myocardial fast transient outward K^+ currents. *J Physiol.* 591(Pt 17):4149-66

174. Anderson D, Mehaffey WH, Iftinca M, Rehak R, Engbers JD, Hameed S, Zamponi GW, Turner RW. (2010) Regulation of neuronal activety by Cav3-Kv4 channel signaling complexes. *Nat Neurosci.* 13(3):333-7

175. Anderson D, Engbers JD, Heath NC, Bartoletti TM, Mehaffey WH, Zamponi GW, Turner RW. (2013) The Cav3-Kv4 complex acts as a calcium sensor to maintain inhibitory charge transfer during extracellular calcium fluctuations. *J Neurosci.* 33(18):7811-24

176. Heath NC, Rizwan AP, Engbers JD, Anderson D, Zamponi GW, Turner RW. (2014) The expression pattern of a Cav3-Kv4 complex differentially regulates spike output in cerebellar granule cells. *J Neurosci.* 34(26):8800-12

177. Huang CY, Chu D, Hwang WC, Tsaur ML. (2012) Coexpression of high-voltage-activated ion channels Kv3.4 and Cav1.2 in pioneer axons during pathfinding in the developing rat forebrain. *J Comp Neurol.* 520(16):3650-72

178. Cai X, Liang CW, Muralidharan S, Kao JP, Tang CM, Thompson SM. (2004) Unique roles of SK and Kv4.2 potassium channels in dendritic integration. *Neuron.* 44(2):351-64

179. Hammond RS, Lin L, Sidorov MS, Wikenheiser AM, Hoffman DA. (2008) Protein kinase A mediates activity-dependent Kv4.2 channel trafficking. *J Neurosci.* 28(30):7513-9

180. Mayer ML, Westbrook GL, Guthrie PB. (1984) Voltage-dependent block by Mg^{2+} of NMDA responses in spinal cord neurones. *Nature.* 309(5965):261-3

181. Nowak L, Bregestovski P, Ascher P, Herbet A, Prochiantz A. (1984) Magnesium gates glutamate-activated channels in mouse central neurones. *Nature.* 307(5950):462-5

182. Ascher P, Nowak L. (1988) The role of divalent cations in the N-methyl-D-aspartate responses of mouse central neurones in culture. *J Physiol.* 399:247-66

183. Jarh CE, Stevens CF. (1987) Glutamate activates multiple single channel conductances in hippocampal neurons. *Nature.* 325(6104):522-5

184. Tonini R, Ferraro T, Sampedro-Castañeda M, Cavaccini A, Stocker M, Richards CD, Pedarzani P. (2013) Small-conductance Ca^{2+}-activated K^{+} channels modulate action potential-induced Ca^{2+} transients in hippocampal neurons. *J Neurophysiol.* 109(6):1514-24

185. Kimm T, Bean BP. (2014) Inhibition of A-Type Potassium Current by the Peptide Toxin SNX-482. *J Neurosci.* 34(28):9182-9